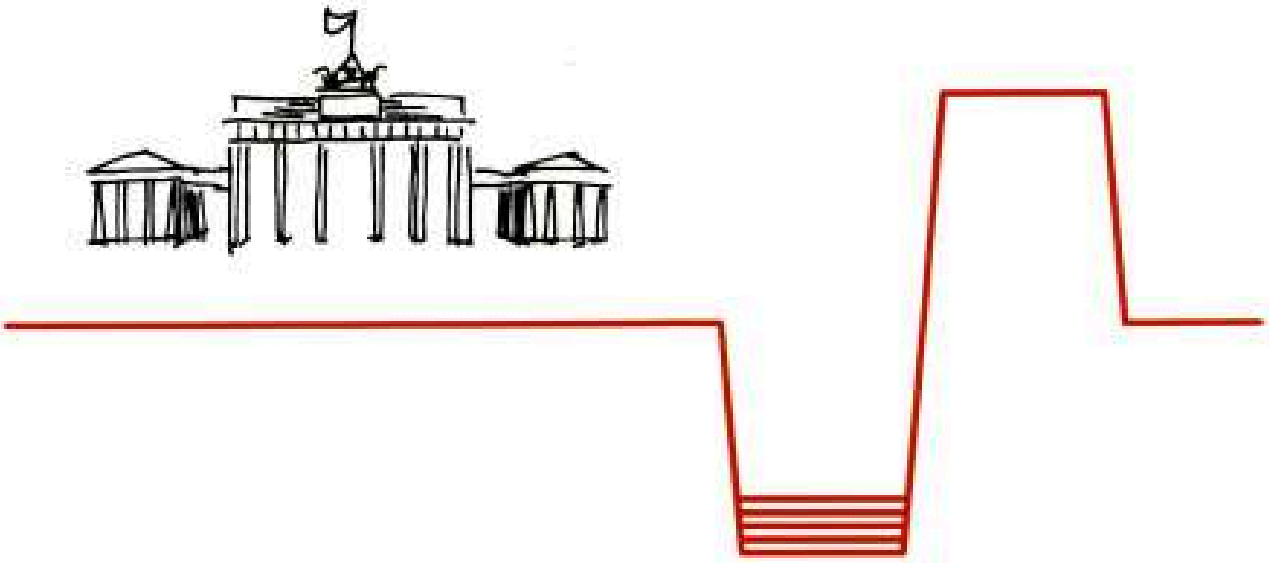

Symposium

Field-Cycling NMR Relaxometry

(Techniques, Applications, Theories)

organized
under the auspices of the Groupement Ampere

Berlin, July 31 - August 2, 1998

Symposium

Field-Cycling NMR Relaxometry

(Techniques, Applications, Theories)

Berlin, July 31-August 2, 1998

(preceding the joint 29th AMPERE-13th ISMAR Conference)

organized

under the auspices of the Groupement Ampere

Contents

General Remarks

Purpose

- to disseminate the information on the technique and on the potential of its applications
- to bring together researchers practising field-cycling methods with those who do not yet but are interested in applying this technique in the future
- to form a discussion forum promoting and cultivating the description of molecular motions in complex systems by spectral densities in relation to recent condensed-matter theories

International Organization and Advisory Committee

R. Kimmich (Ulm, chairman), R. G. Bryant (Charlottesville), N. Fatkullin (Kazan), A. R. Grimmer (Berlin), F. Grinberg (Ulm), J.-P. Korb (Palaiseau), R. N. Muller (Mons), D. Pusiol (Córdoba, AR), E. Rommel (Würzburg), K.-H. Spohn (Ulm)

Scientific Program

The symposium will consist of five sessions including plenary lectures, main lectures, short lectures and poster presentations on the following topics

- Techniques
- Diamagnetic biosystems
- Paramagnetic biosystems and level-crossing experiments
- Polymers and liquid crystals
- Porous media and surface systems

Language The official language of the Symposium will be English.

The venue

The Symposium will be held in the Magnus-Haus, Am Kupfergraben 7, D-10117 Berlin. The Magnus-Haus is located in the old cultural center of Berlin close to the Humboldt University and touristic attractions such as the Pergamon Museum and the Staatsoper unter den Linden. It can conveniently be reached by S- or U-Bahn (subway), station Friedrichstrasse, or by bus line # 100, stop Staatsoper.

The Technical University where the ISMAR/AMPERE conference will take place is only three S-Bahn stops away. Sightseeing spots such as the Brandenburger Tor and the (now unveiled!) Reichstag are located just in the middle between the two meeting sites.

The Magnus-Haus is a conference center of the German Physical Society. Originally it was built in 1760 as a mansion. However, already soon after its completion it became tightly connected with science. The famous physicist J. L. Lagrange lived and worked here. Later in 1840, Gustav Magnus founded a private Physics Laboratory in this building. The German Physical Society which was officially founded in 1845 originates from the Physical Colloquium used to be held here.

Schedule

An informal get-together will take place at the Professorenmensa of the Humboldt University, Unter den Linden 6, entrance at Dorotheenstrasse, on Thursday, July 30, 7 pm - 9 pm.

The scientific program begins on Friday, July 31, 9:15 am. The lectures and the poster exhibition will take place in the Magnus-Haus, Am Kupfergraben 7. The Symposium ends on Sunday, August 2, at 12 am.

The registration desk will be open in the Professorenmensa during the get together on Thursday night, and in the Magnus-Haus beginning with Friday, July 31, 8:00 am.

Common lunch and dinner meals will be arranged for all registrants on Friday and Saturday. The meal tickets and the books of abstracts will be handed over upon registration.

There will be 4 introductory plenary lectures (40 min) by Drs R. G. Bryant, N. Fatkullin, A. G. Redfield, and M. Vilfan. The 10 main lectures (30 min) will be presented by Drs B. Halle, A. J. Horsewill, J.-P. Korb, C. Luchinat, D. J. Lurie, R. N. Muller, D. Pusiol, R.-O. Seitter, S. Stapf, and R. Valiullin. Furthermore, there will be 11 contributed oral communications (20 min). The indicated speaking times include about 5 min for discussion.

Two poster sessions are scheduled on Friday and Saturday afternoon. All posters will be displayed during the whole meeting. The poster format is 100 cm wide and 140 cm high.

Poster Prizes

A prize committee has been formed which will select the two best posters. The prizes will be awarded at dinner on Saturday night. Contributors of oral communications are invited to exhibit posters in addition. In that case, they will take part at the competition for the best posters. Posters from Ulm are excluded from the contest.

Sponsors

The Organizing Committee of the Symposium would like to thank the following sponsors whose financial support is gratefully acknowledged:

Bruker Analytische Messtechnik GmbH, Rheinstetten, Germany

Deutsche Forschungsgemeinschaft, Bonn, Germany

EPIX Medical, Inc, Cambridge, MA, USA

Schering AG, Bereich Pharma, Berlin, Germany

Springer-Verlag, Berlin, Germany

Stelar s.n.c., Mede (PV), Italy

Universität Ulm, Ulm, Germany

Program

Thursday, July 30, 1998

19:00 - 21:00 informal get-together and registration at Humboldt University, Unter den Linden 6, Professorenmensa, entrance at Dorotheenstrasse

Friday, July 31, 1998

8:00 - 9:15 registration at Magnus-Haus, Am Kupfergraben 7
9:15 - 9:30 opening

session "Methods"
chair: A. J. Horsewill

9:30 - 10:10 **A. G. Redfield** (Waltham):
The Early Days of Field Cycling NMR

D. Ivanov, **A. G. Redfield**:
Pure Quadrupole Resonance of Metal Ions and Other Species in Proteins and Other Biopolymers

10:10 - 10:40 **D. J. Lurie** (Aberdeen):
Field-Cycled Magnetic Resonance Imaging - Techniques and Applications

10:40 - 11:10 **coffee break**

11:10 - 11:30 **J. D. King** and A. De Los Santos (San Antonio):
Application of NMR Field Cycling Relaxometry for Detection, Inspection, Identification and Measurement of Long T_1 Materials

11:30 - 11:50 F. Bonetto, **E. Anoardo**, and D. Pusiol (Córdoba):
Fast Field Cycling Study of AC Magnetic Induced Spectral Densities in Doped Gelatins

11:50 - 12:20 **R.-O. Seitter** (Ulm):
A Fast Inexpensive Field-Cycling Relaxometer: The Use of IGBTs and Car Batteries

12:20 - 14:00 **lunch** at restaurant "Die 12 Apostel", Georgenstrasse 177-180
(In den S-Bahn-Bögen)

session "Biopolymers, contrast agents, level crossing"
chair: C. Luchinat

14:00 - 14:30 **R. N. Muller,** P. A. Rinck, and Luce Vander Elst (Mons):
Biomedical Applications of Field Cycling Relaxometry

14:30 - 14:50 A. Ouaksim, A. Roch, **P. Gillis,** and R. N. Muller (Mons):
Characterization of Superparamagnetic Colloids by Analysis of their Water Proton Relaxation Dispersion Profiles

14:50 - 15:10 **V. Denisov,** K. Venu, H. Jóhannesson, and B. Halle (Lund, Hyderabad):
Hydration of Biopolymers in Solution by NMRD

15:10 - 15:30 **E. C. Wiener,** H. Nakamura, A. T. Tatham, and Y. Yamamoto (Urbana, Sendai):
Noncovalent Binding of MR Contrast Agents to Proteins: Assessment with Field-Cycling Relaxometry

15:30 - 15:50 **A. G. Krushelnitsky,** D. V. Markov, A. A. Kharitonov, A. E. Mefed, and V. D. Fedotov (Kazan):
NMR Relaxation in Doubly Rotating Frame as a Tool for Studying Slow Protein Dynamics

15:50 - 16:20 **coffee break**

16:20 - 18:20 **poster presentation**

19:30 **dinner** at restaurant "Zur Nolle", near Bahnhof Friedrichstrasse (S-Bahnbogen 203)

Saturday, August 1, 1998

session "Biopolymers, level crossing, molecular tunnelling"
chair: R. N. Muller

9:00 - 9:40 **R. G. Bryant** (Charlottesville):
Magnetic Relaxation Dispersion of Solutes Using a Sample Switched Spectrometer

9:40 - 10:00 **E. Roduner** (Stuttgart):
Avoided-Level-Crossing Muon Spin Resonance Experiments on Organic Free Radicals in Solids

10:00 - 10:30 **A. J. Horsewill,** D. F. Brougham, C. J. McGloin, and R. I. Jenkinson (Nottingham):
Proton Transfer in the Hydrogen Bond: Incoherent Tunnelling Studied by Field-Cycling NMR Relaxometry

10:30 - 11:00 **coffee break**

11:00 - 11:30 **C. Luchinat** (Florence):
Relaxometry of Paramagnetic Systems with other than Isotropic Zeeman Term in their Electron Spin Hamiltonian

11:30 - 12:00 **D. Pusiol** and E. Anoardo (Córdoba):
^{14}N NQR Studies in Thermotropic Liquid Crystals: T_1 Quadrupole Dips and Double Resonance

12:00 - 12:20 **J. Struppe,** T. Liesener, F. Noack, and M. Vilfan (San Diego, Stuttgart, Ljubljana):
Deuterium Nuclear Quadrupole Resonance Dips in the Proton Spin Relaxation Dispersion of Deuterated Liquid Crystals

12:20 - 14:00 **lunch** at restaurant "Die 12 Apostel", Georgenstrasse 177-180
(In den S-Bahn-Bögen)

session "Polymers, liquid crystals, membranes"
chair: D. Pusiol

14:00 - 14:40 **N. Fatkullin** (Kazan):
Spin-Lattice Relaxation Dispersion in Polymer Melts and Chain Dynamics

14:40 - 15:10 **B. Halle,** S. Gustafsson, Per-Ola Quist, H. Jóhannesson, and K. Venu (Lund, Hyderabad):
Theoretical Aspects of Relaxation Dispersion in Complex Biological Systems

15:10 - 15:30 **F. Grinberg,** R. Kimmich, and S. Stapf (Ulm):
Molecular Dynamics of Microconfined Liquid Crystals Studied by Field-Cycling NMR Relaxometry and the Dipolar-Correlation Effect

15:30 - 15:50 **K. Venu** and V. S. S. Sastry (Hyderabad):
Nuclear Magnetic Relaxation Through Director Fluctuations in Anisotropic Media

15:50 - 16:20 **coffee break**

16:20 - 18:20 **poster presentation**

19:30 **symposium dinner, awards of poster prizes**
at restaurant "Zur Nolle", near Bahnhof Friedrichstrasse
(S-Bahnbogen 203)

Sunday, August 2, 1998

session "Porous media and surface systems"
chair: J. Strange

9:00 - 9:40	**M. Vilfan** (Ljubljana): Investigating Liquid Crystal Dispersions by NMR Relaxometry
9:40 - 10:10	**J.-P. Korb** and R. G. Bryant (Palaiseau, Charlottesville): Anomalous Surface Diffusion of Water Compared to Aprotic Liquids in Nanopores
10:10 - 10:30	**T. Zavada** and R. Kimmich (Ulm): Statistics of Surface Diffusion Probed by Field-Cycling NMR Relaxometry
10:30 - 11:00	**coffee break**
11:00 - 11:30	**S. Stapf** (Nottingham): NMR Relaxometry Studies of Bulk and Confined Plastic Crystals
11:30 - 12:00	**R. Valiullin** (Kazan): Surface Diffusion of Strong Adsorbates: Computer Simulations and NMR Spin-Lattice Relaxation
12:00	adjournment to the ISMAR/AMPERE conference, Technical University, Strasse des 17. Juni 135

Detailed Contents

Invited Lectures and Short Oral Communications

Pure Quadrupole Resonance of Metal Ions and Other Species in Proteins and Other Biopolymers

Dimitri Ivanov and Alfred G. Redfield
Biophysics Program and Department of Biochemistry
Brandeis University
Waltham, MA 02254, USA
FAX (USA) 781-736-2349

If appropriate I will talk briefly about the early days of field cycling NMR in metals (1), and field cycling NMR in general (2). Then I will review our attempt to make field-cycling pure quadrupole resonance (FCPQR) simple and generally applicable to proteins. PQR has been observed without field cycling in at least one protein (of Cu(I) in Cu-Zn Superoxide dismutase, by G. Harbison's group (unpublished)), and quadrupole interactions can be estimated by high-field central transition NMR and other methods. However, we hope that FCPQR will be useful and not too difficult for accurate high-sensitivity observations of low frequency transitions. Our emphasis is on the "rotating frame" methods introduced by one of us and by Slusher and Hahn, and developed by many others including the groups of Minier and Seeger. We are also evaluating a multiple-level crossing method described only, as far as we know, in the thesis of J. C.-K. Koo (with E. L. Hahn, Berkeley, 1969). These are rigid-lattice methods, and to freeze out thermal methyl rotations which would shorten T_1 we operate below 50°K, in a flow dewar (3). The field is cycled by sucking the sample from the center of a 500 MHz magnet to its upper edge, about 1 M above, where the .03 T field and its gradient can be bucked out with a Helmholz coil. The temperature at the top (low field) is 2-4°K higher than at the bottom. We expect to use protein samples dissolved in H_2O-PEG or H_2O-Glycerol, fast-frozen to inhibit water crystallization and, in the case of PEG, as a precipitate, spinning the protein down into the NMR tube just before freezing, to get high concentration. We have obtained promising FCPQR signals from ^{11}B and ^{17}O in small

molecules frozen in glycerol-water glass (3). Generally, we are hampered by short T_1's at zero field, some of which may be due to O_2 that we did not remove, or other impurities. We are now trying to understand the low field T_1's as well as other problems that may make it hard to observe FCQPR of interesting species like Mg and Zn.

1. Y. Masuda in the Encyclopedia of NMR (Wiley 1996, D. Grant, ed.), A. Genack, Phys. Rev. B13, 68 (1976).
2. A. Redfield in "NMR as a Structural Tool" (Plenum, 1996; Rao & Kemple, eds.), D. B. Zax in the Encyclopedia (above); Oja and Lounasmaa, Rev. Mod. Phys. 69, 1 (1997); J. H. Walton et al., Chem. Phys. Lett. 203, 237 (1993).
3. Ivanov and Redfield, Zeit.fur Naturforschung, in press (1998).

Field-Cycled Magnetic Resonance Imaging - Techniques and Applications

David J. Lurie (lurie@abdn.ac.uk)

Dept. of Bio-Medical Physics, University of Aberdeen, Foresterhill, Aberdeen AB25 2ZD, UK

Introduction

A small number of research groups are using field-cycling in conjunction with magnetic resonance imaging (MRI). One use of field cycling in MRI is to produce images in the Earth's magnetic field [1]. Field-cycling is used to pre-polarise the spins in a relatively high, inhomogeneous field, before allowing them to precess in the very low, but very homogeneous Earth's field, with field gradients being used in the usual manner to form an image. "Prepolarised MRI" is also being developed to produce a low-cost, high-sensitivity MRI system [2]. In Aberdeen we have used field-cycling in conjunction with proton electron double resonance imaging (PEDRI) of free radicals [3], and we have constructed a whole-body sized field-cycling imager for this purpose. More recently, the field-cycling imager has been used to measure quadrupole dips in human subjects. The latter two applications will now be discussed in more detail.

Field-Cycled PEDRI

PEDRI is a method for imaging the distribution of free radicals in biological samples or in animals. It is based on the Overhauser effect: an NMR signal is measured while, or after, the EPR resonance of a free radical in solution is irradiated. Under the correct conditions a transfer of polarisation can occur from the electrons to the nuclei, and the NMR signal is enhanced. In PEDRI, proton NMR images are obtained with and without EPR irradiation, and the difference yields an image showing only the free radical distribution. PEDRI produces images with superior resolution to EPR imaging (EPRI), because in EPRI the resolution is degraded by the very broad (~5 MHz) EPR lines of most free radicals. The main difficulty with PEDRI is that it must be performed at very low field (~10 mT) in order to bring the EPR frequency below 300 MHz, for studying biological samples or animals. Even so, excessive RF power deposition is problematical, since the EPR line must be partially saturated. Field-cycled PEDRI (FC-PEDRI) addresses these problems; the basic pulse sequence is shown in Figure 1. The EPR irradiation is applied during the evolution period at field strength B_0^E (~3 mT) at correspondingly low frequency (~50 MHz). The field is then increased for the detection period at field strength B_0^D, where the NMR detection pulse(s) and imaging gradients are applied. The length of the EPR irradiation, T^{EPR} should be of the order of the NMR T_1, to allow the Overhauser enhancement to build up, and the time to ramp the field up to B_0^D should be shorter than T_1, in order not to lose enhancement. Since the EPR irradiation is applied at low frequency, its power deposition is low and it will penetrate easily into biological samples. The signal-to-noise ratio, and hence the sensitivity is improved by detecting at a higher magnetic field. We have used FC-PEDRI to study the exogenous free radical proxyl carboxylic acid (PCA) injected into the bloodstream of living, anaesthetised rabbits [4].

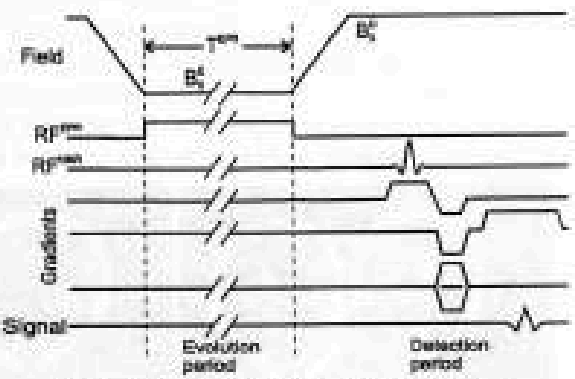

Figure 1: Field-Cycled PEDRI pulse sequence.

Quadrupole Dip Relaxometry and Imaging

It has been known for some time that proton relaxation in proteins and other bio-polymers can be affected by interactions with quadrupolar ^{14}N nuclei, giving rise to "quadrupole dips", which are reductions in the proton spin-lattice relaxation time at NMR frequencies which correspond to the ^{14}N nuclear quadrupole resonance transitions. This effect was studied extensively by

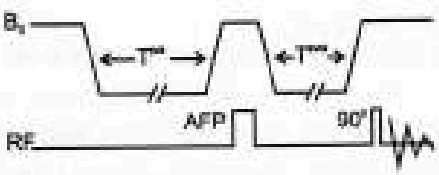

Figure 2: Field-Cycled IR pulse sequence.

Kimmich and co-workers, who measured quadrupole dips in hydrated proteins, and various biological samples including living leeches [5]. Our whole-body field-cycling imager has recently been used to measure quadrupole dips in human muscle and brain. In order to measure T_1 at a range of field strengths, a field-cycled inversion recovery pulse sequence was used, as shown in Figure 2. A polarisation field, identical to the T_1-measurement field, is applied for T^{pol} to bring the spins into equilibrium. A 10 ms adiabatic fast passage (AFP) inverts the magnetisation, and the spins then evolve for T^{evol} at the T_1-measurement field. An interleaved method was used, an identical pulse sequence being applied without AFP at each field strength, to allow T_1 to be calculated by a two-point method. T_1 dispersion spectra were obtained of the author's head and forearm (Figure 3). The timing parameters were T^{pol}=600 ms, T^{evol}=250 ms (head) and T^{evol}=150 ms (arm). T_1 data were collected over the range 30 mT to 80 mT, at intervals of 1 mT. Quadrupole dips at 2.1 MHz (49 mT) and 2.8 MHz (65 mT) can clearly be seen, in good agreement with previous work on muscle [5]. An imaging version of this pulse sequence has also been used, which allows inversion recovery images to be obtained at 57.5 mT (between the dips) and 65 mT (high-field dip). Images of the author's thighs showed considerable differences between the images, most apparent in areas of muscle as shown in Figure 4.

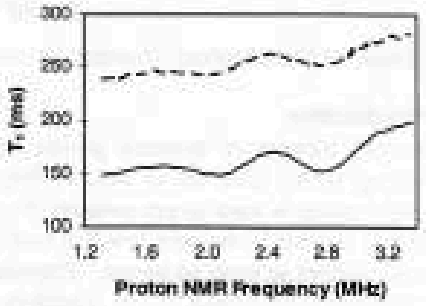

Figure 3: T_1 dispersion plots of human head (dashed) and forearm (solid).

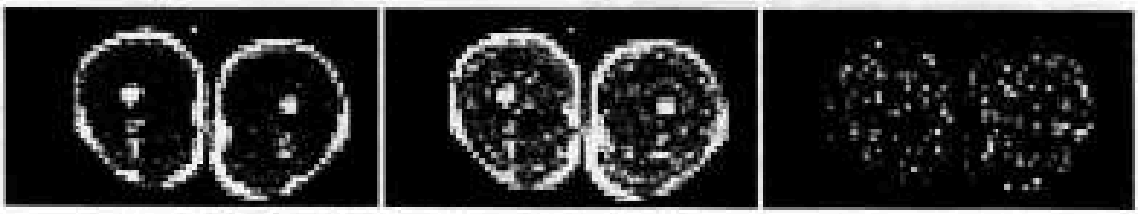

Figure 4: Field-cycling IR images of human thighs. Left: 57.5 mT; middle: 65 mT; right: difference.

Hardware

Experiments were carried out using a whole-body sized field-cycling MRI system [4]. The imager uses a whole-body, ferrite permanent magnet with a vertically-oriented field of 59 mT (Field Effects, USA); this provides the detection magnetic field. Field cycling is accomplished by the field-compensation method: a resistive, saddle-shaped magnet (Magnex Scientific Ltd., UK) is fitted into the bore of the permanent magnet. The field from this secondary magnet can add to or subtract from the permanent magnet's field. A switch-mode power supply amplifier (Copley Controls Inc., USA) is used to drive the secondary magnet; a field change of 59 mT can be achieved in 40 ms, or 30 mT in 10 ms. Eddy currents do not pose a problem with this system, as the structure of the permanent magnet is non-conducting. Field gradient coils are integrated into the structure of the permanent magnet, and the internal bore of the secondary magnet coil is 52 cm in diameter. In the FC-PEDRI work, a split-solenoid coil with i/d 14 cm was used for NMR transmit and receive at 2.5 MHz, and a birdcage resonator (diameter 20 cm) was used for EPR irradiation at 51 MHz. The imager is controlled by a commercial MRI console (SMIS Ltd., UK). A split-solenoid transmit/receive NMR coil with i/d 30 cm was used for the quadrupole dip experiments.

References

[1] Planinsic G., Stepisnik J. and Kos M. J. Magn. Reson. **A110**, 170-174 (1994).

[2] Macovski M. and Conolly S. Magn. Reson. Med. **30**, 221-230 (1993).

[3] Lurie D.J., Hutchison J.M.S., Bell L.H., Nicholson I., *et al.* J. Magn. Reson. **84**, 431-437 (1989).

[4] Lurie D.J., Foster M.A., Yeung D. and Hutchison J.M.S. Phys. Med. Biol. **43(7)**, In Press (1998).

[5] Kimmich R., Winter F., Nusser W. and Spohn K.-H. J. Magn. Reson. **68**, 263-282 (1986).

Application of NMR Field Cycling Relaxometry for Detection, Inspection, Identification and Measurement of Long T_1 Materials

J.D. King, and A. De Los Santos
Southwest Research Institute, San Antonio, TX 78228-0510, U.S.A.

NMR field cycling relaxometry has been applied to several detection, inspection, identification and measurement problems by the authors. The initial research was prompted in the early 1970's by the need to reduce the time required to obtain detectable proton NMR signals from certain explosives - particularly RDX and TNT. The problem with RDX was especially troublesome since T_1 was on the order of 3000 seconds at 28 MHz. It was discovered that manually removing the sample of this material from the NMR coil, bringing it outside the magnet and then returning it to the coil allowed one (only) large amplitude proton NMR FID signal to be obtained. We had to wait 5 minutes before another such signal could be produced. From references in the literature, level crossing of the H[1] NMR with the known N[14] NQR in the RDX was recognized as a possible explanation. This was initially confirmed with more precise translation to known intensities in the stray field of the H_0 magnet. Subsequent measurements showed that a reduction of T_1 from 3000 seconds to about 60 milliseconds at an H_0 intensity which made the proton NMR frequency coincide with the N[14} NQR near 3 MHz. Thus the basic problem of rapid detection was solved and was implemented in the full scale NMR explosive detection system for inspection of baggage and parcels.[1,2] Information on this apparatus is presented and discussed.

Field cycling apparatus for use in the laboratory was designed and assembled to allow more accurate spectra to be obtained of the T_1 reduction in materials at the coincidence of the hydrogen NMR and nitrogen [14] NQR frequencies. This was subsequently used to study[3] hexamethylamine-tetramine (HMT) and many explosives. The apparatus description, operating sequence and level crossing T_1 data from those materials are presented.

In subsequent work the field cycling apparatus was used to conduct a study on level crossing techniques for the quantitative analyses of proteins.[4] Tests were conducted with the samples at room temperature and at liquid nitrogen temperature. Spectra and related data obtained for HMT, Cytosine[5], Uracil[6], Thymine, Glycine anhydride[7], and D-6 Tryptophan are presented.

The field cycling relaxometry apparatus was later investigated as a means to identify the presence of certain plastics in the presence of other similar materials. This work, which will be reviewed, demonstrated the capability to detect the presence of nylon in other thermoplastic materials based on the T_1 effects.

In summary, several practical applications of field cycling relaxometry are discussed and early work with this technology is reviewed.

The contributions of G.A. Matzkanin, P.A. Hornung, E.S. Riewerts, and W.L. Rollwitz (now deceased) to this work is hereby acknowledged.

References:

[1] J.D. King, G.A. Matzkanin and W.L. Rollwitz, "NMR Discrimination Apparatus and Method Therefor", U.S. Patent No. 4,166,972, Sept. 4, 1979.

[2] A. De Los Santos, J.D. King, W.L. Rollwitz, G.A. Matzkanin, P.A. Hornung, "Baggage Inspection Apparatus and Method for Determining Presences of Explosives", U.S. Patent No. 4,514,691, April 30, 1985.

[3] R. Gonano, G.A. Matzkanin, J.D. King, and W.L. Rollwitz, "Hydrogen-Nitrogen Cross Relaxation in Hexamethylamine-tetramine", Proc. 3rd Int'l. Conf. NAR, Tampa, FL, April 1975.

[4] P.A. Hornung, J.D. King, W.L. Rollwitz, "Investigation of Level Crossing Techniques for the Quantitative Analysis of Proteins", Project 15-9233, Southwest Research Institute, December 19, 1980.

[5] D.T. Edmonds and P.A. Speight, *Jour. Mag. Res.*, 6, 265-273 (1972).

[6] R. Blinc, M. Mali, R. Osredkar, A. Prelesnik, J. Seligir and I. Zupancic, *Jour. Chem. Phys.*, **57**, 5087-5093 (1972).

[7] D.T. Edmonds and P.A. Speight, *Phys Ltrs*, **34A**, 325-326 (1971).

Fast Field Cycling Study of AC Magnetic induced Spectral Densities in doped Gelatins.

F. Bonetto, E. Anoardo and D. Pusiol.
Facultad de Matemática, Astronomía y Física. Universidad Nacional de Córdoba. Medina Allende y Haya de La Torre. Ciudad Universitaria. 5010 - Córdoba - Argentina.

Recent studies revealed that lyotropic liquid crystalline mesophases doped with nano-size ferromagnetic particles aquire new properties strongly related with the type of dopant. In particular, a strong particle-molecule interaction becomes responsible of faster magnetic orientational properties [1]. From these studies, it can be assumed that any time dependent magnetic coupling between the ferromagnetic dopants and external fields, will be reflected in a mechanical perturbation of the molecular dynamics. Therefore, a new spectral density can be asociated to this process while a T_1 shortening should be spected.

In order to inquiry about this effect we developed different fast field cycling experiments combined with sinusoidal magnetic field perturbations in doped gelatins and lyotropic systems. An important reduction on the T_1 value was observed in doped gelatins when the perturbing frequency was coincident with the proton Larmor frequency. The experimental technique consist in a polarizing pulse coexisting with the magnetic perturbation. During this step the perturbation plays no significant role while the high Zeeman field (0.4T) is used to polarize the spin system. In a second step the Zeeman field is adiabatically switched off to a relaxation field while the external magnetic perturbation is still actuating on the sample. Finally, the perturbation field is switched off and the Zeeman field is restored to the detection field in order to acquire the NMR signal (figure 1). The whole process is repeated for different evolution times.

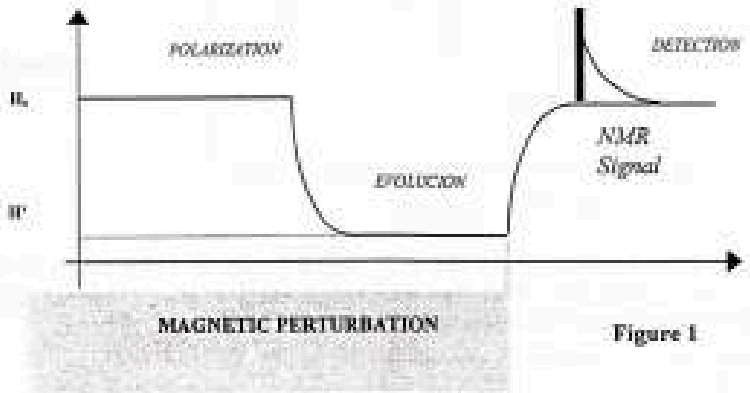

Figure 1

The perturbing field is switched on before polarization and not during the adiabatic demagnetization in order to pre-stablish the desired conditions. Heating of the sample due to the perturbing field was measured to be less than 1°C. The sequence is like a simple T_1 measurement when the perturbing field is not present. We did not observe strong effects when the Larmor frequency corresponding to the relaxation period is greater than the perturbing frequency. On the other hand, in order to increase the magnetic torque on the dopants, the perturbing AC field is perpendicular to the Zeeman field. Therefore, when the perturbing and relaxation spin Larmor frequencies are nearly coisident, an energy absorption from the spin system partially destroy the magnetization during the evolution period. Moreover, this process is superposed to the spin-lattice relaxation, and in consequence, the relaxation evolution becomes non exponential. Figure 2 shows the evolution of the magnetization in a normal T_1 process and when the perturbation is actuating during the relaxation period.

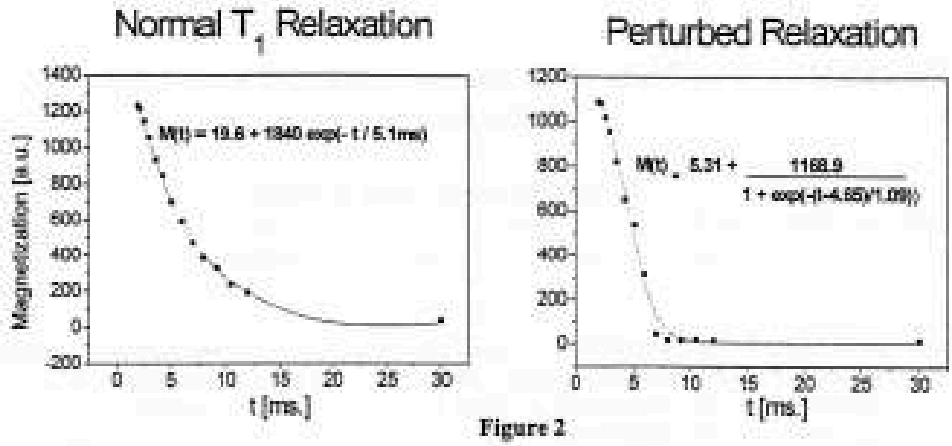

Figure 2

In order to evaluate T_1 when the system is simultaneously absorbing energy from the perturbing field, the experiment must be done with and without perturbation in a doped and nondoped samples. From the 4 obtained magnetization evolution functions, and under certain conditions, it is possible to build a "test function" which is very sensitive to T_1 shortening due to a externally induced forced dynamics. Figure 3 shows computational simulated test functions for the simmilar conditions of the experiment. T_1 in the doped sample at 12 kHz was 5 ms without perturbation. As can be seen in the figure, the test function is very sensitive to a T_1 shortening when the magnetic perturbation actuates on the sample.

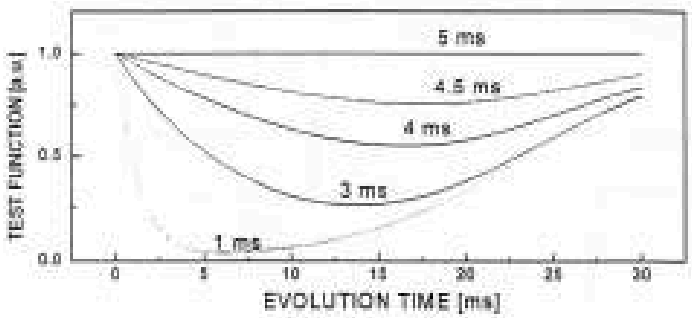

Figure 3

Figure 4 shows the experimental test function for doped gelatin. A T_1 shortening of about 50% was calculated from data fiting. The effect was not present using a sample without dopants (the experimental test function in this case was closer to 1 in the whole evolution time interval).

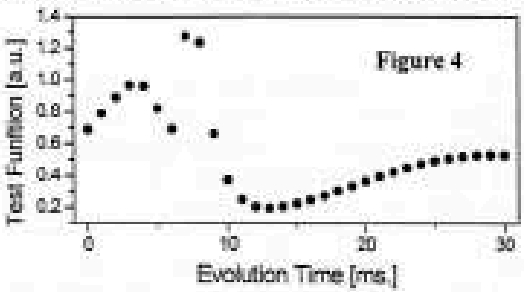

Figure 4

Reference:

[1] - C. Y. Matuo, F. A. Tourinho and A. M. Figueiredo Neto, J. Magn. Mater. 122, 53 (1993).

A fast inexpensive field-cycling relaxometer: The use of IGBTs and car batteries

R.-O. Seitter
Sektion Kernresonanzspektroskopie, Universität Ulm

Field-cycling NMR relaxometry is a versatile and powerful method of investigating molecular dynamics over a large range of time scales [1]. It has been applied to a manifold of materials which show broad distributions of molecular motions, for example proteins [2], liquid crystals [3], synthetic polymers [4] and liquids confined in porous materials [5].
A typical field cycle consists of three intervals: during the *magnetization* or *polarization period* the sample is polarized in a relatively high field B_{0P}. Then the field is switched to a lower level B_{0E}. Within this *relaxation* or *evolution period* the macroscopic magnetization of the sample approaches a new equilibrium value. The corresponding time constant is the spin-lattice relaxation time T_1. At the end of this period the sample is exposed to another strong field B_{0D} to detect the NMR signal. The "relaxation field" may be varied over several orders of magnitude while the "detection field" is kept fixed at the highest possible value with the RF console tuned to this particular field. In this way the features of molecular dynamics can be monitored by recording the Larmor frequency dependence of the spin lattice relaxation time T_1, without changing the frequency of the RF part. The range covered with NMR spectrometers of fixed flux densities is very limited, apart from the fact that the signal-to-noise ratio ($S/N \propto B_0^{3/2}$), and the RF bandwidth decrease the lower the flux density and the frequency become.
In recent years more and more interest arose to measure nuclei with a relatively small sensitivity, such as deuterons, or very diluted samples. Many efforts have been made to improve the stability and the sensitivity of the field-cycling relaxometers, resulting in sophisticated magnet designs and complex current regulation circuits.
Here we describe the setup of a relaxometer with an easy-to-build magnet and a corresponding power supply to ensure the required stability of the current.
In order to facilitate fast field transitions, and to keep occuring induction voltages as small as possible, the inductivity of the magnet should be very low. We decided to built a conventional magnet wound from copper wire. The coil is composed of six double-winding layer split solenoids. The four inner layers consist of 2×21 windings, the two outer layers with 2×18 windings have a 10 mm gap in the center. The magnetic field in the sample volume could be homogenized by adjusting the position of the two outermost layers. The inductivity is 3.2 mH, the room temperature Ohmic resistance 0.46 Ω. The relative inhomogeneity of the flux density was less than $\Delta B/B = 1\cdot10^{-4}$, the current/field ratio amounts to 188.73 A/T.
While the accuracy of the polarization and evolution field is less critical, the detection field is most demanding with respect to strength, stability and reproducibility. Especially samples with a small signal-to-noise ratio require the facility of phase-sensitive detection. A series of 13 ordinary 12 V car batteries turned out to be the best in these regards. In this way a stability of about 10^{-5} at a current of about 300 A can be achieved. The

field corresponds to a Larmor frequency of 62 MHz for protons or 9.5 MHz for deuterons, respectively.
The current of the polarisation and the evolution field is generated by power supplies optimized for different ranges. Fields above 4.2 mT (>800 mA) are produced by a parallel combination of four modules Kepco ATE75-15M. The maximum current in these intervals is 60 A. The resolution below the threshold of 800 mA is improved by a special low current power supply temporarily replacing the Kepco system. Fast field transitions can be facilitated with the aid of a capacitor [6]. During the polarization - evolution transient the energy is transferred from the coil to the capacitor. With opposite polarity it can be used to drive up the current to the detection field. The switches used in the field-cycling circuit are single IGBT modules (Semikron SKM 400 GA) with maximum currents of 400 A at 1200 V.
As the bore of the magnet is relatively small, the RF probehead has a rather compact design. The sample compartment with the RF coil and the temperature sensor is arranged closely to the tune and match capacitors. To prevent the induction of eddy currents during the fast field transients, the RF shielding has to be slit. On the other hand, as every slit works like an antenna, one has to avoid undesired interferences from RF sources outside the probe. A multiple layer shielding with interdigitized slits turned out to be the best in these regards. The length of the exchangeable sample coil is 17 mm with a maximum diameter of 12 mm for the sample containers. The coils can be tuned either for proton or for deuteron resonance.
Measuring both protons and deuterons, the role of inter- and intramolecular relaxation mechanisms can be elucidated, like in polymer melts [7]. Using deuterated water also helps to clarify the mechanisms of water relaxation in biological tissue [8].

References

[1] R. Kimmich, Bull. Magn. Reson. 1, 195 (1980)

[2] S.H. Koenig and R.D. Brown, Progr. Nucl. Magn. Res. Spectr. 22, 487 (1990)

[3] F. Noack, M. Notter and W. Weiss, Liq. Cryst. 3, 907 (1988)

[4] R. Kimmich, N. Fatkullin, H.W. Weber, S. Stapf, J. of Non-Crystalline Solids 172-174, 689-697 (1994)

[5] S. Stapf, R. Kimmich and R.-O. Seitter, Phys. Rev. Let. 75, 15, 2855-2858 (1995)

[6] Redfield A.G., Fite W., and Bleich H.E., Rev. Sci. Instr. 39, 710 (1968)

[7] R. Kimmich, N. Fatkullin, R.-O. Seitter and K. Gille, J. Chem. Phys. 108 (5), (1996)

[8] R. Kimmich, *NMR Tomography, Diffusometry, Relaxometry*, Springer-Verlag, Berlin (1997)

Biomedical Applications of Field Cycling Relaxometry

Robert N. Muller, Peter A. Rinck and Luce Vander Elst
NMR Laboratory, Department of Organic Chemistry
University of Mons-Hainaut, B-7000 Mons, Belgium

Over the last decade, proton field cycling relaxometry has proved its usefulness as a powerful technique in various areas of biomedical research (1). Among other topics, tissue characterization and contrast media development for magnetic resonance imaging (MRI) have attracted the largest attention. The success of this *relaxation spectroscopy* is related to the plentiful structural and dynamic information unveiled by the relaxation parameters of water, the major component of living materials and of their models. Used as a fingerprint of the relaxation behavior of tissues, the NMRD profiles can help in the prediction and optimization of the inherent contrast of MR images (2) and fitted with appropriate models they give a better understanding of the tissue structures and of their alteration induced by pathologies (3).

In the context of the characterization and optimization of paramagnetic and superparamagnetic contrast agents for MRI (4), the analysis of NMRD data, combined with information arising from other techniques like ^{17}O and ^{2}H spectroscopy offers a non-ambiguous and precise description of the intimate mechanisms governing these agents' efficiency (relaxivity) towards the water proton relaxation enhancement. Additionally, protein-binding of paramagnetic chelates and the subsequent increase of relaxivity can be quantitatively followed (5).

The weak points of the method are :

(i) the unability to record transverse relaxation dispersion profiles;
(ii) the rather limited diffusion;
(iii) the technical limits on the upper range of magnetic fields.

Another possible improvement would be the design of systems allowing the investigation of excised and perfused tissues and whole animals enabling the study of living systems.

References

1. Koenig S.H., Brown R.D.
   Relaxometry of Tissue. in: Gupta RK (ed.). NMR Spectroscopy of Cells and Organisms. Vol. 2. Boca Raton, FL (U.S.A.) 1987. 75-114.
2. Rinck P.A., Fischer H.W., Vander Elst L., Van Haverbeke Y., Muller R.N.
   Field Cycling Relaxometry : Medical Application. Radiology 1988; 168: 843-849.
3. Fischer H.W., Rinck P.A., Van Haverbeke Y., Muller R.N.
   Nuclear Relaxation of Human Gray and White Matter: Analysis of Field Dependence and Implications for MRI. Magn. Reson. Med. 1990; 16 :317-334.
4. Vander Elst L., Maton F., Laurent S., Seghi F., Chapelle F., Muller R.N.
   A Multinuclear MR Study of Gd-EOB-DTPA: Comprehensive Preclinical Characterization of an Organ Specific MRI Contrast Agent. Magn. Reson. Med. 1997; 38: 604-614.
5. Muller R.N.
   Contrast Agents in Whole Body MR: Operating Mechanisms. In: Grant DM and Harris R.K. (eds.). Encyclopedia of Nuclear Magnetic Resonance. John Wiley and Sons: Chichester 1996; 1438-1444.

Characterization of superparamagnetic colloids by analysis of their water proton relaxation dispersion profiles.

A. Ouakssim, A. Roch, P. Gillis and R. N. Muller.

Superparamagnetic colloids consist of suspensions of nanometric crystals, each one being made of a ferri- or ferromagnetic domain. The field of applications of these materials is broad: they are used as contrast agents for magnetic resonance imaging (MRI) (1), as therapeutic agent in the context of hyperthermia (2), as well as the basic component of magnetic joints and magnetic inks (3).

In the context of their use as contrast agent in MRI, a precise knowledge of their effects on the water proton magnetic relaxation rates is mandatory. Theories are under development and sometimes conflicting, they derive from the paramagnetic outer sphere relaxation model. Several approaches have been developed which agree with the existence of easy directions in the superparamagnetic crystals and on the oscillation of the magnetization vector. These fluctuations are characterized by a time constant τ_N called the Néel relaxation time. Some contradictions between the theories however arise about the interpretation of the effect of very small crystals ($r < 10$ nm). For those materials called USPIO (Ultra Small Particle Iron Oxide), a low field dispersion appears around 0.5 MHz in the profile representing their « catalytic relaxation efficiency » (relaxivity), those profiles, called NMRD profiles (Nuclear Magnetic Relaxation Dispersion), give the evolution of the water proton relaxation rate with the external magnetic field measured on the aqueous colloidal suspensions. For some authors (4), its origin is the electronic spin precession in an isotropic environment. However, this hypothesis clearly overestimates the low field dispersion experimentally observed.

We have developed another model (5) which takes into account the energy of anisotropy of the crystal, a factor which is known to increase with the volume of the particle, therefore with its diameter. This new model allows a perfect fitting of the NMRD profiles and provides various informations about the particles such as: the estimation of the crystal size, the magnetization of the material and the Néel relaxation time. The energy of anisotropy cannot be extracted from this fitting, but an indication about its value can be obtained from the amplitude of the low field dispersion.

(1) R. N. Muller. Contrast Agents in Whole Body MR: Operating Mechanisms. *Encyclopedia of NMR*, John Wiley, New York 1438-1444 (1996).

(2) I. Hilger, W. Andrä, R. Bähring, A. Daum, R. Hergt, W. A. Kaiser. Evaluation of temperature increase with different amounts of magnetite in liver tissue samples. *Invest. Radiol.* **32(11)**, 705-712 (1997).

(3) K. Nakatsuka. Trends of magnetic fluid applications in Japan. *J. Magn. Magn. Mater.* **122**, 387-394 (1993).

(4) S. H. Koenig, K. E. Kellar. Theory of 1/T1 and 1/T2 NMRD profiles of solutions of magnetic nanoparticles. *Magn. Reson. Med.* **34**, 227-233 (1995).

(5) A. Roch, P. Gillis, A. Ouakssim, R. N. Muller. Proton magnetic relaxation in superparamagnetic aqueous colloids: a new tool for the investigation of the ferrite crystal anisotropy. Abstract « Eight International Conference On Magnetic Fluids » June 29-July 3, 1998 Timisoara, Romania.

Hydration of Biopolymers in Solution by NMRD

V. Denisov, K. Venu, H. Jóhannesson, and B. Halle

Condensed Matter Magnetic Resonance Group,
Department of Chemistry, Lund University, P.O. Box 124, S–22100 Lund, Sweden;
e-mail: vladimir.denisov@fkem2.lth.se; bertil.halle@fkem2.lth.se

The FFC and conventional field variation techniques have been used extensively for almost 30 years [1,2] to study the Nuclear Magnetic Relaxation Dispersion (NMRD) in solutions of biopolymers. The molecular basis of ^{17}O, ^{2}H and ^{1}H NMRD in protein solutions has been recently identified [3-7] with the fast exchange of internal water molecules (trapped in cavities and pockets in the protein structure) with the bulk water [8]. An additional contribution to ^{2}H and ^{1}H relaxation has been shown to come from labile protein hydrogens [5,10]. These methodological advances have allowed accurate determination of the amount, orientational order and residence times of structural water in proteins and DNA, with spatial resolution achieved by designed replacements of specific water molecules [6,7,9,12,14].

NMRD data analysis and time scales. At moderate concentrations, NMRD profiles from protein solutions can be described by the theoretical expression [13]

$$R_1 = R_{bulk} + \alpha + \beta\left[0.2\, j(\omega_0) + 0.8\, j(2\omega_0)\right] \qquad (1)$$

with a Lorentzian spectral density function $j(\omega) = \tau_\beta / [1 + (\omega\tau_\beta)^2]$. Fitting (1) to the observed profiles thus allows determination of the three (essentially model free) quantities: the correlation time, τ_β, the (scaled) NMRD magnitude, $\beta N_T / \omega_{RL}^2 = N_\beta S^2$, and the (scaled) high-frequency plateau, $\alpha N_T / R_{bulk} = N_\alpha \rho$. For data interpretation on the molecular level, knowledge of the water/protein mole ratio N_T, and the rigid-lattice quadrupole (or dipole) frequency for the water molecules giving rise to NMRD, ω_{RL}, is required [13]. To fully contribute to the NMRD magnitude, the residence time of a water molecule should satisfy the criterion $\tau_R < \tau_{res} < (\omega_{RL}^2 S^2 \tau_R)^{-1}$, where τ_R is the rotational correlation time of the protein and S is the water orientational order parameter. Water molecules at the protein surface, with residence times less than ca. 1 ns, contribute to the high-frequency plateau, α.

NMRD magnitude. The ^{17}O NMRD magnitude, $N_\beta S^2$, provides information on the number, N_β, of long-lived water molecules (typically, with residence times, τ_{res}, in the range 0.01 - 1 μs), and their average orientational order parameter, S. Comparison with protein crystal structures [3-9] showed a fair correlation between N_β and the number of internal (structural) water molecules (Fig. 1) residing in protein cavities, surface pockets, and metal centers, and having low solvent accessibility, high positional order, and strong hydrogen bonds to the protein [8]. In accord with this, quantitative changes in $N_\beta S^2$ were seen when designed number of structural water molecules was removed by protein mutation [6,9], extraction of metal ions [7], drug binding [12,14], and protein unfolding [15,16]. The pH-dependent contribution from labile protein hydrogens to the ^{2}H and ^{1}H NMRD magnitude can be quantitatively accounted for, if both the acid dissociation constants and the rate constants for hydrogen exchange are known [5,10]. If this contribution is under control, comparison of the ^{17}O, ^{2}H and ^{1}H NMRD can in favourable cases yield information on libration amplitudes of internal waters [11] (due to unequal effect of the three librational modes on the ^{17}O, ^{2}H and ^{1}H order parameters) and on their residence times [6,9] (due to unequal intrinsic relaxation times for ^{17}O, ^{2}H and ^{1}H). A deeply buried water in BPTI was thus found to have $\tau_{res} = 170$ μs and not to contribute to ^{17}O NMRD at 27 °C [9].

High-frequency plateau. The primary contribution to the high-frequency plateau, $N_\alpha\rho$, arises from N_α water molecules at the protein surface, with an average dynamic retardation factor $\rho = \left(\tau_\alpha/\tau_{bulk} - 1\right)$ [13]. Estimating N_α from the solvent accessible surface area (ASA), $\rho = 4$ - 5 was found for a number of small proteins (Fig. 2) [8], with $N_\alpha\rho$ increasing with ASA upon protein

unfolding [15,16]. Larger proteins exhibit increase in $N_\alpha\rho$, most probably due to numerous surface pockets, containing water molecules with subnanosecond residence times (fast local motions in clusters of internal water may also contribute to this term) [8]. The high-frequency plateau can thus be used as a measure of protein solvent accessibility and surface roughness.

Correlation time. If $\tau_{res} \leq \tau_R$ (but $\tau_{res} \geq$ ca. 1 ns) for N_β water molecules, τ_{res} can be obtained directly from the correlation time, τ_β. Mean τ_{res} was thus determined to be 8 ns at 27 °C for the structural water in RNase A [15], and 0.9 ns at 4 °C (11 ns at -20 °C) for the minor groove water in a DNA dodecamer [12,14]. If $\tau_{res} > \tau_R$, the correlation time τ_β provides information on the protein hydrodynamic volume, irrespectively of the structural integrity of the biopolymer (due to labile hydrogens contribution to $^2H/^1H$) [15].

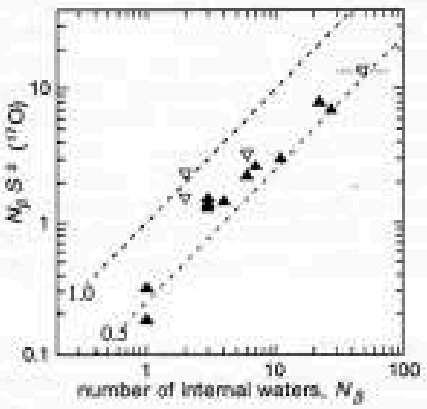

Fig. 1. Correlation of the (scaled) ^{17}O NMRD magnitude, $N_\beta S^2$, from solutions of several proteins, with the number of internal water molecules identified in the known protein crystal structures (filled symbols) or deduced from related crystal structures (open symbols). The dashed lines correspond to the indicated values of the average order parameter, S.

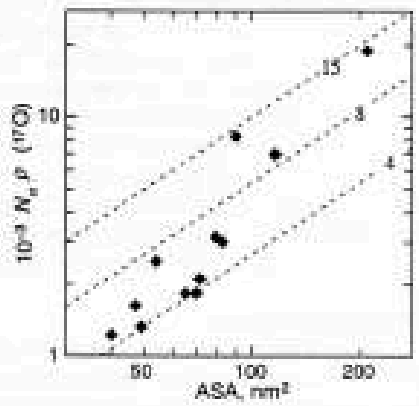

Fig. 2. Correlation of the (scaled) ^{17}O NMRD high-frequency plateau, $N_\alpha\rho$, obtained from solutions of several small and middle-size proteins, with the protein accessible surface area, ASA. The dashed lines correspond to the indicated values of the dynamic retardation factor, ρ.

References

[1] S.H. Koenig and W.E. Schillinger, J. Biol. Chem. 244, 3283 - 3289 (1969)
[2] R. Kimmich and F. Noack, Z. Naturforsch. 25a, 1680 - 1684 (1970)
[3] V.P. Denisov and B. Halle, J. Am. Chem. Soc. 116, 10324 - 10325 (1994)
[4] V.P. Denisov and B. Halle, J.Molec.Biol., 245, 682 - 697 (1995)
[5] V.P. Denisov and B. Halle, J.Molec.Biol., 245, 698 - 709 (1995)
[6] V.P. Denisov, B. Halle, J. Peters, and H. D. Hörlein, Biochemistry, 34, 9046 - 9051 (1995)
[7] V.P. Denisov and B. Halle, J.Am.Chem.Soc., 117, 8456 - 8465 (1995)
[8] V.P. Denisov and B. Halle, Faraday Discuss., 103, 227 - 244 (1996)
[9] V.P. Denisov, J. Peters, H.D. Hörlein and B. Halle, Nature Struct. Biol., 3, 505 - 509 (1996)
[10] K. Venu, V.P. Denisov, B. Halle, J. Am. Chem. Soc. 119, 3122 - 3134 (1997)
[11] V.P. Denisov, K. Venu, J. Peters, H.D. Hörlein and B. Halle, J.Phys.Chem. B 101, 9380-9389 (1997)
[12] V.P. Denisov, G. Carlström, K. Venu and B. Halle, J. Molec. Biol., 268, 118-136 (1997)
[13] B. Halle, V.P. Denisov, K. Venu, in: Modern Techniques in Protein NMR, L.J. Berliner and N.R. Krishna, eds., Vol. 16B, Plenum, NY, in press (1998)
[14] H. Jóhannesson and B. Halle, J.Am.Chem.Soc., in press (1998)
[15] V.P. Denisov and B. Halle, Biochemistry, in press (1998)
[16] V.P. Denisov, B.-H. Jonsson and B. Halle, submitted (1998)

"Noncovalent Binding of MR Contrast Agents to Proteins: Assessment with Field-Cycling Relaxometry"

E.C.Wiener*, H. Nakamura, A.T. Tatham*, and Y.Yamamoto** *University of Illinois at Urbana Champaign, IL USA, **Tohoku University, Sendai, Japan.**

Introduction:

We have used field cycling relaxometry to measure the interaction of a dual labeled magnetic resonance imaging (MRI) and neutron capture therapy (NCT) probe with proteins found in the blood. The specific aim of this research is to improve treatment planning in NCT by providing an agent that allows for the quantitative measurement of the drug distribution with in a tumor. Boron Neutron Capture therapy (NCT) is a binary technique that delivers a non-radioactive agent to the tumor. Neutron irradiation then converts the agent in to a radioactive compound. In the past both poor tumor to blood ratios and unknown radiation dose to the tumor have hindered clinical applications of NCT. Dosimetric calculations can be used to predict the effectiveness of NCT, but these calculations require an a priori knowledge of the drug concentration and distribution. One method for determining the [B] uses an indirect method which measures the [Gd] of a dual labeled agent with MRI. Magnetic resonance imaging uses gadolinium labeled compounds to achieve tumor contrast enhancement. The [Gd] can be calculated from changes in T_1. Fast T_1 mapping techniques such as inversion recovery snapshot flash can be used. This method requires an understanding of the magnetic properties of the agents under physiological conditions.

We are studying the use of a diethylenetriaminepenta-acetate-Gd(III)-carborane derivative (Gd-DTPA-carborane) for dual MRI and NCT applications. We characterized the efficiency of the agent's proton relaxation by using a field cycling relaxometer. We found that this agent binds to serum albumin and has a high relaxivity. When the agent is bound to the protein, the water residence time limits the relaxation efficiency.

Materials and Methods:

We compared the dimeglumine salt of Gd(III)-DTPA to a carborane derivative of Gd(III)-DTPA. The Gd-DTPA-carborane was synthesized as described by Nemoto, et al.[1] Solutions were prepared with varying concentrations of the agents dissolved in either phosphate buffered saline (PBS) or PBS with 1%BSA w/v.

The longitudinal relaxation rates, $1/T_1$, were obtained on an IBM field cycling relaxometer. Nuclear magnetic relaxation dispersion, (NMRD), profiles were obtained as described by Wiener, et al.[2] The magnetic field ranged from 0.47 mT to 1.17T. Relaxivities were determined from the slope of the graph of $1/T_1$ versus the [Gd] and/or by subtraction of the relaxation rate in the absence of the paramagnetic ion from that containing Gd and dividing this quantity by the [Gd].

The [Gd] in each sample was determined by inductively coupled plasma mass spectroscopy using a Perkin-Elmer Sciex ELAN 5000 ICP-MS.

Results and Discussion:

Carboranes are lipophilic. We therefor examined if the Gd-DTPA-carborane formed micelles in the PBS solution. The longitudinal relaxation rate was a linear function of the [Gd]. This coupled with the NMRD shape indicates that the concentration range used was below any possible critical micelle concentration. The relaxivity of the Gd-DTPA-carborane at 30 MHZ was 3.92 +/- 0.01 ($sec^{-1}mM^{-1}$). Many lipophilic agents bind to serum albumin. We therefor tested whether the agent possessed different NMRD profiles in PBS/BSA relative to PBS alone (Figure 1). The relaxivity of the Gd-DTPA-carborane with BSA at 30 MHZ was 32.6 +/- 0.8 ($sec^{-1}mM^{-1}$). The peak in the NMRD profile observed in the PBS/BSA indicates slower molecular tumbling of the Gd-DTPA-carborane relative to the PBS solution. This may result from either noncovalent binding of the agent to the serum albumin or from the higher viscosity.

In order to differentiate between a viscosity or binding effect, we compared the NMRD profile of the Gd-DTPA-carborane with the dimeglumine salt of Gd-DTPA in PBS/BSA. The NMRD profile of Gd-DTPA lacks the peak observed in the profile of the Gd-DTPA-carborane (Figure 2). These data imply that the carborane derivative noncovalently binds to serum albumin.

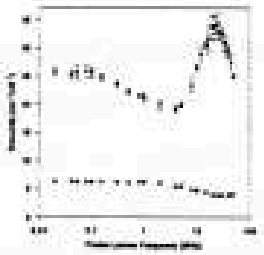

Figure 1. Serum Albumin Increases the Relaxivity of Gd-DTPA-Carboranes. NMRD profile at 35 °C in PBS/BSA,■, and PBS,●.

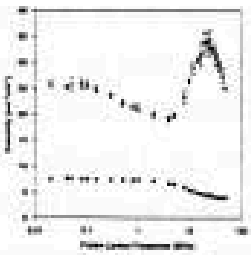

Figure 2. Gd-DTPA-Carboranes Bind to Serum Albumin. NMRD profile at 35 °C in PBS/BSA of Gd-DTPA-Carborane,●, and Gd-DTPA,■.

Low molecular weight Gd-DTPA complexes have fast rotational correlation times, τ_r, and long water residence times, τ_m, on the order of 240 ns.[1] For these complexes τ_m has little impact on the relaxivity relative to τ_r. However for longer τ_r , τ_m of these magnitudes may limit the relaxivity. We therefor examined the effect of τ_m on the relaxivity with temperature studies. Increasing the temperature decreases τ_r and should the relaxivity. We observed that increasing the temperature from 5 to 35 °C increased the relaxivity, 30 MHz, from 19 ± 3 to 32.6 ± 0.8 $(s * mM)^{-1}$. This increase is consistent with a decrease in τ_m associated with an increase in temperature.

The results presented above indicate that the carborane derivative binds to serum albumin noncovalently, has a high relaxivity, and a relatively long τ_m. Thus this agent can be used as a blood pool agent for angiography or tumor blood volume determinations like other agents specifically designed to bind to serum albumins. One may also use this agent to measure the intratumoral [B] and distribution providing that one is careful not to exceed the in vivo binding capacity. Further studies comparing the relaxivity in and on cells to that in serum are underway.

Acknowledgments:

This work was supported by PHS 5 P41 RR05964-06, the University of Illinois, and the Servants Foundation.

References:

1. Nemoto, H.; Cai, J.' Yamamoto, Y.; *Tet. Letters* , 37, 539-542, 1996.
2. Wiener, E.C.; Brechbiel, M.W.; Brothers, H.; Magin, R.L.; Gansow, O.A; Tomalia, D.A.; Lauterbur, P.C. *Mag. Reson. in Med.*, 31, 1-8, 1994.
3. Micseki, K.; Powell, D.H.; Helm, L.; Bruchen, E.; Merbach, A.E. *Mag. Reson.Chem* , 31, 1011-1020, 1993.

NMR relaxation in doubly rotating frame as a tool for studying slow protein dynamics.

A.G. Krushelnitsky, D.V. Markov, A.A. Kharitonov, A.E. Mefed*, V.D. Fedotov.
Kazan Institute of Biochemistry and Biophysics, Kazan, Russia
*Institute of Radiotechnics and Electronics, Fryazino, Russia
e-mail: krushelnitsky@sci.kcn.ru

Many techniques are being applied for studying molecular dynamics of proteins. Infrequent large amplitude conformational transitions are of primary interest since these types of motions rather than fast low amplitude oscillations are usually more important for biological function of proteins. Field cycling NMR relaxometry has been used to obtain information for studying slow motions in proteins and polypeptides in solid state [1-3]. However, this method has a natural limitation in that molecular motions having correlation times longer than the inverse frequency of the local field of the sample are not accessible by standard T_1 relaxation techniques. In most cases, the local field for protons is 10-20 kHz; therefore, for studying slower motions, other approaches must be used.

The method of proton magnetic relaxation in doubly rotating frame [4-6] permits averaging of the local magnetic field by means of magnetization rotation under the magic angle condition and in this way much slower motions become accessible. In this method, two fields simultaneously are applied to the nuclear system: standard B_1 and a weaker field B_2. The latter is created by phase modulation of B_1, and the depth of this modulation defines the resonance frequency in the doubly rotating frame. The spin-lattice relaxation time in the doubly rotating frame is defined as [6]:

$$\frac{1}{T_{1\rho\rho}} = \frac{1}{4 \cdot N} \cdot \left[3 \cdot J(\omega_1) + J(2 \cdot \omega_1)\right] \cdot \sum_{i \neq j} b_{ij}^2 +$$

$$+ \frac{9}{64 \cdot \omega_1^2} \cdot \frac{1}{N} \cdot \left[\left\{ \frac{29}{24} \cdot J(\omega_2) + \frac{49}{8} \cdot J(3 \cdot \omega_2) \right\} \cdot \sum_{i \neq j \neq k} b_{ij}^2 \cdot b_{ik}^2 + \right.$$

$$\left. + \left\{ \frac{5}{12} \cdot J(\omega_2) + \frac{49}{4} \cdot J(3 \cdot \omega_2) \right\} \cdot \sum_{i \neq j \neq k} b_{ij} \cdot b_{ik} \cdot b_{jk}^2 + J(\omega_2) \cdot \sum_{i \neq j} b_{ij}^4 \right]$$

$$b_{ij} = \frac{1}{2} \cdot \gamma^2 \cdot \hbar \cdot \left(1 - 3 \cdot \cos^2 \Theta_{ij}\right) \cdot r_{ij}^{-3}$$

where N is the number of protons in the molecule; $J(\omega)$ is a spectral density of the motion, and Θ_{ij} is an angle between the internuclear vector r_{ij} and the magnetic field B_2.

As shown in the equation above, $T_{1\rho\rho}$ gives information concerning spectral densities of motion at two resonance frequencies: ω_1 and ω_2. The latter can be easily changed by varying the depth of phase modulation of the B_1 field within the range 200 Hz - 10 kHz. In addition, $T_{1\rho\rho}$ is sensitive to the motion of three nuclei with respect to each other, whereas the standard relaxation is defined only by pairwise nuclear interactions. Thus, the relaxation in the doubly rotating frame can be a very informative tool for selecting an appropriate motional model.

Using this method we have studied hen egg lysozyme as a dry powder. The temperature dependence of $T_{1\rho\rho}$ from -130°C to 70°C was measured at three $\omega_2/2\pi$ frequencies: 1.5, 3 and 6 kHz. $\omega_1/2\pi$ was equal to 100 kHz. Analysis of the data was performed using a model free approach assuming a distribution of internal motional correlation times. Lattice sums $\sum_{i\neq j} b_{ij}^2$, $\sum_{i\neq j\neq k} b_{ij}^2 \cdot b_{ik}^2$, $\sum_{i\neq j\neq k} b_{ij} \cdot b_{ik} \cdot b_{jk}^2$ and $\sum_{i\neq j} b_{ij}^4$ (see the equation above) were calculated from the PDB coordinates for lysozyme. These sums were calculated assuming powder averaging and fast methyl rotation around the symmetry axis of the methyl group to average the internuclear interaction.

For fitting the data, it was realized that the order parameter for different lattice sums (see the equation above) can be different even for the same motion. For simplicity we used only two order parameters that correspond to the standard second moment $\sum_{i\neq j} b_{ij}^2$ and other lattice sums, respectively. The analysis has shown that the correlation time for the slow internal motion has a broad distribution and is about 10-50 μs at room temperature. Both amplitude and frequency parameters for this motion have been defined more reliably than it was done for the same sample using standard T_1 and T_2 relaxation methods [7].

References.

1. R. Kimmich, F. Winter, W. Nusser and K.-H. Spohn. J. Magn. Res. (1986) 68, 263-282.
2. W. Nusser, R. Kimmich and F. Winter. J. Phys. Chem. (1988) 92, 6808-6814.
3. W. Nusser and R. Kimmich. J. Phys. Chem. (1990) 94, 5637-5639.
4. A. Mefed and V. Atsarkin. Phys. Stat. Sol. (A) (1986) 93, K21.
5. A. Mefed, V. Atsarkin and M. Zhabotinsky. JETP (1986) 91, 671-676.
6. V. Atsarkin, T. Khazanovich. JETP (1984) 87, 279-288.
7. A.G. Krushelnitsky, V.D. Fedotov, J. Spevacek and J. Straka. J. Biomol. Struc. Dynam. (1996) 14, 211-224.

Magnetic Relaxation Dispersion of Solutes Using a Sample Switched Spectrometer. R. G. Bryant, Department of Chemistry, University of Virginia. Charlottesville, Virginia 22901 USA.

The magnetic field dependence of the nuclear spin-lattice relaxation rate provides considerable information about molecular dynamics over a very wide frequency range [1]. Constraints on resolution and sensitivity have limited applications of magnetic relaxation dispersion to solute species, which are often of considerable chemical or biochemical importance. We have assembled a spectrometer that utilizes two magnets and a pneumatic sample shuttle system that permits direct characterization of solute spin relaxation dispersion profiles.

The high field is provided by a Magnex 7 T superconducting solenoid modified to withstand the stresses of an iron shield that is in close proximity. The secondary field is provided by a GMW 4-inch electromagnet driven by a Danfysik System 8000 magnet power supply controlled in a feed-back loop with a Hall probe to sense the magnetic field. The magnet control system is operated from an Internatonal Instruments Labview platform. The remainder of the NMR spectrometer was constructed in this laboratory and operates with a Tecmag Libra interface and data system that is controlled by a Macintosh Quadra 800 computer that serves as the master control for the spectrometer. Data processing is largely accomplished off-line. Samples are housed in plastic containers machined to fit loosely in a 6 mm shuttle tube that is activated pneumatically using dc solenoid valves controlled by the Libra interface. Shuttle times are generally rapid compared with settling times, but we may collect data 100 ms after the shuttle movement is initiated.

As in current switched systems [2], the usual data acquisition cycle is to polarize the spins in the high field, move the sample to the satellite field where it may relax for a simultaneously specified time, then return it to the high field and sample the magnetization. Because we detect in a static high resolution 7 T field, we may readily resolve different chemical shifts and measure the relaxation dispersion of several components simultaneously. Because the polarization and detection field is 7 T, the sensitivity of the instrument is high and permits multinuclear observation of solute spins including protons, lithium-7, cesium-133, fluorine-19, cadmium-111. The price of the high resolution is a rather long shuttle time between fields, which may limit the range of relaxation rates easily measured with this approach. Nevertheless, results on electrolytes, peptides, and protein solutions are very promising and demonstrate that there are many new opportunities for studying molecular dynamics over the time scale range from 10^{-4} to 10^{-12} seconds. [3]

[1] A. Noack, Progr. NMR Spectrosc. 18, 171-276 (1986).
[2] A. G. Redfield, W. Fite, H. E. Bleich, Rev. Sci. Instrum. 39, 710 (1968). K. H. Schweikert, R. Krieg, F. Noack, J. Magn. Reson. 78, 77-96 (1988). G. Schauer, W. Nusser, M. Blanz, R. Kimmich. J. Phys. E. Sci. instrum. 20, 43-6(1987).
[3] T. R. J. Dinesen, R. G. Bryant, J. Magn. Reson.,1998 in press. T. R. J. Dinesen, S. Wagner, R. G. Bryant, J. Am. Chem. Soc. 1998, in press.

Avoided-Level-Crossing Muon Spin Resonance Experiments on Organic Free Radicals in Solids

Emil Roduner
Institute of Physical Chemistry, University of Stuttgart, Pfaffenwaldring 55
D-70569 Stuttgart, Germany
roduner@indigo01.chemie.uni-stuttgart.de

Avoided-Level-Crossing Muon Spin Resonance (ALC-μSR) is a technique that is closely related to field-cycling NMR relaxometry. It is based on energetic positive muons (μ^+, a spin one-half elementary particle with a mass of one-ninth the proton mass and a lifetime of 2.2 μs) which are available at the ports of suitable accelerators with a spin polarization of close to 100% (1). They are stopped in the experimental sample which is placed in an applied magnetic field with the field direction parallel or antiparallel to the polarization of the muons in the beam.

Upon thermalization, the muons capture an electron from the environment, forming a bound state which has been dubbed muonium (Mu $\equiv \mu^+e^-$). This is a hydrogen-like one-electron atom, and in a chemical sense it is a light isotope of hydrogen with a mass of one-ninth the mass of H. Since its Bohr radius and its ionization potential are within 0.5% the same as those of H its chemical behavior is the same as that of H, except when kinetic isotope effects are involved. Like H, it reacts with unsaturated molecules by addition, for example with benzene

under formation of a Mu-substituted free radical in which the muon is chemically bound as a polarized spin label. The muon polarization is detected via observation of the decay positron which for reasons of conservation of angular momentum is emitted preferentially along the instantaneous muon spin direction at the moment of its decay. A plot of the muon decay asymmetry as a function of the externally applied longitudinal field reveals resonances at fields where avoided crossings of magnetic energy levels allow the muon spins to relax. The resonance fields permit the determination of the muon and proton hyperfine coupling constants. Quantitative analysis of the line width and shape leads to detailed information about the radical reorientation dynamics on a critical time scale of typically 30 ns [1]. In particular, there is one type of resonance that is driven by the dipolar part of the muon hyperfine interaction. It is strongest in the solid state but absent in the liquid or gas. For radicals in a directing environment (e.g. adsorbed on surfaces) it may disappear with increasing temperature either by broadening, or by narrowing and loss of amplitude, depending on the exact nature of the motion [2,3].

The effect was proposed originally by Abragam [4]. The relaxation at avoided crossings is common to the field cycling techniques, and therefore the theories about line positions and shapes are basically the same. The difference is that owing to the high genuine polarization of the muons no cycling of the field is needed. Furthermore, the read-out is via a single particle counting technique instead of an induction coil.

A typical example of an ALC-μSR spectrum, obtained for cyclohexadienyl radicals in a benzene-loaded ZSM-5 zeolite at 334 K, is displayed in the figure. The line near 1.88 kG is a muon spin flip transition which is present only under anisotropic conditions, the others are muon-proton spin flip-flop transitions which are seen also in the liquid or gaseous phase. The line shapes demonstrate that the radical performs fast uniaxial rotation about an axis perpendicular to the molecular plane, and the line widths show that this rotation is superimposed by some type of wobbling which leads to an extensive but not isotropic averaging of the hyperfine anisotropy. The wobbling amplitude decreases below ca. 100 K, and around 50 K the entire motion freezes. In a copper-loaded zeolite of the same structure a strong additional resonance appears due to a small hyperfine interaction of the unpaired electron with the copper nucleus [5].

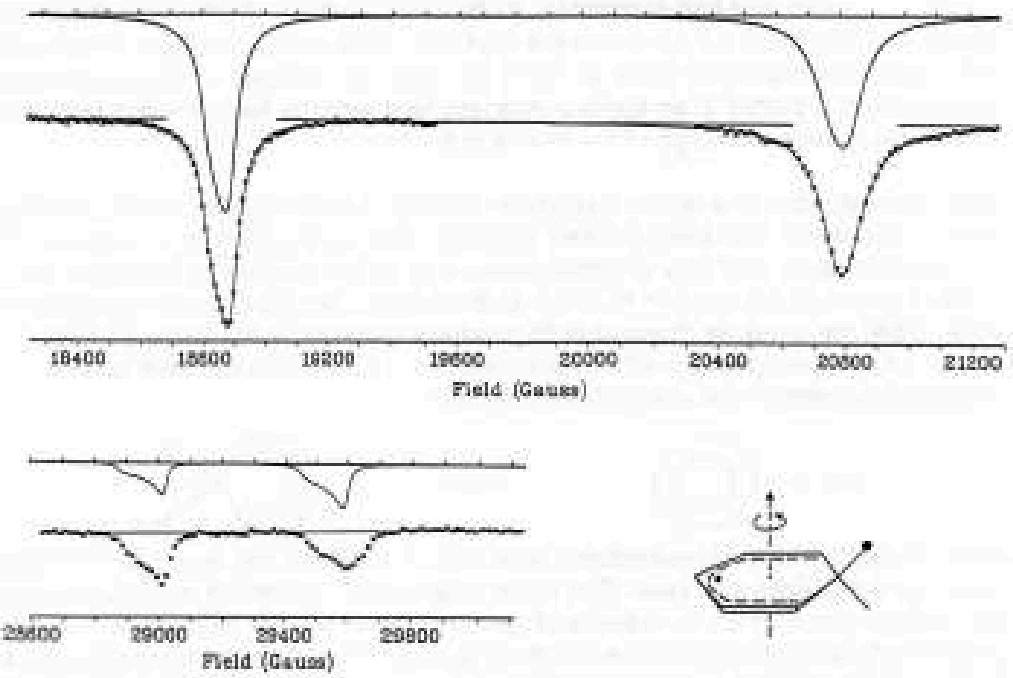

The experimental technique will be introduced, and its application for studying structure and dynamics of organic free radicals in the solid phase will be discussed.

[1] E. Roduner, *Polarised positive muons probing free radicals: a variant of magnetic resonance*, Chem. Soc. Reviews, **22** (1993) 337.

[2] E. Roduner et al., *Reorientational dynamics of C_{60} in the solid state. An avoided level crossing muon spin resonance study*, Chem. Phys. **192** (1995) 231.

[3] P. Tregenna-Piggott et al., *Calculation of the ALC-μSR response for various stochastic motion by use of Monte-Carlo methods*, Chem. Phys. **203** (1996) 317.

[4] A. Abragam, *Résonance magnétique - Spectrométry par croisements de niveaux en physique du muon*, Comptes Rendus Acad. Sci. Paris **229** (1984) 85.

[5] M. Stolmár and E. Roduner, *Complexation of copper by cyclohexadienyl radicals in Cu/ZSM-5 zeolite*, J. Amer. Chem. Soc. **120** (1998) 583.

Proton Transfer in the Hydrogen Bond: Incoherent Tunnelling Studied by Field-Cycling NMR Relaxometry

A.J. Horsewill*, D.F. Brougham, C.J. McGloin and R.I. Jenkinson

Department of Physics, University of Nottingham, Nottingham, NG7 2RD, UK

Introduction

The motion of atomic and molecular particles under the influence of a potential energy surface is ubiquitous to condensed matter science. In particular, the quantum mechanical aspects of the motion are of fundamental importance because the wave-like nature of the particles permits barrier penetration by tunnelling processes. We have investigated the proton transfer process in the hydrogen bond, one of the most fundamental chemical reactions.[1] In this system, the small mass of the proton, together with the relatively small nuclear displacements involved, means that quantum mechanical tunnelling contributes to and often dominates the reaction dynamics. In many systems, in particular in those of biological interest such as the nucleic acid-base pairs, there exist two tautomer structures corresponding to the minima of the double well potential energy surface (PES), which governs the transfer. The correct description of the PES and the evaluation of the dynamics on this surface are required for a quantitative understanding of this reaction and motivate much experimental and theoretical work.

A direct measurement of the frequency spectrum of the stochastic jumps of the proton in the hydrogen bond can be made by QENS and field-cycling NMR relaxometry.[2,3] In both cases, the recorded spectra characterising the frequency spectrum of this dynamics exhibit Lorentzian lineshapes with linewidths determined by the inverse correlation time for the motion, τ_c^{-1}. We shall demonstrate the complementarities of these different methods and describe the temperature dependence of τ_c^{-1} in proton transfer systems. These measurements cover the particularly interesting temperature range in which the transition from direct tunnelling at low temperatures to a rate process characterised by an Arrhenius law at high temperatures is observed.

Experimental Results

The information on the rates and frequencies that characterise the motion is encoded within the nuclear spin relaxation properties. The proton spin-lattice relaxation rate, T_1^{-1}, is the Fourier Transform of the dipolar correlation function and for a powder sample represents the superposition of two Lorentzian spectral density functions with widths in the ratio 1:2 and amplitudes in the ratio 4:1 as follows,

$$T_1^{-1}(\omega_L) = C\, p_a p_b \left[\frac{\tau_c}{1+\omega_L^2 \tau_c^2} + \frac{4\tau_c}{1+(2\omega_L)^2 \tau_c^2} \right] = C\, p_a p_b \left[L(\omega_L, \tau_c) + 4L(2\omega_L, \tau_c) \right] \qquad \textbf{Eqn.1}$$

$\omega_L = \gamma B_r$ is the proton Larmor frequency in the externally applied magnetic field, B_r. The modulation of the dipolar interactions determines the constant, C, and p_a and p_b are the populations of the two tautomeric forms. In Fig. 1 the dispersion of the proton spin-lattice relaxation rate, T_1^{-1}, in benzoic acid at 13.6 K recorded by field-cycling NMR is plotted. The data have been reflected in the zero frequency axis as a visual aid. The solid line is the fit to the superposition of two Lorentzians, Eqn. 1, and the two individual spectral density components arising from the fit are illustrated by dashed lines. The FWHM of the $L(2\omega,\tau_c)$ line determines the inverse correlation time, $\tau_c^{-1} = (1.22 \pm 0.02) \times 10^8\ s^{-1}$. From the temperature independence of this linewidth we have shown that the dynamics are dominated by incoherent tunnelling.[2,3] The quality of the fit in Fig.1 supports the assumptions made in developing the two-site

jump model leading to Eqn. 1, in particular the stochastic nature of the proton jumps exemplified by the exponential form of the dipolar correlation functions.

In Fig. 2 the dynamic range accessible to the field-cycling spectrometer at Nottingham is illustrated by measurements of the spectral density for proton transfer in four different carboxylic acid dimers. The spectrometer possesses a superconducting magnet with an inductance of 0.2 H, a maximum B-field of 3 T and a field switching rate of 0.7 T s^{-1}.

Figure 1

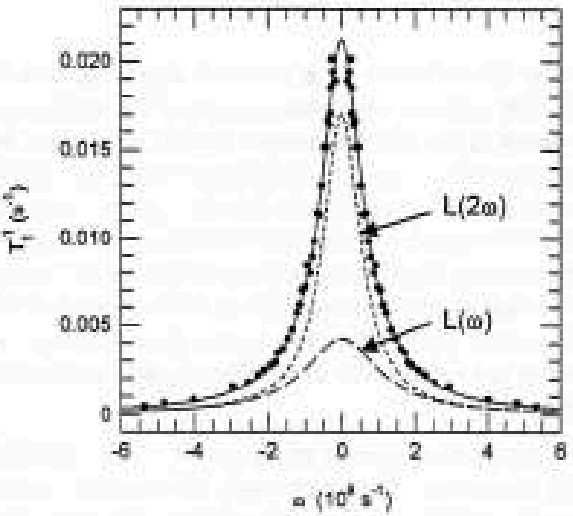

Figure 2

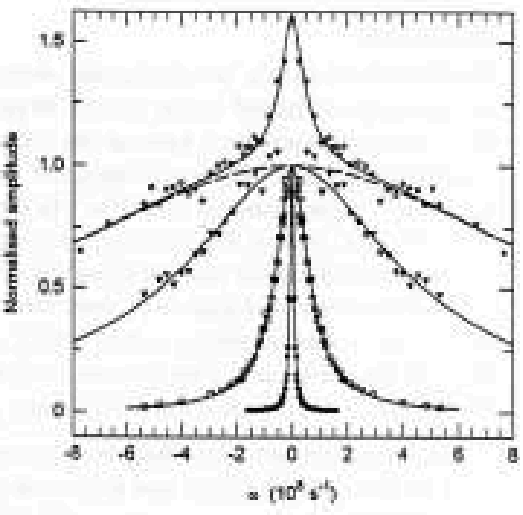

The high resolution of the field-cycling NMR technique has enabled us to measure the isotope effects associated with the nuclei of the heavy atoms, O and C, on the skeletal framework of the molecule. The proton transfer process involves displacements of these heavy atoms, in addition to the displacements of the proton in the hydrogen bond. The tunnelling rate is highly sensitive to the mass of the quasi-particle that is associated with the tunnelling co-ordinate, so this experiment is important in the context of the multi-dimensional description of the PES.

The effect of disorder in the crystals has been investigated using samples that are doped with low concentrations of substitutional impurities; the proton transfer dynamics and PES of dimers within the sphere of influence of the impurities were affected and measured. This experiment has provided insight into the tunnelling behaviour of two-level systems in disordered materials and, because it has been undertaken on a system that is well characterised in the pure form, it is important to the methodology, interpretation and development of field-cycling NMR in disordered systems.

Additional applications of Field-Cycling NMR Relaxometry to a variety of proton transfer systems will be discussed.

This work is supported by the EPSRC.

* Email address: A.Horsewill@nottingham.ac.uk

[1] H.-H. Limbach and J. Manz, Edts, 'Hydrogen Transfer: Experiment and Theory', Ber. Bunsenges. Phys. Chem. **102** (1998) pp. 298-586

[2] A.J. Horsewill, D.F. Brougham, R.I. Jenkinson, C.J. McGloin, H.P. Trommsdorff and M.R. Johnson, Ber. Bunsenges. Phys.Chem. **102** (1998) pp. 317-324

[3] D.F. Brougham, A.J. Horsewill and R.I. Jenkinson, Chem.Phys.Letters **272** (1997) pp. 69-74

Relaxometry of Paramagnetic Systems with other than Isotropic Zeeman Term in their Electron Spin Hamiltonian

C. Luchinat

Department of Soil Science and Plant Nutrition, University of Florence, P.le delle Cascine 28, 40144 Florence, Italy, and European Large Scale Facility on NMR of Paramagnetic Biomolecules PARABIO, University of Florence, Via G. Capponi 7, 50121, Florence, , Italy.
E-mail: luchinat@lrm.fi.cnr.it

The advantages of relaxometry (or nuclear magnetic relaxation dispersion, NMRD) as a tool are particularly pronounced for paramagnetic systems. This fact derives from the general feature that nuclear relaxation in a paramagnetic system is usually governed by a sum of spectral densities containing the nuclear as well as the electron Larmor frequencies. As the two associated dispersions are about three orders of magnitude far from one another, only field-cycling instruments, possibly supplemented by high-field instruments, permit to effectively cover both dispersions. The theory for nuclear relaxation in the presence of an electron spin Hamiltonian constituted solely by an isotropic Zeeman term has been developed by Solomon (1) for the dipolar interaction, Bloembergen for the contact interaction, (2) and Gueron (3) and Vega and Fiat (4) for the interaction with the time averaged electron magnetic moment. In many real cases, the electron spin Hamiltonian is more complicated, and the classical theory breaks down. This is expecially striking in slow-rotating systems, where the role played by other terms in the Hamiltonian, that are often anisotropic, is enhanced (5,6).

We have been interested for many years in biological macromolecules containing, or interacting with, paramagnetic metal ions, (7,8) and found that in no case the NMRD of these systems resembled the theoretical predictions. These observations prompted us to investigate the origin of the breakdown, and to develop the proper equations. The aim was to i) fill in the missing parts of the theory and ii) exploit NMRD to extract quantitative structural and electronic information on the biological systems of interest.

The various cases investigated will be presented according to the specific term in the electron spin Hamiltonian that needed to be introduced. First, the anisotropy of the g-factor will be discussed (9): this case had been considered in the early literature (10) but the treatment was not valid in the slow-motion limit. Hyperfine coupling with the metal nucleus itself if often present and generally important (9,11): both the isotropic and anisotropic cases have been developed (9). Then, the effect of static zero field splitting (ZFS) has been taken into account: a perturbative approach (ZFS >> Zeeman) valid for S=1 (12) has been initially followed and extended to S=3/2 (13,14) and larger (15) spin systems. Later, numerical programs were developed (16) to account for the whole NMRD profile through the region where ZFS << Zeeman. The program, in its present version, can calculate NMRD profiles of systems containing anisotropic Zeeman and both hyperfine and ZFS terms. More recently, the effect of ZFS has also been independently investigated by Sharp (17-20). Finally, the case of isotropic hyperfine coupling of the paramagnetic center with a second paramagnetic center has been worked out (21).

An important parameter in nuclear relaxation induced by paramagnetic centers is the electron spin relaxation time, τ_s, which, especially in slow-rotating systems, is often the relevant correlation time for the electron-nuclear interaction (5,6). Electron relaxation is also a complicated phenomenon per se: the early treatment of Blombergen and Morgan (22) of electron relaxation as caused by modulation of the quadratic transient ZFS showed that τ_s can be field-dependent. Rubinstein, Baram and Luz (23) then showed that for S > 1 systems more than one τ_s should be considered. Finally, Kowalewski et al. pointed out that the Redfield limit may not always hold for electron relaxation and consequently it may not be possible to even define τ_s under these conditions (24-26). A computer program that calculates nuclear relaxation in the

presence of both static and transient ZFS, that is valid beyond the Redfield limit has been developed by Kowalewski et al. (24-26). An early comparison of the Florence and the Stockholm programs showed that the two treatments were in agreement in the Redfield limit. Since then, efforts have been directed to define an effective τ_s that could be still used as a parameter outside the Redfield limit (27,28). Recent progress in this area will be illustrated (29).

Electron relaxation in dimetallic systems has also been addressed. The importance of dimetallic systems in biomolecules is increasingly recognized (30). We have developed a simple theoretical approach to estimate the alteration of τ_s of a metal when coupled to another metal, in the assumption of isotropic coupling and in the absence of other electron relaxation mechanisms that may become operative in the pair (31).

Bibliography

1. I. Solomon and N. Bloembergen, *J Chem Phys* **25**, 261 (1956).
2. N. Bloembergen, *J Chem Phys* **27**, 572 (1957).
3. M. Guéron, *J Magn Reson* **19**, 58 (1975).
4. A.J. Vega and D. Fiat, *Mol Phys* **31**, 347 (1976).
5. L. Banci, I. Bertini, and C. Luchinat, " Nuclear and electron relaxation. The magnetic nucleus-unpaired electron coupling in solution" VCH, 1991. Weinheim.
6. J. Kowalewski, L. Nordenskiöld, N. Benetis, and P.-O. Westlund, *Progr NMR Spectrosc* **17**, 141 (1985).
7. I. Bertini and C. Luchinat, " NMR of paramagnetic molecules in biological systems" Benjamin/Cummings, 1986. Menlo Park, CA.
8. I. Bertini and C. Luchinat, " NMR of paramagnetic substances" p. 1. Coord.Chem.Rev. 150, Elsevier, 1996. Amsterdam.
9. I. Bertini, F. Briganti, C. Luchinat, M. Mancini, and G. Spina, *J Magn Reson* **63**, 41 (1985).
10. H. Sternlicht, *J Chem Phys* **42**, 2250 (1965).
11. D. Pfeifer, D. Michel, D. Sames, and H. Sprinz, *Mol Phys* **11**, 591 (1966).
12. V.U. Lindner, *Ann Phys* **16**, 319 (1965).
13. I. Bertini, C. Luchinat, M. Mancini, and G. Spina, *J Magn Reson* **59**, 213 (1984).
14. I. Bertini, C. Luchinat, and K.V. Vasavada, *J Magn Reson* **89**, 243 (1990).
15. L. Banci, I. Bertini, F. Briganti, and C. Luchinat, *J Magn Reson* **66**, 58 (1986).
16. I. Bertini, O. Galas, C. Luchinat, and G. Parigi, *J Magn Reson Ser A* **113**, 151 (1995).
17. R.R. Sharp, *J Chem Phys* **98**, 2507 (1993).
18. T. Baybutt and R.R. Sharp, *J Chem Phys* **92**, 5892 (1990).
19. R.R. Sharp, *J Magn Reson* **100**, 491 (1992).
20. R.R. Sharp, *J Chem Phys* **98**, 912 (1993).
21. I. Bertini, G. Lanini, C. Luchinat, M. Mancini, and G. Spina, *J Magn Reson* **63**, 56 (1985).
22. N. Bloembergen and L.O. Morgan, *J Chem Phys* **34**, 842 (1961).
23. M. Rubinstein, A. Baram, and Z. Luz, *Mol Phys* **20**, 67 (1971).
24. I. Bertini, C. Luchinat, and J. Kowalewski, *J Magn Reson* **62**, 215 (1985).
25. J. Kowalewski, T. Larsson, and P.-O. Westlund, *J Magn Reson* **74**, 56 (1987).
26. N. Benetis, J. Kowalewski, L. Nordenskiöld, Wennerstrom, and P.-O. Westlund, *Mol Phys* **48**, 2 (1983).
27. S.M. Abernathy and R.R. Sharp, *J Chem Phys* **106**, 9032 (1997).
28. P.-O. Westlund, *J Chem Phys* (1998).(in press)
29. I. Bertini, J. Kowalewski, C. Luchinat, T. Nilsson, and G. Parigi, " Nuclear spin relaxation in paramagnetic complexes of low symmetry. A comparison of different models" 1998.(UnPub)
30. Clementi, V and C. Luchinat, *Accounts of Chemical Research* (1998).(in press)
31. I. Bertini, O. Galas, C. Luchinat, G. Parigi, and G. Spina, *J Magn Reson* **130**, 33 (1998)

^{14}N NQR STUDIES IN THERMOTROPIC LIQUID CRYSTALS: T_1 QUADRUPOLE DIPS AND DOUBLE RESONANCE§

D.J. Pusiol† and E. Anoardo‡

Facultad de Matemática, Astronomía y Física, Universidad Nacional de Córdoba, Ciudad Universitaria, 5000 Córdoba, Argentina - e-mail: pusiol@fis.uncor.edu -.

Nuclear Quadrupole Resonance (NQR) spectrum in Liquid Crystals (LCs) has been established to be a powerful technique for studying local molecular ordering [1, 2]. The main advantage is due to the easy identification of the NQR nuclei spectrum in comparison with the always complex proton NMR spectra. Conventional NQR experiments in liquid crystalline mesophases have been up to now unsuccessful mainly because: *i)* the relative low abundance of quadrupole nuclei even in the simplest LC molecules, and *ii)* the strong averaging of the electric field gradients (EFGs) at the quadrupole sites. However, NQR has been indirectly measured via two similar proton Zeeman-quadrupole cross relaxation techniques: *i.e.*, *i)* by crossover relaxation in the laboratory frame at a fixed relaxation period (COR) [1] and *ii)* by the quadrupole dips in the spin-lattice relaxometry (QDs) [3, 4, 5, 6]. In both techniques the Zeeman magnetic field is scanned over a range wide enough to overlap both the quadrupole and the Zeeman spin systems. Consequently, the NQR spectrum reconstructed from the QD minima is distorted by the Zeeman field. In solids the unperturbed NQR spectrum can be alternatively recorded from the zero-field Nuclear Quadrupole Double Resonance (NQDOR) technique [7]. The experiment involves both Fast Field Cycling NMR of protons together with the irradiation of the quadrupole ^{14}N nuclei by means of a second radiofrequency just during the period of zero-magnetic field. As dipolar interaction between protons and nitrogens is quenched at zero field, we used the spin mixing by level crossing (LCNQDOR) procedure [8]. In our knowledgement NQDOR was not previously carried out in a non-solid material.

The phenomenon, referred to as QD is due to a resonant effect occurring when the Zeeman levels of a spin specie (^1H) and the combined quadrupolar and Zeeman levels of a quadrupolar spin system (for instance, ^{14}N or ^2H) match. Compared with protons, quadrupolar nuclei are in general strongly coupled to the lattice and their spin-lattice relaxation rate is much faster. A net flow of energy takes place from protons to quadrupolar nuclei and then to the lattice. The consequence of this resonant process is an increment in the proton relaxation rate. This effect produces a dip in the proton $T_1(\nu)$ dispersion profile. In the case of spin $I = 1$ nuclei sensing an EFG with non-zero asymmetry parameter, three QD are generally expected: one at low frequency and a doublet at higher frequency. The dips have been previously observed in polyvinyl chloride [9], plastic crystalline phases of $CFCl_2CFCl_2$ [10], hydrated solid proteins, polypeptides, DNA, some living systems [11].

LCNQDOR combine electronically fast field cycling and two different radiofrecuency excitations of the sample. The experiment consist on three different phases: polarization of the sample, irradiation of quadrupole transitions at zero-field and detection of proton nuclear magnetic resonance (NMR) signal. During polarization the spin system is allowed to reach thermal equilibrium with the high magnetic field at the lattice temperature. In a second step, the external field is adiabatically switched off, and an allowed ^{14}N quadrupole transition is irradiated with a pulsed radiofrequency. If the RF pulse frequency is coincident with the quadrupole transition one, this can be saturated. The irradiation period might be of course shorter than proton T_1 at zero field. At the end of this phase, the RF pulse is switched off and the magnetic field is switched on again. During raising and lowering of the external field, all ^{14}N quadrupole transitions are "level crossed" by the Zeeman splitting, and thermal contact between the different spin systems takes place.

Thermal contact can be very effective in spite of the occurrence of multiple quantum transitions in addition to the single ones. When this happens, polarization is transferred from one spin system to the other. If a quadrupole transition is saturated, proton spin polarization is partially destroyed when switching on the field, and in consequence, the proton NMR signal at high field during the detection step will be smaller than without the quadrupole level saturation.

The fast field cycling NMR spectrometer (FFC) is based on a specially designed air cored 0.5 T low resistance electromagnet. The electronics of the magnetic field switch and control was entirely home-made in our Laboratory [12].ansar95. Additional pulsed coils are used for shimming the detection magnetic field. The earth magnetic field is compensated by an external pair of dc driven Helmholtz coils. The relaxation field B_r was tested by means of a double resonance experiment in a sample of water where no QD takes place. During the relaxation period, the water is irradiated with a second rf pulse of frequency ν_r. Absorption of the second frecuency is produced just as the relation $\gamma B_r = \nu_r$ is met. The quantity $\gamma \Delta\nu_r$, which is extracted from the rf absorption at ν_r, is conveniently scanned giving us a measure of the B_r dispersion. In the frequency range of our interest we have for instance a dispersion in B_r of approximately 0.5% (at $\nu_r = 400\,\mathrm{kHz}$) and 0.1 % (at $\nu_r = 2\,\mathrm{MHz}$) respectively. Very fine adjustments of the B_r electronic control were necessary before reaching the final performance. The double resonance spectrometer is a modified version of our homemade Fast Field Cycling relaxometer. The same rf coil is used for irradiation at both ν_l and ν_r. A reed relay bank connects that coil with the respective high and low frequency resonant circuits.

Careful measurements of $T_1(\nu)$ at the Larmor frequency range from 3 kHz to 4 Mhz in the Smectic C and Nematic mesophases of 4-4'-bis-heptyloxy-azoxy-benzene. Arizing from the QDs positions in the relaxometry profile, perturbed quadrupole spectra were recorded at several temperatures. In addition, zero-field homologous were also adquired by means of the LCNQDOR technique. Making the Zeeman perturbation reductions, spectra obtained by the two techniques match very well. Three chemically inequivalent Nitrogen nuclei have been detected, denoting the existence of two non-equivalent molecules. We conclude that a bimolecular (dimeric) structure can be asociated with the elemental liquid crystalline unit [14, 15, 16].

References

[1] J. Seliger, R. Osredkar, V. Žagar and R. Blinc, *Phys. Rev. Lett.* **38**, 411 (1977).

[2] R. Blinc, J. Dolinsek, M. Luzar and J. Seliger, *Liq. Cryst.* **3**, 663 (1988).

[3] D. Pusiol and F. Noack, *Proc. 10th AMPERE Summer School*, R. Blinc, M. Vilfan and J. Slak Ed., Portorož (1988).

[4] D. Pusiol and F. Noack, *Liq. Cryst.* **5**, 377 (1989).

[5] D. Pusiol, R. Humpfer and F. Noack, *Z. Naturforsh.* **47a**, 1105 (1992).

[6] E. Anoardo, D. Pusiol and C. Aguilera, *Phys. Rev.* **B49**, 9600 (1994).

[7] D. T. Edmonds, *Physics Reports* **29**, 233 (1977).

[8] G. W. Leppelmeier and E. L. Hahn, *Phys. Rev.* **141**, 724 (1966).

[9] F. Winter and R. Kimmich, *Mol. Phys.*, **45**, 33 (1982).

[10] H.T. Stoker, T.A. Case, D.A. Aillion and C.H. Wang, *J. Chem. Phys.*, **70**, 3563 (1979).

[11] R. Kimmich, F. Winter, W. Nusser and K.-H. Spohn, *J. Magn. Reson.*, **68**, 263 (1986).

[12] E. Anoardo, Thesis, Universidad Nacional de Córdoba (1996).

[13] E. Anoardo, E.A. Romero, W. Zanimetti, C.A. Marquéz y D. Pusiol, *Rev. Fis. Appl. e Instrum. (Brasil)*, **20**, 55 (1995).

[14] E. Anoardo and D.J. Pusiol, *Phys. Rev. Lett.* **76**, 3983 (1996).

[15] E. Anoardo y D.J. Pusiol, *Phys. Rev. E*, **55**, 7079 (1997).

[16] E. Anoardo y D.J. Pusiol, *Phys. Rev. B*, **56**, 2348 (1997).

---

§Partially financed by Fundación Antorchas, CONICOR and CONICET of Argentina.
†Holder of a Fellowship from the National Research Council, CONICET.
‡Fellow of CONICET

Deuterium nuclear quadrupole resonance dips in the proton spin relaxation dispersion of deuterated liquid crystals

J. Struppe[†], T Liesener, F. Noack.
Physikalisches Institut der Universität Stuttgart, D-70550 Stuttgart, Germany
[†] Department of Chemistry and Biochemistry, University of California San Diego, La Jolla Ca. 92093, USA

M. Vilfan
J. Stefan Institute, University of Ljubljana, 6111 Ljubljana, Slovenia

The Proton spin relaxation of selectively deuterated nematic liquid crystals like 5CB-$d_{2,\alpha}$ reveals at very low Larmor frequencies (20 –50 kHz) resonant proton deuterium couplings ("quadrupole dips"), where both spin systems exchange energy. Similar effects were previously observed at much higher Larmor frequencies (50 – 500 kHz) for non-deuterated liquid crystals with nitrogen bonds and ascribed to a resonant proton – nitrogen interaction. The analysis of the ^{2}H-^{1}H dips in comparison with the ^{14}N-^{1}H dips [1,2] demonstrates however, that the main mechanism responsible for the number of resonances is quite different in both systems. It is the dipolar line splitting $\Delta\nu$ in the case of deuterium [3] and the asymmetry η of the electric field gradient at the bond in the case of nitrogen, respectively. The angular dependence of these dips should support this finding. A final analysis however, has not been done yet.

[1] D. Pusiol and F. Noack, Liquid Crystals 5, 377 (1989).
[2] D. Pusiol, R. Humpfer and F. Noack, Z. Naturforsch. 47a, 1105 (1992).
[3] Th. Liesener, Diplomarbeit, Uni-Stuttgart (1993).

Spin-lattice relaxation dispersion in polymer melts and chain dynamics

N. Fatkullin

Department of Molecular Physics, Kazan State University, Kremlevskaya-st. 18,
420008 Kazan, Tatarstan/Russia
e-mail: nail.fatkullin@ksu.ru

The well-known and most influential tube/reptation model predicts a frequency dependence of the spin-lattice relaxation time $T_1 \propto \omega^{-3/4}$ in entangled polymer melts in the wide frequency range $\tau_s^{-1} \gg \omega \gg \tau_R^{-1}$, where τ_s is the segmental relaxation time, $\tau_R = \tau_s N^2$ is the Rouse relaxation time, N is the number of Kuhn segments per chain [1]. This power-law dependence has never been observed in NMR relaxation experiments [2 – 5], despite the broad frequency range accessible with existing experimental techniques: $\omega/2\pi = 10^2 - 10^8$ Hz. Typical attempts to explain this situation are the following: "When a monomer goes back and forth, and comes back to its original position, it recovers the original alignment if the tube is very narrow (say 3 Å diameter). This would then lead to interesting memory effects. Unfortunately, the tubes are much wider (~ 50 Å). Then the alignment upon return is completely decoupled from the original alignment. The low ω features (of NMR) do not reflect reptation" [6]. Briefly speaking, the T_1-dispersion does not reveal global chain dynamics.

The main experimental support for the reptation model comes from neutron spin echo (NSE) techniques, dealing with a time window of 1 – 20 ns [7], which is adequate for the crossover region from Rouse behavior to entangled dynamics. The T_1-dispersion time/frequency window is evidently much broader than that of NSE. It seems to be extremely surprising that NMR T_1-dispersion could not see what NSE can see. In our presentation, this situation is discussed in detail. We argue that NMR T_1 relaxation experiments have important advantages compared to other techniques for the following reasons:

1. For frequencies $\omega T_1 \gg 1$, corresponding to $T_1 \geq 10^{-2}$ s as a rule, the approximation of short correlation times is applicable with high accuracy. This provides theoretically well-defined expressions for the spin-lattice relaxation rate T_1^{-1}.

2. For temperatures of interest $T \gg 10^{-3}$ K, due to weak interactions of spins with an external magnetic field and with each other as compared to the thermal energy, the high-temperature approximation with respect to spin variables works with an extremely high accuracy. This allows to describe T_1^{-1} in terms of dynamical pair correlation functions, which are the simplest ones for theoretical interpretations.

3. The existence of intra- and interchain dipole-dipole interaction contributions to T_1^{-1} allows, in principle, the investigation of single chain and two-chain dynamical correlations separately using deuteron NMR techniques.

Moreover, recently we formulated the Twice Renormalized Rouse Model which perfectly describes NMR properties of entangled polymer melts [8].

Financial support by Deutsche Forschungsgemeinschaft and Russian Fond of Fundamental Research (grant N 98-03-3307a) is gratefully acknowledged.

References

[1] P. G. de Gennes, J. Chem. Phys. (1971) **55**, 572.

[2] H. W. Weber and R. Kimmich, Macromolecules (1993) **26**, 2597.

[3] N. Fatkullin, R. Kimmich and H. W. Weber, Phys. Rev. E (1993) **47**, 4600.

[4] N. Fatkullin and R. Kimmich, J. Chem. Phys. (1994) **101**, 822.

[5] R. Kimmich, N. Fatkullin, R.-O. Seitter, and K. Gille, J. Chem. Phys. (1998) **108**, 2173.

[6] P. G. de Gennes (private communication)

[7] B. Ewen, D. Richter, Adv. in Polym. Sci., (1977) **134**, 3.

[8] N. Fatkullin, R. Kimmich, and M. Krout'eva, J. Chem. Phys. (submitted)

Theoretical Aspects of Relaxation Dispersion in Complex Biological Systems

Bertil Halle, Stefan Gustafsson, Per-Ola Quist, Haukur Jóhannesson and Kandadai Venu

Condensed Matter Magnetic Resonance Group, Department of Chemistry,
Lund University, P.O. Box 124, S-22100 Lund, Sweden
E-mail: bertil.halle@fkem2.lth.se

Nuclear magnetic relaxation dispersion (NMRD) measurements can provide valuable information about the dynamics and structure of complex biological systems such as dense macromolecular solutions, fluid bilayer membranes, and tissues. Within the motional-narrowing regime, the available information is contained in one (isotropic fluids) or several (anisotropic fluids) *spectral density functions* (SDFs). In the strongly coupled systems considered here, the SDF is usually non-Lorentzian with the dispersion extending over several decades. Although such stretched dispersions can be measured by the fast field cycling (FFC) technique, their interpretation in terms of microscopic interactions, structure, and dynamics can be highly nontrivial. This lecture addresses three aspects of the interpretation problem. In each case, new theoretical results are presented and applied to NMRD data.

- A model-free approach is presented for analyzing stretched relaxation dispersion profiles in situations where a microscopic model is not (yet) available. A major advantage of this approach is the unambiguous separation of the equilibrium and dynamic information content of the SDF.
- A theoretical description is presented of spin relaxation induced by elastic distortions in a multilamellar stack of fluid membranes. In particular, it is shown how the subtle effects of orientational correlations and membrane coupling give rise to the well-known $1/\omega$ dispersion.
- A non-perturbative theory of spin relaxation in semisolid systems is described that is valid under conditions where the standard motional-narrowing theory breaks down. This theory is relevant for understanding the molecular basis of soft tissue contrast in clinical magnetic resonance imaging (MRI).

Model-Free Analysis of Stretched Relaxation Dispersions [1]

In water ^{1}H NMRD studies of concentrated protein solutions, the relaxation dispersion often extends over a wide frequency range and therefore cannot be described by a Lorentzian SDF. A *model-free approach* for analyzing such *stretched dispersion profiles* is described. Unlike the usual empirical fitting procedures, the model-free approach is based on rigorous theory and produces parameters with well-defined physical significance. The model-free approach is validated with the aid of synthetic relaxation data, showing that it is robust and accurate, and is then applied to new water ^{1}H NMRD data from solutions of the protein bovine pancreatic trypsin inhibitor (BPTI). By *separating the static and dynamic information content* of the NMRD data, the model-free analysis shows that the dramatic salt effect observed in BPTI solutions is due almost entirely to a slowing down of protein rotation with little change of protein structure. An analysis of the same data in terms of an empirical dispersion function, first introduced by Hallenga and Koenig, leads to a qualitatively different picture. It is demonstrated that this widely used dispersion function is unphysical and that its parameters do not have the physical meaning usually ascribed to them.

Relaxation Dispersion in Lamellar Fluid Membrane Phases [2-4]

The orientation and frequency dependence of nuclear spin relaxation rates can provide detailed information about the amplitudes and rates of *collective orientational fluctuations* (director fluctuations) in liquid crystals. In particular, the low-frequency relaxation dispersion from a lamellar phase of fluid bilayers reflects the *membrane bending rigidity* and the *intermembrane forces*. Such data have usually been analyzed in terms of an effectively *two-dimensional* membrane model, which ignores the mutual

coupling of the individual membranes. A theory of spin relaxation induced by small-amplitude, long-wavelength elastic distortions in a multilamellar stack of fluid membranes is presented. This theory shows that *membrane coupling can profoundly affect the spin relaxation behavior* via its effect on the amplitudes and rates of membrane distortion modes. A physical basis for the resulting, rather intricate, spin relaxation behavior is provided by analyzing the spatial correlation function for the local membrane orientation. We find that the decay of this function involves two correlation lengths: one is related to interactions with the two adjacent membranes and the other reflects the coherent fluctuation modes in the entire membrane stack. This analysis explains why the time correlation function has the asymptotic form $1/t^2$, rather than $1/\tau$ as expected for a two-dimensional system. The new theory is applied to published ^{2}H and ^{31}P relaxation data from phospholipid bilayer membranes and to new ^{23}Na relaxation data from a sterically stabilized lamellar phase.

Stochastic Theory of Relaxation Dispersion in Semisolid Systems [5,6]
In isotropic solutions of biomolecules (of MW < ca. 1 MDa), all orientation-dependent spin couplings are averaged to zero by biomolecule tumbling at a rate exceeding the anisotropic coupling frequencies. Since the biomolecules in a semisolid material are not free to tumble (or do so very slowly), orientational randomization of spin couplings in internal water molecules (and labile hydrogens) is brought about by *exchange* into the bulk water phase. If the exchange rate is comparable to the residual coupling, however, the conventional second-order perturbation theory of spin relaxation breaks down and a more general (non-perturbative) theory must be used. Starting from the *stochastic Liouville equation*, a *generalized spectral density function* is derived that describes the relaxation dispersion under such conditions. If there is a broad distribution of exchange rates (as expected for proteins), the ^{2}H relaxation dispersion will be dominated by water molecules with exchange rates comparable to the (residual) quadrupole coupling frequency. *The (apparent) correlation time derived from the dispersion profile is then determined by the nuclear quadrupole frequency*, which is independent of temperature and protein structure. This behavior has been observed with chemically cross-linked and with highly concentrated protein solutions. Similar considerations apply to dipolar ^{1}H relaxation in semisolid systems, and are thus important for understanding *relaxation-based contrast* in MRI images of soft tissues.

References

[1] B. Halle, H. Jóhannesson & K. Venu, Model-free analysis of stretched relaxation dispersions, *J. Magn. Reson.*, in press.

[2] B. Halle & S. Gustafsson, Orientational correlations and spin relaxation in lamellar fluid membrane phases, *Phys. Rev. E* **56**, 690–707 (1997).

[3] S. Gustafsson & B. Halle, Spin relaxation by collective director fluctuations and molecular diffusion in lamellar phases. Continuum theory of relaxation anisotropy and dispersion, *J. Chem. Phys.* **106**, 9337–9352 (1997).

[4] P.-O. Quist & B. Halle, Fluid membrane interactions probed by nuclear spin relaxation, *Phys. Rev. Lett.* **78**, 3689–3692 (1997).

[5] B. Halle, Spin dynamics of exchanging quadrupolar nuclei in locally anisotropic systems, *Progr. NMR Spectrosc.* **28**, 137–159 (1996).

[6] B. Halle & V. P. Denisov, A new view of water dynamics in immobilized proteins, *Biophys. J.* **69**, 242–249 (1995).

Molecular Dynamics of Microconfined Liquid Crystals Studied by Field-Cycling NMR Relaxometry and the Dipolar-Correlation Effect

F. Grinberg, R. Kimmich and S. Stapf
Sektion Kernresonanzspektroskopie, Universitaet Ulm, 89069 Ulm, Germany
e-mail: farida.grinberg@physik.uni-ulm.de

Confinements by pores produce strong effects on order and dynamics of collective molecular motions in liquid crystals. Field-cycling NMR-relaxometry[1] allows one to probe orientational director fluctuations (ODF) which represent a significant mechanism of spin-lattice relaxation of liquid crystals[2] at frequencies below $10^5 - 10^6$ Hz. The low-frequency scale accessible by this method however ends at a few KHz. Recently, a new technique based on the dipolar-correlation effect[1,2] (DCE) on the stimulated echo has been suggested allowing one to monitor slow dipolar correlations on the time scale from $\approx 10^{-4}$ s up to the order of spin-lattice relaxation times. The low frequency range of the field-cycling relaxometry can thus be extended by additional 3 orders. In this work we report the application of the field-cycling NMR-relaxometry and the DCE to studies of ordering effects and slow director fluctuations in a nematic liquid crystal 4'-n-pentyl-4-cyanobiphenyl (5CB) confined in porous glasses.

Figure 1 shows frequency (ν) dependences of the spin-lattice relaxation time (T_1) of 5CB in bulk and confined in Bioran glasses with pore diameters 30, 70 and 200 nm. The data refer to 303 K and 316 K. Above the isotropization temperature (T_c = 308.5 K), only flat dispersions were observed both in bulk and confined samples. Below T_c, a square-root term characteristic for three-dimensional ODF dominates the spin-lattice relaxation of bulk 5CB in the low-frequency range[4]. Dispersion curves of confined samples exhibit sudden sharp changes from $\nu^{\frac{1}{2}}$ towards ν^2-law at frequencies below the MHz-range. These changes cannot be ascribed to local field effects, which under certain circumstances may mask contributions of dynamical processes to spin-lattice relaxation at low frequencies. This conclusion is based on spectral linewidths of the confined samples increasing with pore diameters from 5000 Hz at 30 nm to 7000 Hz at 200 nm. If local field effects were relevant they would become stronger (or at least not weaker) at higher frequencies for bigger pores. However, the finding is that the deviations from the square-root law appear rather at lower frequences for bigger pores. The observed behaviour of T_1-dispersion curves in confined samples must therefore originate from the lack of long wavelength fluctuations in the ODF spectrum due to finite pore sizes. However, abrupt cut-offs imposed by pores, that is, the absence of any fluctuation modes with wavelengths bigger than the pore size, would result in low-frequency plateaus of the dispersion curves. In the investigated samples, instead, a clear tendency towards the ν^2-law typical for single-correlation-time processes was observed. This indicates that one or a few fluctuation modes survive at the low-frequency end of the spectrum of director fluctuation modes.

The modes below 10^4 Hz reveal themselves in the DCE-studies, as shown in Fig. 2. The experimentally measured quantity is the quotient of the stimulated and the primary echoes[3] as a function of the time interval (τ_1) in the standard three 90^0-pulse sequence $\pi/2 - \tau_1 - \pi/2 - \tau_2 - \pi/2$. Above T_c, the quotient of all bulk and confined samples equals a constant value independent on τ_1, as expected for isotropic liquids, where dipolar interactions are averaged out by fast stochastic motions. Below T_c, the attenuation curves reflect director fluctuations on the time scale of the interpulse spacings. The attenuation rate of the quotient exhibits a strong dependence on the pore size. It is determined by the mean squared fluctuation of the dipolar coupling constant characterising the distribution of director fluctuation modes[5]. The mean squared fluctuation decreases exponentially with decreasing mean pore diameter.

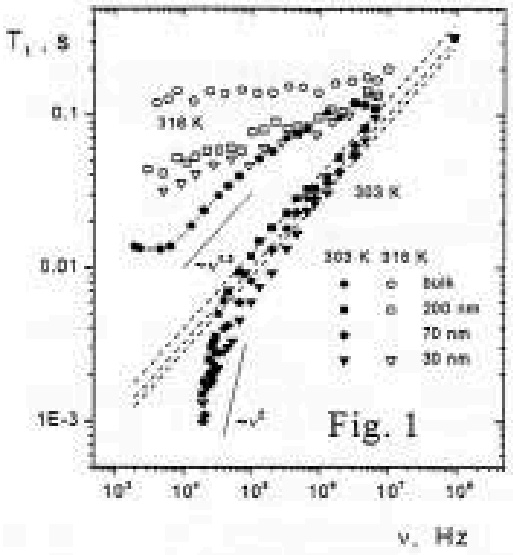

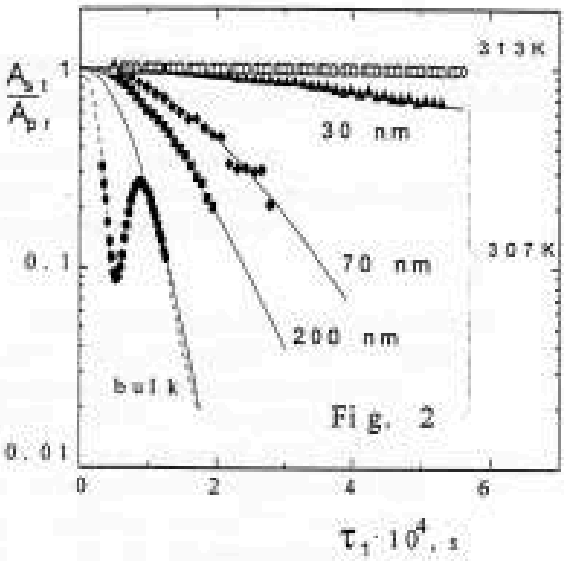

Fig. 1. Frequency dependences of the spin-lattice relaxation time of 5CB in bulk and when confined in Bioran glasses with pore diameters 200 nm, 70 nm and 30 nm. Filled symbols refer to the nematic state at 303 K, open symbols refer to an isotropic state at 316 K. Straight lines serve as guides for the readers eye.

Fig. 2. The quotient of stimulated and the primary echo amplitudes of bulk 5CB and when confined in Bioran glasses in dependence on τ_1. Filled symbols refer to the nematic state at 307 K. Open symbols refer to a temperature above T_c.

This reflects the decrease of director fluctuations caused by surface interactions which dictate fixed local orientations of the molecules and thus hinder spontaneous fluctuations. The critical mean pore size for the onset of bulk behaviour was found to be of the order of 120 nm.

In the isotropic state, pronounced differences were observed for pore diameters ≤ 10 nm compared to that in bigger pores. Experimental results in samples with $d \geq 30$ nm are typical for those of isotropic liquids, that is, the constant values of the quotient of stimulated and primary echoes as function of τ_1 and only minor dispersions of spin-lattice relaxation rates were observed. Strong frequency dependences, $T_1(\nu)$, appear when $d \leq 10$ nm. In the same samples, the stimulated echo amplitudes become modulated due to a spin exchange between inequivalent protons. These phenomena are discussed from the view point of molecular ordering at the pore walls.

References

1. R. Kimmich, NMR: Tomography, Diffusometry, Relaxometry. Heidelberg: Springer-Verlag, 1997.
2. F. Noack, M. Notter, W. Weiss, Relaxation dispersion and zero-field spectroscopy of thermotropic and lyotropic liquid crystals by fast field-cycling NMR. *Liquid Crystals* **3**, 907-925, (1988).
3. F. Grinberg, R. Kimmich, Characterization of order fluctuations in liquid crystals by the dipolar-correlation effect of the stimulated echo. *J. Chem. Phys.* **103**, 365-370, (1995).
4. R. Köllner, K. H. Schweikert, F. Noack, NMR field-cycling study of proton and deuteron spin relaxation in the nematic liquid crystal 4'-n-pentyl-4-cyanobiphenyl. *Liquid Crystals* **13**, 483-498, (1993).
5. F. Grinberg, R. Kimmich, Pore size dependence of the dipolar-correlation effect on the stimulated echo in liquid crystals confined in porous glass. *J. Chem. Phys.* **105**, 3301-3306, (1996).

Nuclear Magnetic Relaxation Through Director Fluctuations in Anisotropic Media

K. Venu and V.S.S. Sastry
University of Hyderabad, School of Physics, Hyderabad 500 046, India
e-mail : kvsp@uohyd.ernet.in

Introduction :

Field Cycling NMR (FCNMR) spectroscopy permits detailed study of magnetic relaxation dispersion (NMRD) at very low (kHz) frequencies with typical nuclei like proton and deuterium [1, 2]. Slow processes in liquid crystals like the fluctuations of order director, smectic order, etc., dominate the low frequency regions of spectral density of molecular dynamics, and FCNMR is now an established tool to investigate them [3]. The application of the existing theoretical formalism [4, 5] to extract useful information on visco-elastic properties of this medium, however, requires certain improvements. The initial model for the evaluation of the contribution to nuclear magnetic relaxation rate (R_{1DF}) from the nematic director (DF) fluctuations based on the single (elastic) constant approximation [6] was refined in two ways: (1) introduction of anisotropy of visco-elastic constants, however incorporating only the upper cut-off frequencies for the DF modes [5]; and (2) introduction of both lower and upper cut-off frequencies, but within the single constant approximation [6]. These modifications describe DF adequately in two situations : (1) NMRD in many nematics for which visco-elastic properties are nearly isotropic; and (2) NMRD in the high frequency region available from conventional spectrometers. The situation is typically more complex in nematics with underlying smectic phases : the visco-elastic properties are perceptibly more anisotropic on one hand; and the presence of cybotactic clusters (smectic organisations) may impose restrictions on the DF modes leading to the upper and lower cut-off frequencies. In this context, this work is concerned with the evaluation of R_{1DF} incorporating these two effects, and the present results are compared with earlier models through simulations. This analysis is demonstrated with the NMRD data (obtained with our FCNMR facility) on a binary liquid mixture with an interesting phase diagram (having variable nematic and smectic stabilities) [7].

Evaluation of R_{1DF} :

The relaxation rate for Zeeman order R_{1DF} is proportional to the spectral density $J_1(\omega)$ for small angle director fluctuations, given by (with the notation of [4, 5])

$$J_1(\omega) = C_1(\Delta)\sum_{\alpha=1}^{2}\eta_\alpha \int_{q_{z\omega}}^{q_{z\max}} dq_z \int_{q_{\perp\omega}}^{q_{\perp\max}\left[1-\left(\frac{\eta_z}{\eta_{\max}}\right)^2\right]^{1/4}} \frac{q_\perp dq_\perp}{(K_\alpha q_\perp^2 + K_3 q_z^2)^2 + \omega^2\eta_\alpha^2} \qquad \ldots(1)$$

which, upon integration, leads to

$$J_1(\omega) = C_1(\Delta)\sum_{\alpha}\frac{\sqrt{\eta_\alpha}}{K_\alpha\sqrt{K_3}\sqrt{\rho\omega}}\left[f(D_{\omega},A_{\omega}) - f(D_{\omega},A_{z\omega}) - f(B_{\omega},A_{\omega}) + f(B_{\omega},A_{z\omega})\right] \qquad \ldots(2)$$

where

$$f(D,A) = B\tan^{-1}\left(D^2 + A^2\right) + \frac{B\sqrt{\sqrt{1+A^4}+A^2}}{2\sqrt{2}D}\ln\left|\frac{\sqrt{1+A^4}+\sqrt{2}\sqrt{\sqrt{1+A^4}-A^2}\;D+D^2}{\sqrt{1+A^4}-\sqrt{2}\sqrt{\sqrt{1+A^4}-A^2}\;D+D^2}\right| \qquad \ldots(3)$$

$$-\frac{B_z\sqrt{\sqrt{1+A^4}-A^2}}{\sqrt{2}D}\left\{\tan^{-1}\left(\frac{\sqrt{2}D-\sqrt{\sqrt{1+A^4}-A^2}}{\sqrt{\sqrt{1+A^4}+A^2}}\right)+\tan^{-1}\left(\frac{\sqrt{2}D+\sqrt{\sqrt{1+A^4}-A^2}}{\sqrt{\sqrt{1+A^4}+A^2}}\right)\right\}$$

and $f(B,A)$'s can be obtained by replacing D by B in Eqn.(3).

Here

$$D_{ab}^2 = B_{ab}^2 - A_{ab}^2 \ , \ D_{al}^2 = B_{al}^2 - A_{ab}^2\left(\frac{q_{\perp al}}{q_{\perp ah}}\right)^2$$

$$A_{ab(l)}^2 = \frac{K_a q_{\perp ah(l)}^2}{\omega \eta_a} \ , \ B_{ab(l)}^2 = \frac{K_a q_{\perp ah(l)}^2}{\omega \eta_a}$$

and $q_{\perp ah(l)} = \dfrac{2\pi}{\lambda_{\perp al(h)}}$ and $q_{\perp ah(l)} = \dfrac{2\pi}{\lambda_{\perp al(h)}}$

where $\lambda_{\perp ah(l)}$ and $\lambda_{\perp al(h)}$ are the upper (lower) cut off wave length of DF modes along and in the perpendicular directions of the director respectively with the corresponding cut off frequencies given by

$$\nu_{\perp ah(l)a} = \frac{K_a q_{\perp ah(l)}^2}{2\pi\eta_a} \quad \text{and} \quad \nu_{\perp al(h)a} = \frac{K_a q_{\perp al(h)}^2}{2\pi\eta_a}$$

$$C_1(\Delta) = f(\Delta)\frac{2S^2 k_B T}{(2\pi)^2}$$ where $f(\Delta)$ describes the angular dependence [4].

This expression reduces to the earlier results in appropriate limits.

Discussion :

The principal difference between the Eqn.2 and similar expression obtained earlier [5] (where DF modes were assumed to be extending down to zero frequency) is in the two terms involving low frequency cut-off. Effect of incorporating the low frequency cut-off is demonstrated by computing data from Eqn.2 with $K_a = 10^{-6}$ dyn, $\eta_a = 0.5$ P, $\lambda_{\perp al} = \lambda_{\parallel al} = 30$Å, $\lambda_{\perp ah} = \lambda_{\parallel ah} = 1\text{x}10^4$Å, $C = 5\text{x}10^{-3}$ s$^{3/2}$ and for different values of K_s in the range of 10^{-12} to 10^{-5} dyn (Fig.1). Here $J_1(\omega)$ varies as $\nu^{-1/2}$ ($\omega = 2\pi\nu$ where ν is Larmor frequency) between upper (140 MHz) and lower (1.3 kHz) cut-off frequencies for isotropic case ($K_s = 10^{-6}$ dyn). Above the upper cut-off frequency $J_1(\omega)$ varies as ν^{-2} whereas it is essentially independent of frequency below lower cut-off frequency. As K_s increases $\nu_{\parallel ah}$ increases, but $\nu_{\perp ah}$ remains the same leaving the effective upper cut-off to be still 140 MHz. On the other hand, $\nu_{\parallel al}$ also increases, thus effectively increasing the lower cut-off frequency, as seen from the flat region extending to higher frequencies (cutting down $\nu^{-1/2}$ region). Similar effects are seen in Fig.2 as well. These plots are for K_s fixed at 10^{-5} dyn and $\lambda_{\perp ah} = \lambda_{\parallel ah} = 5\text{x}10^3$Å, and $\lambda_{\parallel al} = \lambda_{\perp al}$ is varied from 5 - $5\text{x}10^4$ Å. Here

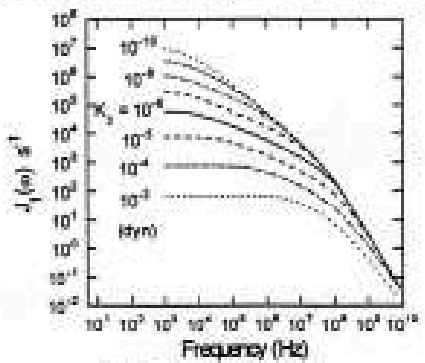

Figure 1.

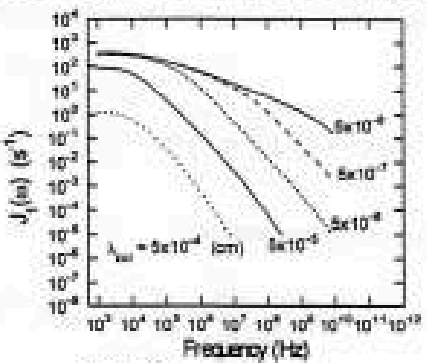

Figure 2.

$\nu_{\parallel al}$ (32 kHz) is four orders of magnitude larger than $\nu_{\perp al}$ and hence $\nu_{\parallel al}$ is the effective lower cut-off frequency. Now as λ_{al} is increased the upper cut-off frequencies reduce, shrinking the $\nu^{-1/2}$ region. This suggests the possibility of observing $J_1(\omega)$ which starts with practically no frequency dependence at very low frequencies, moving over to a ν^{-2} dependence without ever showing $\nu^{-1/2}$ dependence as the

Larmor frequency increases. This could be a feasible scenario, for example, in a nematic having an underlying smectic phase, with substantial increase in K_3 and containing cybotactic clusters which effectively increase the lower cut-off wavelengths.

Analysis of Experimental Data :

This analysis is applied to the proton R_1 data measured earlier [7] in a binary mixture of liquid crystals 7BCB and 8CN. This system exhibits an interesting phase diagram, with an induced smectic island for intermediate concentrations, while the two constituents have no smectic phase. NMRD data in nematic phases at two relative concentrations, one having no underlying smectic phase (pure 8CN) (Fig.3) and the other with a smectic phase (70% 8CN) (Fig.4) are analysed, by writing the relaxation rate R_1 as :

$$R_1 = R_{1DF} + R_{1SD} + R_{1R} \qquad \ldots(4)$$

where R_{1DF} is given by Eqn.2 with $C_1(\Delta)$ replaced by A_{DF} ($\propto C_1(\Delta)$), R_{1SD} is the contribution from the self diffusion, given by Torrey's formula [8], and R_{1R} represents contributions from individual reorientations with Lorentzian type dispersion. Results of the non-linear least squares fitting of the data to Eqn.4 (relevant fit parameters being K_3, cut-off frequencies and A_{DF}) are shown in Figs. 3 and 4. The dispersion in pure 8CN is essentially dominated by DF with a constant contribution from R (and possibly SD). The mixed system on the other hand shows frequency dependent contributions from all the mechanisms. Further, K_3 is found to be higher ($2.4 \pm .5 \times 10^{-5}$ dyn) and DF are cut-off much earlier ($\nu_{co} \approx 33$ MHz) in the mixture (compared to 10^{-6} dyn and above 100 MHz, respectively, in the pure system). In this context, it is interesting to note that the mixture has an underlying smectic phase and perhaps the observed difference in the elastic properties and cut-off frequencies could be a consequence of this.

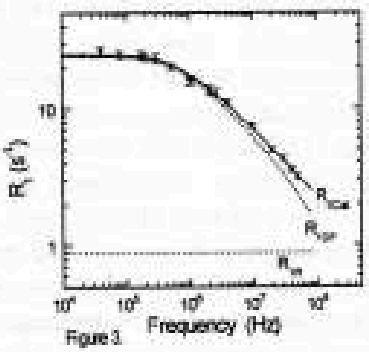

Figure 3

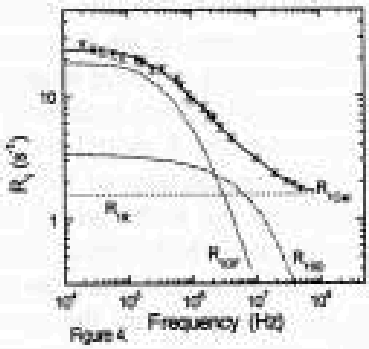

Figure 4

References :

[1] F. Noack in Encyclopaedia of Nuclear magnetic Resonance, Ed. D.M. Grant and R.K. Harris, Wiley, New York (1995) pp 1980-1990.

[2] S. Stapf, R. Kimmich and R.-O. Seitter, Phys. Rev. Letts. 75, 2855 (1995).

[3] F. Noack, S. Becker and J. Struppe, Annu. Rep. NMR Spectrosc. 33, 1 (1997).

[4] R. Blinc, NMR Basic Principles Progress 13, 97 (1976).

[5] R.R. Vold and R.L. Vold, J. Chem. Phys. 88, 4655 (1988).

[6] P. Pincus, Solid State Commun. 7, 415 (1969).

[7] V. Satheesh, D. Loganathan, K. Venu, V.S.S. Sastry, R. Dabrowsky and M. Brodzik., Proceedings of International Society for Optical Engineering, 3318, 245 (1997).

[8] H.C. Torrey, Phys. Rev. 92, 962 (1953)

Investigating Liquid Crystal Dispersions by NMR Relaxometry

M. Vilfan
J. Stefan Institute, Jamova 39, 1000 Ljubljana, Slovenia
e-mail: mika.vilfan@ijs.si

Since the discovery of easily fabricated liquid crystal dispersions in 1986 [1], the interest in this field of liquid crystals has been steadily growing, partly because of their electrically controllable optical properties. Liquid crystals in spherical cavities within a solid polymer (PDLC), in cylindrical cavities of organic and inorganic membranes, in silica aerogel matrices and porous glasses, and those constrained by polymer networks have been investigated [2]. The most important characteristic of liquid crystal dispersions is a high surface-to-volume ratio which makes the surface effects dominant over the bulk ones. Conventional NMR spectroscopy and NMR relaxometry have been used to study director configurations, degree of orientational order, and molecular dynamics in liquid crystal dispersions with pores of submicrometer size [3], which are not accessible by standard optical techniques.

Proton spin-lattice relaxation of liquid crystals within an organic polymer is usually faster than in the bulk counterpart. The increase is caused by the **cross-relaxation** between the protons of the liquid crystal and of the surrounding polymer at the interface between the two systems. This effect is not limited to a particular frequency or temperature range. It is present in the nematic as well as in the isotropic phases and influences - or even dominates - the proton relaxation in the MHz and kHz regime. Cross-relaxation was detected first by measuring T_1 at MHz frequencies [4], then by the spin-lattice relaxation in the rotating frame [4], and finally by the field-cycling relaxometry in the frequency range extending from 10^3 to 10^8 Hz [5]. Special NMR techniques, including selective magnetization inversion [6] and polarization transfer with off-resonance irradiation [7], have been used as well. A rather large cross-relaxation rate of $\sim 10^4$ s^{-1}, found in the liquid crystal 4'-pentyl-4-cyanobiphenyl (5CB) in a PDLC material, indicates that there is a thin liquid crystal layer at the surface with molecular translational and/or rotational mobility different from that in the rest of the cavity. The exchange of molecules between both states takes place at a rate which is small compared to the Larmor frequency. The cross-relaxation rate itself is governed by several processes like the average dwelling of molecules at the surface, the transfer of spin energy across the boundary, and the spread of magnetization across the polymer, which have rates of comparable magnitude and are therefore not easy to distinguish.

The most specific relaxation mechanism in liquid crystals, **order director fluctuations**, is only mildly influenced by the confinement unless the pores are smaller than ~ 100 nm [8]. The characteristic $\nu_L^{-1/2}$ frequency dependence of the relaxation rate, typical for protons and deuterons in the kHz range in the nematic phase [9], has been observed in the microconfined liquid crystals as well [10]. The low frequency cut-off, however, below which the relaxation rate becomes frequency independent, is determined by the size of the cavity and not by the discontinuities in the orientation as in the bulk. It is important to note that the low frequency plateau takes place no matter how many spatial dimensions of the liquid crystal are restricted. The effect of confinement on the collective molecular orientational excitations is expected to increase drastically in the vicinity of a structural phase transition (from one director field configuration into another) due to the critical slowing-down of the transition-driving mode. A strong decrease of order director

fluctuations owing to the confinement has been observed by Grinberg and Kimmich in the cavities of nanometer size within a porous glass [11]. They used the dipolar-correlation effect on the stimulated echo to show how the surface interactions hinder spontaneous director fluctuations in such small cavities.

The deuteron spin-relaxation in confined liquid crystals is interesting in particular in **the isotropic phase**. Here a weak orientational order, induced by the inner surfaces, is observed far above the nematic-isotropic transition. The orientational order parameter S_0 is constant within a thin layer at the surface to decay then exponentially with the distance from the surface. The value of S_0 is associated with the wetting of internal surfaces with the nematic phase above the transition temperature and consequently with the strength of liquid crystal - solid substrate coupling. This residual orientational order does not affect the spin-lattice relaxation rate of deuterons in the MHz regime. On the other hand, the transverse deuteron relaxation rate T_2^{-1} is considerably increased - for about a factor of two - in the confined systems [3,12]. The additional relaxation mechanism is translational diffusion of spin-bearing molecules through the regions with different degree of orientational order and, in some cases, of different director orientation at the surface. The resulting relaxation rate in the kHz regime consists basically of two terms. The first one results from the penetration of molecules into the surface layer with constant order parameter S_0. It is only weakly temperature dependent in systems where S_0 exhibits no pretransitional increase. The second term is due to the diffusion of molecules through the region with exponentially decaying order parameter and is roughly proportional to $(T-T^*)^{-1}$, where T^* denotes the supercooling limit of the isotropic phase. Both terms have been clearly identified in the deuteron transverse relaxation rates of 5CB in an epoxy PDLC material and of its homologue 8CB in Anopore membranes. The analysis of the experimental data yields S_0 and τ_s as the two adjustable parameters. It is important to note that the deuteron T_2^{-1} yields S_0 also in systems with non-uniform director orientation at cavity walls with respect to the magnetic field, where the more conventional NMR method, based on the splitting of the NMR spectrum, fails.

[1] J. W. Doane, N. S. Vaz, B. G. Wu, and S. Žumer, Appl. Phys. Lett. **48**, 269 (1986).

[2] G. P. Crawford, J. W. Doane, and S. Žumer, *Handbook of Liquid Crystals* (Eds. P. J. Collings and J. S. Patel, Oxford, 1996), p. 347-414.

[3] M. Vilfan and N. Vrbančič-Kopač, *Liquid Crystals in Complex Geometries* (Eds. G. P. Crawford and S. Žumer, Taylor & Francis, London, 1996), p. 159-186.

[4] M. Vilfan, V. Rutar, S. Žumer, G. Lahajnar, R. Blinc, J. W. Doane, and A. Golemme, J. Chem. Phys. **89**, 597 (1988).

[5] D.Schwarze-Haller, F.Noack, M.Vilfan, and G.P. Crawford, J. Chem. Phys. **105**, 4823 (1996).

[6] O. Jarh and M. Vilfan, Liq. Cryst. **22**, 61 (1997).

[7] C. W. Cross and B. Fung, J. Chem. Phys. **96**, 7086 (1992) and **99**, 1425 (1993).

[8] P. Ziherl, M. Vilfan, and S. Žumer, Phys. Rev. E **52**, 690 (1995).

[9] W. Wölfel, F. Noack, and S. Stohrer, Z. Naturforsch. A **30**, 437 (1975); W. Wölfel, *Kernrelaxationsuntersuchungen der Molekülbewegung in Flüssigkristal PAA* (Minerva, München, 1978).

[10] J. Struppe and F. Noack, Liq. Cryst. **20**, 595 (1996).

[11] F. Grinberg and R. Kimmich, J. Chem. Phys. **105**, 3301 (1996).

[12] M. Vilfan, N. Vrbančič-Kopač, B. Zalar, and G. P. Crawford, *Proceedings of "27. Arbeitstagung Flüssigkristalle"*, Freiburg, 1998, p. P27.

Anomalous surface diffusion of water compared to aprotic liquids in nanopores

J.-P. Korb and R. G. Bryant[1]
Laboratoire de Physique de la Matière Condensée, C.N.R.S.,
Ecole Polytechnique, 91128 Palaiseau, France
[1]Department of Chemistry, University of Virginia, Charlottesville, Virginia 22901, USA.

Introduction

Liquid dynamics at solid surfaces is central to understanding transport properties in heterogeneous systems such as rocks, catalytic materials, or biological tissues. Characterization of liquids at surfaces is difficult because the small fraction of liquid in a surface layer is generally in rapid exchange with bulk phases in contact with it. Nuclear magnetic relaxation dispersion, the measurement of nuclear spin-lattice relaxation rates as a function of Larmor frequency provides a powerful approach for characterizing molecular dynamics, including surface dynamics [1-3]. Here we report remarkable differences in the ^{1}H spin-lattice relaxation dispersion between water and other common solvents such as acetone when in contact with high surface area calibrated microporous chromatographic glasses that contain trace paramagnetic impurities located at the pore surface. We show that these differences come from the spatial extent of the surface explored by the diffusing liquid and the possibility of water to coordinate directly to relaxation centers which are unambiguously at the origin of the nuclear relaxation mechanism.

Water surface diffusion probed by magnetic relaxation dispersion

Water is unique in that it is small, has extensive hydrogen bonding capabilities and may exchange protons with other molecules or surface sites. It may behave as both a Lewis acid or base, and may coordinate to most metal ions. Proton nuclear magnetic relaxation rates were measured using a field cycling instrument of the Redfield design and constructed with S. Koenig and R. Brown as described elsewhere [2]. Controlled pore chromatographic glass was obtained from the Sigma Company with mean pore diameters of 75Å and 159Å and specific area of 140m^2/g and 90.9 m^2/g, respectively. The water proton spin-lattice relaxation rate, $1/T_1$, is fundamentally different from other liquids studied on glasses to date in that it shows power law dependence on magnetic field strength (Fig.1). We demonstrate that this dependence results from correlations that persist much longer in the surface region than in the bulk and that the relaxation in close proximity to the surface is dominated by processes that appear to be one dimensional. This seemingly paradoxical result is interpreted through surface diffusion of water mediated by the bulk phase permitting long range 1-dimensional exploration along the pores between metal sites at which water relaxation is efficient. On the contrary the slower diffusion of acetone at proximity of the pore surface, precludes such anomalous diffusion and a 2-dimensional diffusional model for the surface dynamics around each paramagnetic impurity is sufficient to account for the bilogarithmic dependence of the nuclear relaxation rate on Larmor frequency

(Fig. 2) [3].

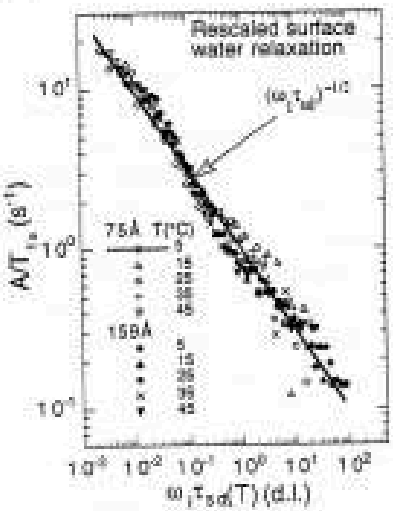

Fig.1 Logarithmic plot of the re-scaled magnetic field dependence of the surface ^{1}H spin-lattice relaxation rates, $A/T_{1S}(\omega_I)$, of water in packed samples of calibrated porous glass beads of pore diameters 75 Å and 159Å at various temperatures as function of the dimensionless variable $\omega_I\tau_{sd}(T)$. The migration within the surface layer is described by a correlation time of diffusion, τ_{sd} and A is a constant. The continuous line is the best fit obtained with a one-dimensional diffusion: $1/T_1 = [\omega_I\tau_{sd}(T)]^{-1/2}$.

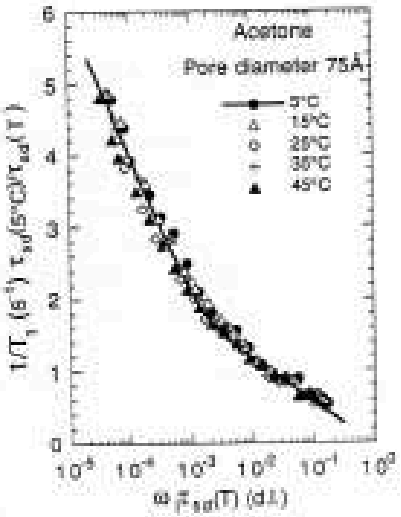

FIG. 2. Semilogarithmic plot of the re-scaled magnetic field dependence of the ^{1}H spin-lattice relaxation rates of acetone in packed samples of calibrated porous glass beads of pore diameter 75 Å at various temperatures as function of the dimensionless variable $\omega_I\tau_{sd}(T)$. The continuous line is the best fit to Eq. (19) of ref [3].

[1] R. Kimmich and H.W. Weber, Phys.Rev. B **47**, 11788 (1993); S. Stapf and R. Kimmich, J. Chem. Phys. **103**, 2247 (1995); S. Stapf, R. Kimmich and R.O. Seitter, Phys. Rev. Letters **75**, 2855 (1995).

[2] M. Whaley-Hodges, A.J. Lawrence, J.-P. Korb, R. G. Bryant, Solid State Nuclear Magn. Resonance **7**, 247 (1996).

[3] J.-P. Korb, M. Whaley-Hodges, R. G. Bryant, Phys.Rev. E **56**, 1934 (1997)

E-mail:
Jean-Pierre.Korb@polytechnique.fr
rgb4g@virginia.edu

Statistics of Surface Diffusion Probed by Field-Cycling NMR Relaxometry

T. Zavada and R. Kimmich
Sektion Kernresonanzspektroskopie, Universitaet Ulm, 89069 Ulm, Germany
e-mail: tatjana.zavada@physik.uni-ulm.de

The frequency dependence of the spin-lattice relaxation time in liquids confined in nanoporous glasses was found to depend on the adsorbate-surface interactions [1]. In the limit of weak adsorption, a flat T_1-dispersion was observed in the experimental frequency range. A steep T_1-dispersion in the strong-adsorption limit was shown to appear as a result of surface diffusion. The relaxation mechanism of the *reorientations mediated by surface displacements* (RMTD) was proposed [2, 3] to account for the effect of surface diffusion on the T_1-dispersion.

Molecules participating in surface diffusion probe the structure of the pore surface. The fractal properties of the rugged surface are taken into account by the radial orientation structure factor $S(k)$, provided the system under consideration is isotropic. k is a surface wave vector. According to the RMTD model, surface diffusion reveals itself in the autocorrelation function of spin fluctuations:

$$G(t) = 2\pi \int_0^\infty S(k)p(k,t)\,dk. \tag{1}$$

$p(k,t)$ is the Fourier transform of a two-dimensional distribution of effective displacements along the surface.

Surface diffusion can occur in the topologically 2D or 3D pore space. Effective diffusion in the two-dimensional liquid layer is expected to be similar to Fickian. In this case, $p(k,t)$ decays as e^{-Dtk^2} according to Gaussian statistics of surface displacements. D is the apparent diffusion coefficient.

In contrast to that, bulk-mediated surface diffusion results if the molecules strongly adsorbed on the surface exchange with the bulk-like phase [4]. The anomalous surface diffusion caused by the strong adsorption is governed by Lévy statistics on a certain displacement scale. In the short-time limit, $p(k,t)$ decays as e^{-ctk}, where c has dimensions of velocity.

Through the RMTD mechanism, the statistics governing the surface dynamics is encoded in the intensity function $\mathcal{I}(\omega)$ (scanned by the experimental T_1-dispersion):

$$\mathcal{I}(\omega) = 2\int_0^\infty G(t)\cos(\omega t)\,dt = \int_0^\infty S(k)\frac{2\tau_k}{1+\omega^2\tau_k^2}\,dk. \tag{2}$$

τ_k is the correlation time of the RMTD process reflecting the relevant length scales. $\tau_k \propto 1/k^2$ and $\tau_k \propto 1/k$ for Fickian diffusion and for a Lévy process, respectively [4]. A power-law T_1-dispersion observed for liquids filling porous systems can be described by $S(k) \propto k^{-x}$ [5]. Thus, for the topologically 2D Fickian diffusion in a thin surface layer, one obtains

$$1/\mathcal{I}(\omega) \propto \omega^{(1+x)/2}. \tag{3}$$

For Lévy walks along the surface, we find

$$1/\mathcal{I}(\omega) \propto \omega^{x}. \tag{4}$$

Hence, the slope of the T_1-dispersion curves given by expressions (3) and (4) is determined by the statistics of surface displacements, closely related to the effective topology of the pore surface.

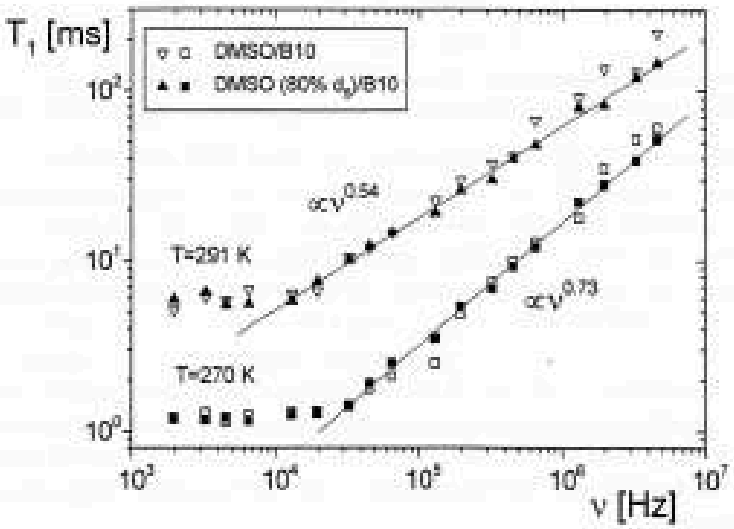

Figure 1: Frequency dependence of the proton spin-lattice relaxation time for dimethylsulfoxide (DMSO) in porous glass B10 and for an isotopically diluted sample (80 % DMSO-d_6) above and below the phase transition. Below the melting point, the data relate to the slowly decaying component of a NMR signal which corresponds to the non-frozen DMSO layers.

For low-molecular liquids, the pore space of a porous glass B10 used in this study (a mean pore diameter d=10 nm) can be considered as isotropic and three-dimensional. Non-frozen surface layers of partially frozen systems form an isotropic network of interconnected topologically two-dimensional pores. The reduction of the topological dimension of the pore space resulting from the phase transition is expected to influence the statistics. The change in the surface dynamics was examined by use of proton NMR field-cycling relaxometry.

Fig. 1 shows the T_1-dispersion of dimethylsulfoxide (DMSO) and of the DMSO isotope mixture (80% b.w. DMSO-d_6 mixed with 20% b.w. DMSO) filling the porous glass B10. The experimental data for both pure and isotopically diluted samples coincide on both sides of the phase transition. Therefore, intermolecular dipolar couplings and any influence of surface paramagnetic impurities on the course of the dispersion curves discussed by Korb *et al* [6] can be ruled out. The dispersion region was found to be a power-law $T_1 \propto \nu^{0.54}$ for the unfrozen system. The slope of 0.54 is in a good agreement with the results obtained for other polar liquids confined in porous glasses [1]. For the system which is partially frozen, $T_1 \propto \nu^{0.73}$ is observed. The difference in the slopes of the dispersion regions of $T_1(\nu)$ can be attributed to the difference in the statistics of surface displacements as predicted by expressions (3) and (4). Thus, the experimental data provide evidence that the interface dynamics of strongly adsorbing systems containing a bulk-like phase is controlled by Lévy statistics.

[1] S. Stapf, R. Kimmich and R.-O. Seitter, *Phys. Rev. Letters* (1995) **75** (15), 2855-2858.
[2] R. Kimmich and H. W. Weber, *Phys. Rev. B* (1993) **47** (18), 11788-11794.
[3] R. Kimmich "NMR Tomography, Diffusometry, Relaxometry" (1997). Springer-Verlag, Berlin Heidelberg.
[4] O. V. Bychuk and B. O'Shaughnessy, *J. Phys. II France* (1994) **4**, 1135-1156.
[5] S. Stapf, R. Kimmich, and J. Niess, *J. Appl. Phys.* (1994) **75**, 529-537.
[6] J.-P. Korb, M. Whaley-Hodges, and R. G. Bryant, *Phys. Rev. E* (1997) **56** (2), 1934-1945.

NMR RELAXOMETRY STUDIES OF BULK AND CONFINED PLASTIC CRYSTALS

Siegfried Stapf *
Sektion Kernresonanzspektroskopie, Universität Ulm, D-89069 Ulm, Germany
* current address: Dept. of Chemistry, University of Nottingham, Nottingham NG7 2RD, UK

Several plastically crystalline materials [1] were investigated employing NMR field-cycling and pulsed field gradient techniques. In bulk, these species are characterized by two dominating reorientational motions: fast anisotropic molecular rotations and slow translational jumps. While the rotational process usually fulfils the extreme narrowing condition, the average jump correlation times are of the order 10^{-7} s or longer. Thus, field-cycling relaxometry with its capability of determining longitudinal relaxation times at Larmor frequencies down to the kHz region is a suitable means for investigating these slow processes [2]. The frequency dependence is found to follow a $T_1 \propto \omega^2$ dependence over up to four orders of magnitude in relaxation time. The intermolecular character of this relaxation contribution is shown by proton measurements in samples diluted with the deuterated compound [3]. Absolute values and activation energies of the jump frequencies are presented along with a measure of the residual correlation after anisotropic rotation. The self-diffusion coefficients obtained by this method are in good agreement with values determined directly by fringe-field diffusometry.

Hydrogen bonding between the molecules can result in a more complex dynamical behaviour which is reflected in a further T_1 dispersion step well above the jump frequency. Moreover, a coexistence of plastic and liquid phases well below the melting point is observed for some of the investigated materials [4]. The frequency dependences for both phases are well resolved in the field-cycling experiment.

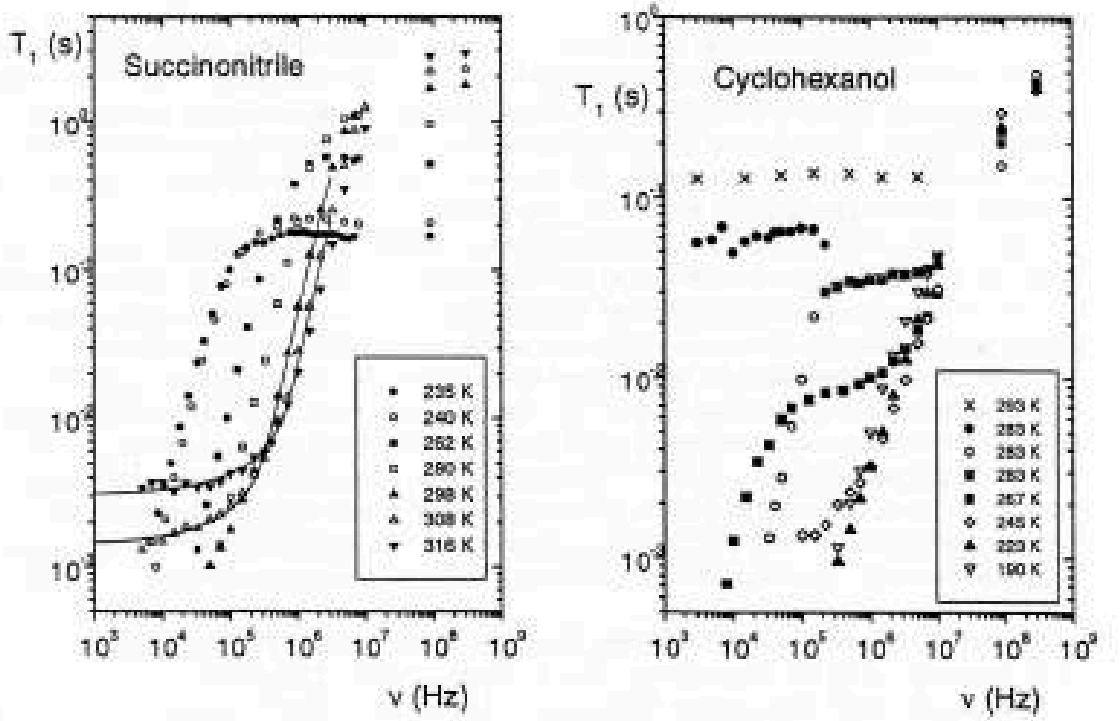

Figure 1: The $T_1(\nu)$-dispersion for succinonitrile is as expected for a system undergoing anisotropic molecular rotation and translational jumps. The dynamical behaviour of cyclohexanol involves correlated molecular motions; a coexistence between liquid and plastic phases is observed at T=283 K.

The observations in the bulk plastic crystal are compared to measurements performed with cyclohexane confined in porous glasses of well-defined pore sizes between 4 nm and 200 nm. The behaviour of the crystals inside the pores is characterised by a size-dependent freezing point depression [5]. Below a critical pore size, freezing does not occur and the supercooled state of the liquid leads to a temperature-dependent dispersion $T_1(\nu)$ [3]. Above this threshold, an unfrozen film at the surface is observed in addition to the intraporous plastic crystal. Despite of its small extension of about two monolayers, which results in a high tortuosity of the space available for diffusion, this film possesses liquid-like properties. Temperature-dependent relaxation measurements indicate a crossover between fast and slow exchange processes. In the fast-exchange limit, the relaxation rate consists of two components $T_1^{-1}(\nu) = c_1\,\nu^{-2} + c_2\,\nu^{-\gamma}$. $\gamma = 0.75 \pm 0.05$ is found which corresponds to the results obtained for surface layers of liquids forming ordinary crystals [6]. Diffusion experiments were performed entirely in the fast exchange regime; they give evidence for a component with a diffusion coefficient at least two orders of magnitude larger than in the plastically crystalline state.

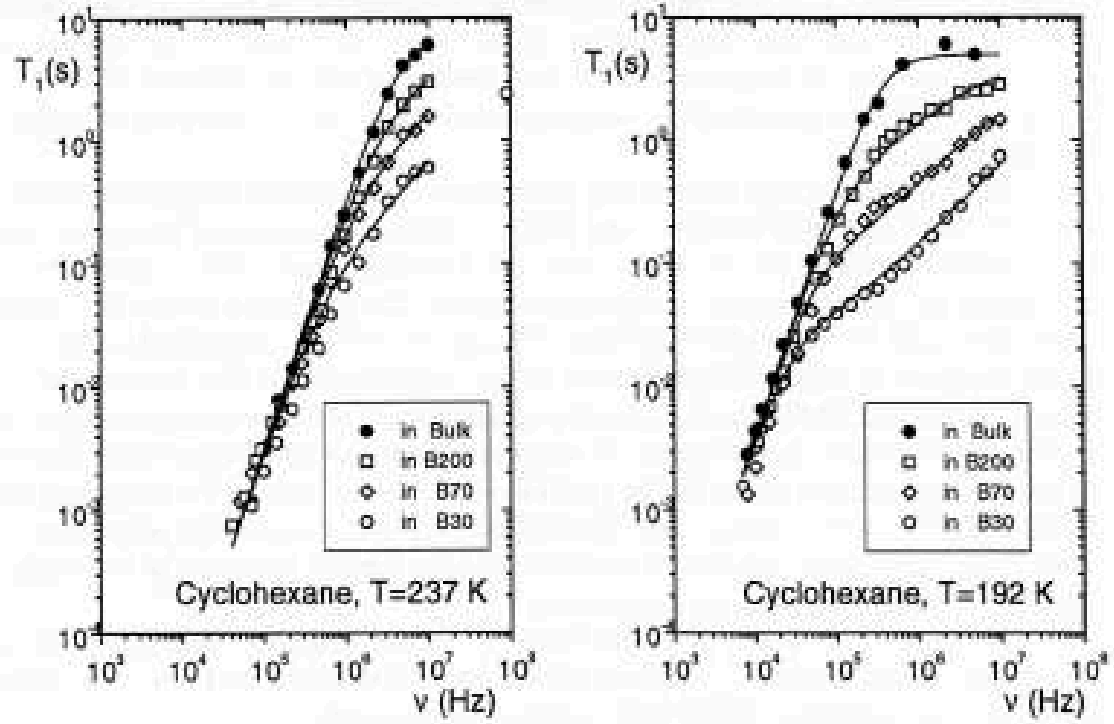

Figure 2: Frequency-dependence of $T_1(\nu)$ for cyclohexane confined in porous glass of 30, 70 and 200 nm pore size, respectively, as compared to the bulk. A crossover from $T_1 \propto \omega^2$ to $T_2 \propto \omega^{0.75}$ is observed, indicating exchange between the intraporous plastic crystal and the surface layer.

References

[1] J. N. Sherwood, *The Plastically Crystalline State*, Wiley & Sons, Chichester (1979)

[2] R. Kimmich, *NMR: Tomography, Diffusometry, Relaxometry*, Springer-Verlag, Heidelberg (1997)

[3] S. Stapf, R. Kimmich, T. Zavada, *Appl. Magn. Reson.* **12**, 199 (1997)

[4] S. Stapf, R. Kimmich, *Molec. Phys.* **92**, 1051 (1997)

[5] J. H. Strange, M. Rahman, E. G. Smith, *Phys. Rev. Lett.* **71**, 3589 (1993)

[6] T. Zavada, S. Stapf, R. Kimmich, *Magn. Reson. Imaging, in press*

e-mail address of corresponding author: pcsssx@unix.ccc.nottingham.ac.uk

Surface diffusion of strong adsorbates: computer simulations and NMR spin-lattice relaxation.

R. Valiullin
Kazan State University, Kazan, Russia

Field-cycling NMR relaxometry of polar liquids in porous media indicates the existing of correlation times of the adsorbate orientation up to eight orders magnitude longer than in bulk [1-2]. The mechanism can be explained on the basis of reorientations mediated by translational displacements (RMTD) of molecules on the surface. In contrast to the case of nonpolar liquids, bulk mediated surface diffusion (BMSD) of strong adsorbates was predicted [3], which is described by Cauchy statistics for the short displacements limit.

Using a Monte-Carlo method, the displacements distribution along infinite planar and spherical liquid-solid interfaces and NMR correlation function $G(t)$ were simulated for a random walker. In the latter case, the planar patches with a finite surface orientation correlation length r_c were also considered. The prediction expected in strong adsorption limit for the surface diffusion [3] was reproduced. In particular, the Levy walks character of surface displacements in the short-time limit was demonstrated in agreement with the BMSD model. Concave spherical surfaces show some deviations due to finite bulk volume in the sphere. It was shown that the NMR correlation function decay due to molecules escape to the bulk becomes relevant only in the long-time limit relative to the retention time t_h, which characterizes the surface-adsorbate interaction. At short times, correlation loss occurs mainly due to the surface geometry in the sense of RMTD mechanism enhanced by Levy walks.

The conclusion is that on a time scale $t << t_h$ the frequency dependence of the spin-lattice relaxation time T_1 of strong adsorbates is determined by Levy walk surface diffusion in combination with the surface topological properties.

[1] S.Stapf, R.Kimmich, and J.Niess *J.Appl. Phys.* **75** (1), 529 (1994).
[2] R.Kimmich, *NMR: Tomography, Diffusometry, Relaxometry* (Springer-Verlag, Berlin, 1997).
[3] O.V.Bychuk, and B.O'Shaugnessy *Phys. Rev. Lett.* **74**, 1795 (1995).

Posters

Relaxometric Properties of Gd(III) Complexes as Contrast Agents for Magnetic Resonance Imaging

Silvio Aime, Mauro Botta, Mauro Fasano, Enzo Terreno
Dipartimento di Chimica I.F.M., Università di Torino, Via P. Giuria 7 - 10125 Torino (Italy).

The use of paramagnetic substances for altering and controlling the magnetic relaxation of water protons has found wide applications in the NMR techniques for medical imaging and diagnosis [1]. The reason is that contrast in NMR images depends less on the local tissue water protons density than on their T_1 and T_2 relaxation times. Moreover, despite the beauty and the inherent spatial resolution of NMR images of native tissues, a large improvement in contrast is achieved by the introduction of exogenous paramagnetic agents able to significantly alter water protons relaxation times. The attention has been primarily focused on complexes of Mn(II) and Gd(III) since these metal ions with S state electronic structures couple a large magnetic moment with a long electron spin relaxation time (~10^{-9} s), two properties that ensure an optimum efficiency for nuclear spin relaxation [2]. The anionic complex $Gd(DTPA)^{2-}$ and $Gd(DOTA)^{-}$ are the first complex entered into clinical practice and they represent the prototype and the reference for the development and the evaluation of new agents presence of isomeric species and the elucidation of their interconversion processes. Many other complexes, mainly functionalized derivatives of DTPA and DOTA ligands, are currently under intense scrutiny in order to optimize properties such as thermodynamic stability, dissociation kinetics, relaxivity, residence time in circulating blood and accumulation at specific target tissues or organs. An important step in the design and characterization of more effective CA is represented by the investigation of the relationship between the chemical structure and the factors determining relaxivity in aqueous solutions as well as the study of the solution structure and dynamics of the metal chelates, the possible

In the last few years we have investigated many of these aspect, through relaxometric and high resolution NMR techniques and here we summarize the relevant results obtained from relaxometric studies on several Gd^{3+}-complexes of both linear and macrocyclic ligands [3].

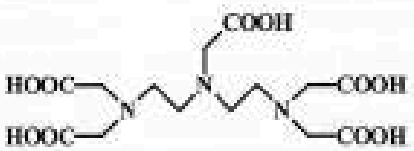

DTPA

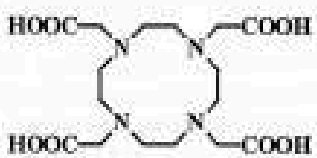

DOTA

Although it is not yet possible to predict accurately the relaxation properties of a Gd(III)-complex based solely on its chemical structure, mainly because of the lack of a complete and adequate theory of the metal ion electronic relaxation, the data collected in the recent past over a reasonably large number of complexes with both linear and macrocyclic ligands allows some general trends to be firmly established [1]. The mechanism of outer- sphere relaxation, for complexes with q = 1 (such as $Gd(DOTA)^{-}$ and $Gd(DTPA)^{2-}$) makes a contributions of roughly 50% to the observed relaxivity that, at high-field (> 10 MHz), is about the same for complexes of similar size and molecular weight. The coordinated water molecules are in fast-exchange with the bulk water, having a mean residence lifetime τ_m of several nanoseconds. The relaxivity in the high magnetic field region is mainly controlled by the reorientational correlation time τ_r which depends upon the molecular dimension of the complexes, as shown by the good

correlation between relaxivity and molecular weight for a number of structurally similar complexes. The low-field region of the NMRD profiles substantially differs among different complexes according to the zero-field value of their electronic relaxation times (τ_{S0}). These latter are remarkably long for axially symmetric complexes (DOTA) and much shorter for linear chelates (DTPA) and are also sensitive to the symmetry of the complex and to the chemical nature of the coordinating groups.

Currently the search for new CA for MRI is mainly directed toward the synthesis of Gd^{3+} complexes of functionalized derivatives of DTPA and DOTA ligands without altering their chelating abilities. We prepared a number of new complexes derived from the macrocyclic structure of DOTA by introducing one or more β-benzyloxy-α-propionic residues. All the Gd^{3+} complexes have significantly higher relaxivities than $Gd(DOTA)^-$ over the entire magnetic field range investigated. The differences in relaxivity among the chelates are due to their different values of τ_r and τ_{S0}. At high fields the relaxivities show a almost linear dependence from τ_r which in turn is strictly related to the molecular weight and the dimension of the complexes, while at lower fields the relaxivity differences are well accounted for the different values of τ_r and τ_{S0}. The effect of the latter parameters is particularly evident when the relaxivity profiles of the disubstituted isomeric complexes are compared with each others. In this case the low field differences in this inner- and outer-sphere relaxivities are completely accounted for by the different electronic relaxation times of the two complexes. The value of τ_{S0} seems to reflect the changes in symmetry introduced in the coordination sphere of the Gd^{3+} ion by the insertion of one, two or three β-benzyloxy-α-propionic residues. In fact, τ_{S0} of the mono-substituted complex (417 ps) is lower than that of the highly symmetric DOTA-complex (460 ps). Moreover, the difference in τ_{S0} between the Gd^{3+} complexes of disubstituted ligands cis (275 ps) and trans (443 ps) is particularly impressive and may result from the lower symmetry of the 1,4-disubstituted isomer. The value of τ_{S0} depends not only on the change introduced in the molecular geometry but also on the nature of the substituent group. In fact the amidation of a DOTA and DTPA carboxyl group produces a dramatic decrease in τ_{S0}, which results in a lower water proton relaxivity at low fields. Moreover the data obtained on a series of monoamide derivatives of DOTA indicate that τ_{S0} is almost independent of the nature of the amide substituent (120-140 ps). It is likely that the observed decrease in this parameter depends on the decreased donor ability of the amide oxygen with respect to the carboxylate oxygen. Therefore, the τ_{S0} parameters acts as a molecular amplifier of the minor differences in the coordination of the carboxylate vs amide groups.

At the magnetic field strengths currently employed in MRI (0.5-1.5 T) the ability of the small Gd^{3+} chelates to enhance the solvent proton longitudinal relaxation rate is largerly determined by this molecular reorientational time τ_r. it follows that the achievement of higher water relaxation rates may be pursued through an increase of this parameter, since the increase of the number q of water molecules in the inner coordination sphere of the Gd^{3+} ion is likely accompained by a decrease of the stability of the complex. A convenient route for increasing τ_r consists in the formation of host-guest non-covalent interactions between suitably functionalized complexes and slowly tumbling macromolecules. We have studied the non-covalent interactions between a series of β-benzyloxy-α-propionic substituted derivatives of $Gd(DTPA)^{2-}$ and $Gd(DOTA)^-$ and some model substrates. In this case we exploited the presence of aromatic residue on the complexes for investigating the extent and the effect on the solvent protons relaxation properties of hydrophobic interactions with β-cyclodextrin (β-CD) and cationic micelles, useful models that can mimic the non-covalent binding occuring within living matrices. A quantitative analysis of the profiles indicates, as expected, that only τ_r changes remarkably following the formation of the inclusion compounds.

References:

[1] S. H. Koenig, *Acta Radiol.*, Suppl. 374, 17 (1990)

[2] S. H. Koenig, R. D. Brown III, *Progr. NMR Spectr.*, 22, 487 (1990)

[3] S. Aime, M. Botta, M. Fasano, E. Terreno, *Chemical Society Reviews*, 27, 19 (1998)

Relaxometric Investigation of Molecular Motions in Molecular Solids.

S. Aime[x], G. Digilio[x], G. Ferrante[o]and S. Sykora[o]

[x] *Dipartimento di Chimica IFM, Università di Torino, Italy.*

[o] *Stelar, Mede (Pavia), Italy.*

Solid State NMR signals of abundant nuclei (spin ½, high isotopic abundance and high concentration) are usually featureless and very broad (up to 100 KHz). Narrowing of the lines is caused by the presence of molecular motions. The occurrence of molecular motions provides a relaxation path through the modulation of the dipolar interaction. Thus, the measurement of relaxation times provides a route to assess and quantify the molecular motions. In fact, the measurement of relaxation times at different temperatures offers a straightforward method to the determination of the energy barrier of the motional process. The most accessible parameter for such measurement is proton T_1.

The availability of a field cycling (FC) relaxometer significantly extends the range of motional processes that can be investigated by measuring ^{1}H-T_1 at the solid state. In fact the problem associated to the small magnetization vector at low magnetic field strength (which has limited the range of the available fields for direct measurements) can now be overcome by creating the initial (strong) magnetization at high field followed by the fast shift to the desired (low) magnetic field. This approach appears to be particularly useful to investigate low/intermediate frequency motions whose detection is usually difficult (or impossible) by other techniques.

The obtained NMRD profiles are fitted to the T_1 values computed on the basis of the dipolar relaxation term :

$$\frac{1}{T_1} = C\left[\frac{\tau_c}{1+\omega^2\tau_c^2} + \frac{4\tau_c}{1+4\omega^2\tau_c^2}\right]$$

where C is the dipolar interaction (which may be evaluated by the VanVleck theory), ω are the Larmor frequencies and τ_c is the correlation time for the dynamic process. Examples

dealing with organic and organometallic systems will be shown whose measured ^{1}H-relaxation times are down to the order of magnitude of one millisecond.

^{2}H-^{1}H Cross Relaxation in the Rotating Frame using Spin-Lock Adiabatic Field Cycling Imaging (SLOAFI) .

E. Anoardo[1] and R. Kimmich[2].

1- Facultad de Matemática, Astronomía y Física. Universidad Nacional de Córdoba. Medina Allende y Haya de La Torre. Ciudad Universitaria. 5010 - Córdoba - Argentina.
Email: anoardo@mail.famaf.unc.edu.ar

2- Universität Ulm, Sektion Kernresonanzspektroscopie, 89069 Ulm, Germany.
Email: Rainer.Kimmich@physik.uni-ulm.de

Spin-Lock Adiabatic Field Cycling Imaging (SLOAFI) is a useful experimental NMR technique for the fast study of spin-lattice relaxation in the rotating frame [1,2]. In this method, the magnetization is spin-locked while a magnetic field gradient G_X is adiabatically switched on to produce a spatial distribution of the effective Larmor frequency along the sample. This condition is held during a relaxation period where the locked magnetization relaxes at the corresponding effective frequency depending on the position. At the end of the interval the gradient is adiabatically switched off and the remaining magnetization is refocused along the spin-lock field. Finally, the partially relaxed magnetization is imaged using the gradient echo sequence. The experiment is repeated for different relaxation intervals in order to obtain the temporal evolution of the profiles, from where the effective rotating frame spin-lattice relaxation dispersion can be evaluated. The effective Larmor frequency interval covered in the experiment extends from few kHz (depending on the spin-lock amplitude) to more than 100 kHz (depending on the magnetic field gradient strength). The figure shows the pulse scheme of SLOAFI.

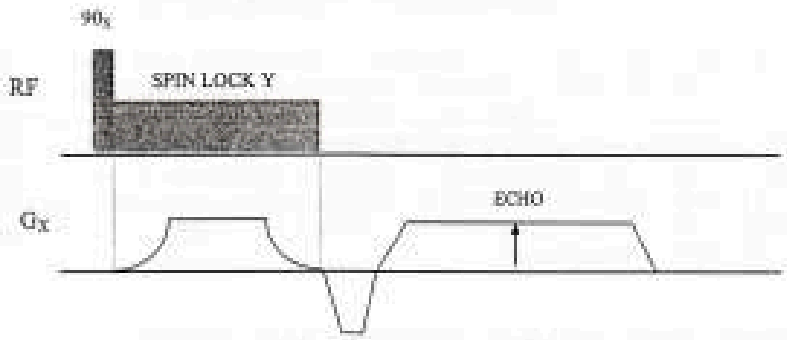

SLOAFI is a powerfull tool combined with traditional field cycling T_1 measurements at low Larmor frequencies. Both techniques provide information about the envolved low frequency spectral densities. However, the experimental conditions could be strongly different from one case to the other: SLOAFI experiment can be carried out using a tomograph with a strong *constant* Zeeman magnetic field, while in general, in the Zeeman fast field cycling relaxometry, the maximun field is under 1.5T and *continuosly switched* between diferent values. Therefore, comparing the spectral densities obtained from both experiments in the same frequency range, important information about the role of the magnetic field can be obtained. This point can be critic for mesomorphic systems with noticeable magnetic anisotropy (like some thermotropic liquid crystals), where the magnetic history and field strength can influence the orientational and dynamical properties of the molecular system.

The aim of the present work was to study the mentioned effect and the rotating frame cross-relaxation spectral density originated from proton spin-lattice relaxation via coupling with other quadrupolar nuclei (SLOAFI quadrupole dips). It is well known the existence of quadrupole dips in the T_1 dispersion profile; however, the phenomena was never systematically studied in the rotating frame.

First experiments were intended in thermotropic liquid crystals (HpAB, 5CB and 8CB) where ^{14}N-^{1}H dips are well known from T_1 field cycling experiments [3,4]. Unfortunatelly, SLOAFI experiment becomes difficult because T_2 in this samples are too short for imaging with the gradient echo technique. In order to avoid this problem we studied a deuterated gelatin (45% D_2O) at 20°C and 47°C. The graph shows the results obtained at the lowest temperature, where clear dips are present at 77 and 100 kHz while a hardly

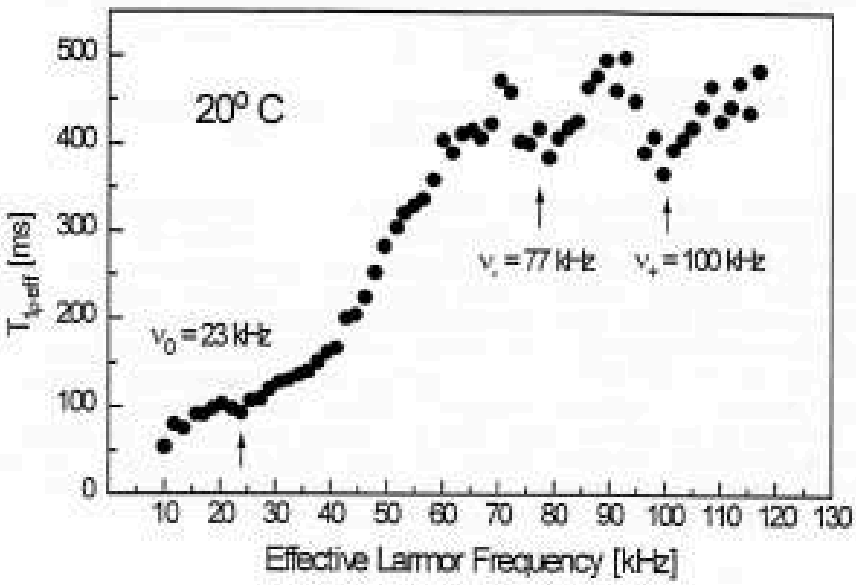

noticiable dip appears at 23 kHz. It is interesting to observe that even when the experiment was developed in a 5T magnetic field, the deuterium quadrupole resonances are not directly perturbed by the presence of the field ($\nu_+ - \nu_- = \nu_0$). Moreover, at this high field limit the Zeeman energy is dominat for the deuterons. Theoretical considerations about this point will be discussed in the conference. The dips are also present in conventional field cycling T1 dispersion experiments. No dips were found at 47 °C, while the big frequency dispersion observed at 20°C is completely absent at the higher temperature (it becomes isotropic-like). It can be concluded that SLOAFI relaxometry is a usefull tool for detecting quadrupole dips at very low frequencies.

[1] - R. Kimmich, J. Barentz and J. Weis, J. Magn. Reson. A117, 228 (1995).
[2] - R. Kimmich, *NMR Tomography, Diffusometry and Relaxometry*, Springer - Berlin (1997).
[3] - E. Anoardo and D. Pusiol, Phys. Rev. E55, 7079 (1997).
[4] - D. Pusiol and F. Noack, Liq. Cryst. 5, 377 (1989).

Chain dynamics in entangled polymers studied by field-cycling nuclear magnetic relaxometry and the dipolar (quadrupolar) correlation effect

M. Assfalg, R. Kimmich, R. Seitter and F. Grinberg
Sektion Kernspinresonanzspektroskopie, Universität Ulm,
Albert-Einstein-Allee 11,89069 Ulm, Germany

N. Fatkullin
Department of Molecular Physics, Kazan State University
420008 Kazan, Russia

The field-cycling nuclear magnetic relaxometry [1] allows one to examine chain modes of entangled polymers in a broad frequency range 10^2 Hz $< \nu < 10^8$ Hz. Experimental frequency dispersions of the proton spin-lattice relaxation time (T_1) show typical crossovers between the power laws $T_1 \sim \nu^{0.50\pm0.05}$ (region I), $T_1 \sim \nu^{0.25\pm0.05}$ (region II) and $T_1 \sim \nu^{0.45\pm0.05}$ (region III) from high to low frequencies. As shown in previous papers [2–4] these power laws essentially reflect the characteristics of collective chain dynamics.
Regions I und II are identified as limits of a theory based on the renormalised Rouse theory and assuming the dominant intrasegment dipolar interactions [2,3]. The justification of the crossover to Region III however demands taking into account intersegment interactions at low frequencies as well. The intermolecular contribution to spin-lattice relaxation strongly depends on the model assumed. Investigations of mechanisms governing the spin-lattice relaxation at low frequencies therefore appear to be especially important for testing polymer theories.

A direct way to examine the relative contributions of intra- and intersegment interactions is to perform a comparative analysis of proton and deuteron relaxations in polymers of equivalent chain length. Proton relaxation is dominated by dipole-dipole couplings. Therefore there are contributions from the intra- as well as intersegment dipole pairs. In contrast to this, deuteron relaxation is a single particle mechanism. It is governed by the coupling of the nuclear quadrupole moment to the local (intrasegment) electric field gradient. The intersegment dipole-dipole interactions can be neglected in this case.

Another efficient investigation tool is based on studies of dipolar and qudrupolar correlation effects on the stimulated echo [1, 5-7]. This method probes ultraslow dipolar (or quadrupolar) correlations on the time scale of the pulse sequence composed of three 90° pulses ($\pi/2 - \tau_1 - \pi/2 - \tau_2 - \pi/2$) that extends the low frequency limit of the field-cycling relaxometry by additional three orders. Again, the presence of non-vanishing intersegment dipolar interactions is to be taken into account only in the case of the protonated (DCE) but not in the case of the deuterated (QCE) samples.

In this work we report results of an experimental study of spin-lattice relaxation and correlation effects in polymers based on the above approach. Figure I shows frequency dependences of the spin lattice relaxation time in protonated and deuterated iso-polybutadiene at 55°C.

In the case of deuterons, no significant change of the dispersion slope $T_1 \sim \nu^{0.25}$ was observed in the experimental frequency range 10^3-10^8 Hz. The protonated sample, in contrast, shows a well observable crossover from the power law $T_1 \sim \nu^{0.22}$ in the MHz range to $T_1 \sim \nu^{0.49}$ below 10^5 Hz. We assume that this finding indicates the dominating role of intersegmential interactions at low frequencies.

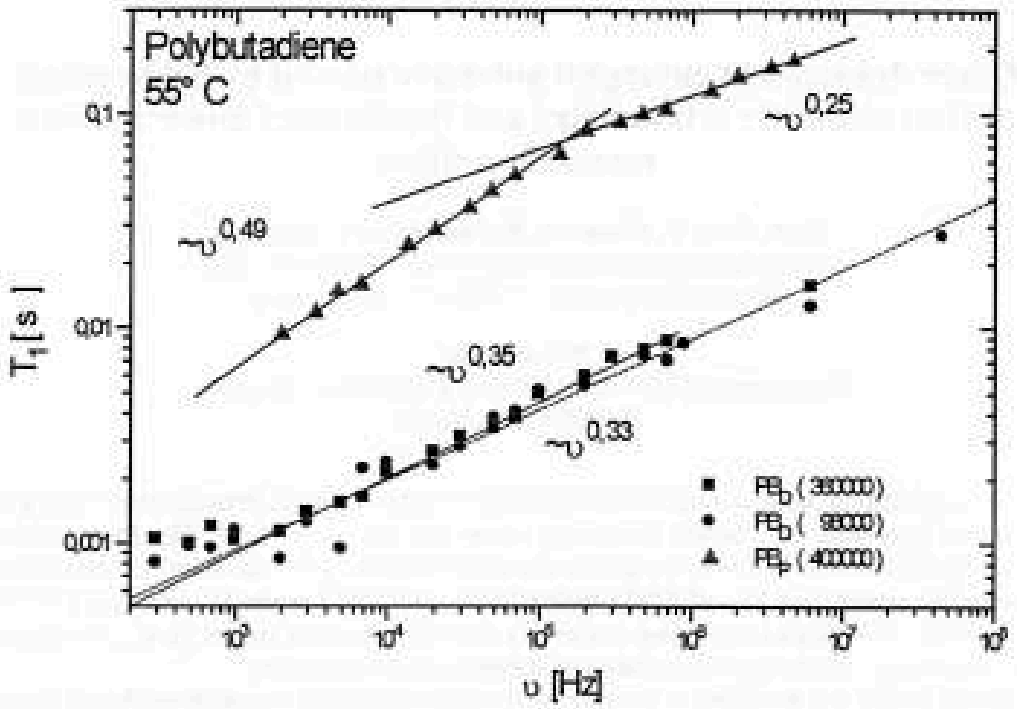

FIG. 1: Frequency dependencies of the proton and deuteron spin-lattice relaxation times of PB_H and PB_D

The DCE and QCE studies were performed with protonated and deuterated polyethyleneoxide samples. The experimentally measured quantity was the quotient of the stimulated and the primary echo amplitudes as a function of the time interval τ_1. Strong attenuations of the quotient were observed in both cases. The attenuation rate in general depends on the mean squared value of the residual coupling constant (second moment) and on the correlation losses during the interpulse intervals. We performed the correction for the second moments associated with the dipolar and quadrupolar coupling constants so that the normalised attenuation curves are comparable with respect to the correlation losses. The results obtained are discussed in terms of inter-and intrasegment interactions and spin diffusion.

This work was supported by DFG and the RFBR (grant No. 98-330-33307).

[1] R. Kimmich, NMR: Tomography, Diffusometry, Relaxometry Springer Verlag, Berlin, 1997

[2] N. Fatkullin, R. Kimmich and H.W. Weber, Phys. Rev. E **47**, 4600, (1993)

[3] N. Fatkullin and R. Kimmich, J. Chem. Phys. **101**, 822, (1994)

[4] N. Fatkullin, R. Kimmich H.W. Weber and S. Stapf, J. of Non-Crystal. Solids, **172-174**, 689, (1994)

[5] F. Grinberg, R. Kimmich, J. Chem. Phys. **103**, 365-370, (1995)

[6] R. Kimmich, E. Fischer, P. Callaghan and N. Fatkullin, J. Magn. Reson., **117**, 53-61, (1995)

[7] F. Grinberg, R. Kimmich, M. Möller, and A. Molenberg J. Chem. Phys., **105**, 9657, (1996)

NMRD of diamagnetic proteins

V. Clementi[1], G. Ferrante[2] and G. Parigi[1]

[1]Dipartimento di Chimica, Università degli Studi di Firenze, via G. Capponi, 7 - 50121 Firenze, Italia
e-mail: valeria@risc1.lrm.fi.cnr.it ; giacomo@risc1.lrm.fi.cnr.it
[2]Stelar snc, via Fermi, 4 - 27035 Mede (PV), Italia
e-mail: stelinf@tin.it

NMRD is an important tool to develop the theoretical grounds for MRI. Natural MRI contrast originates mostly from the different relaxation properties of organic matter in tissues. NMRD profiles of tissues are strongly non-Lorentzian, resembling those of polymers, and theoretical models have been proposed to account for this behavior [1-7].

Proteins are an important component of organic matter in tissues. Proteins can be free in solution, partially aggregated or totally immobilized in supramolecular assemblies like membranes. Often NMRD profiles of diamagnetic proteins in solution acquired over the years exhibit a stretched dispersion [6-14], although the deviation from Lorentzian behavior is less dramatic than for entire tissues. Among them, bovine serum albumin, carbonic anhydrase, hemoglobin, alkaline phosphatase, apoconcanavalin, apotransferrin, alcohol dehydrogenase, immunoglubulin G, hemocyanin, cytochrome c, azurin, lysozyme, phthalate deoxygenase, spanning a range of molecular weights between 10,000 and 200,000. However, none of the existing models for immobilized systems can be extended to proteins in a clear and satisfactory way, and the need itself for this extension may be questionable. Indeed, it is possible that protein aggregation may be at least in part responsible for the deviation from a Lorentzian profile.

NMRD profiles of diamagnetic proteins are either assumed Lorentzian [15] or empirically fitted with the Cole-Cole expression [16], which is an empirical equation of the type

$$R_1 = R_{1w} + D + A \cdot \mathrm{Re}\left[\frac{1}{1+(i\nu/\nu_c)^{\beta/2}}\right] \qquad (1)$$

where ν is the proton Larmor frequency, R_{1w} is the bulk relaxation rate of water, i stands for $\sqrt{(-1)}$, Re stands for the real part of the bracketed expression and D, A, β and ν_c are heuristic parameters. Both A and D are found to be linearly dependent on protein molar concentration and temperature [6]. The value of β, which represents the steepness of the dispersion, is usually found between 1 and 2. For β=2 the field dependent part would reduce to a Lorentzian dispersive term, with inflection at $\nu=\nu_c$. Therefore, the value of ν_c is related to the correlation time of the water protons-protein interaction, τ_c. In this case, it can be easily demonstrated that the dispersive term is a good approximation of two transition dipole-dipole relaxation, with correlation time corresponding to the Brownian rotational time τ_R of solute protein molecule, given by the Stokes' law. This accounts for the reported behavior with molar concentration and temperature.

From literature data and our own measurements on different diamagnetic proteins, we notice that in most cases β has values smaller than 2 and therefore the field-dependent part of eq. (1) has a slower variation with ν than the Lorentzian. This effect could be an intrinsic molecular property or be ascribed to a sizable spread of correlation times due to aggregation mechanisms.

To better clarify the NMRD behavior of proteins in solution we started to record new sets of ^{1}H NMRD profiles of different proteins of different molecular weights, at different

concentrations at temperatures to complement or check literature data. Measurements have been performed using both the relaxometers installed in our Department, a Koenig-Brown relaxometer [17] (from 0.01 to 50 MHz) and the new Stelar relaxometer [18](from 0.01 to 15 MHz). Taking advantage of the larger relaxation rates which can be measured by the latter, higher protein concentrations can be studied. These measurements start to show a trend that confirms that part of the non-Lorentzian effect is concentration dependent. An analysis in terms of protein aggregation (specific) versus increase of microscopic solution viscosity (aspecific effect) is attempted. The residual non-Lorentzian behavior is carefully tested under a variety of experimental conditions including different instruments and different experimental conditions for each instrument.

Bibliography

[1] Bryant R.G., Mendelson D.A., Coolbaugh Lester C., Magn. Reson. Med. (1991) 21, 117-126
[2] Hills B.P., Mol. Phys. (1992) 73, 509-523
[3] Kimmich R., Winter F., Progr. Colloid. & Polymer. Sci. (1985) 71, 66-70
[4] Rorschach H.E., Hazlewood C.F., J. Magn. Reson. (1986) 70, 79-88
[5] Hackman A., Ailion D.C., Ganesan K., Laicher G., Goodrich K.C., Cutillo A.G., J. Magn. Reson. Series B (1996) 110, 132-135
[6] Koenig S.H., Brown III R.D., Progr. NMR Spectrosc. (1990) 22,487-567
[7] Koenig S.H., Brown III R.D., Ugolini R., Magn. Reson. Med. (1993) 29,77-83
[8] Lindstrom T.R., Koenig S.H., J. Magn. Reson. (1974) 15,344-353
[9] Hallenga K., Koenig S.H., Biochemistry (1976) 15, 4255-4264
[10] Koenig S.H., Bryant R.G., Hallenga K., Jacob G.S., Biochemistry (1978) 4348-4358
[11] Banci L., Berners-Price S., Bertini I., Clementi V. Luchinat C., Spyroulias G.A., Turano P., Mol. Phys., submitted
[12] Kroes S.J., Salgado J., Parigi G., Luchinat C., Canters G.W., JBIC (1996) 1, 551-559
[13] Bertini I., Luchinat C., Mincione G., Parigi G., Gassner G.T., Ballou D.P., JBIC (1996) 1, 468-475
[14] Koenig S.H., Brown III R.D., Bertini I., Luchinat C., Biophys. J. (1983) 41, 179-187
[15] Venu K., Denisov V.P., Halle B., J. Am. Chem. Soc. (1997) 119, 3122-3134
[16] Cole K.S., Cole R.H., J. Chem. Phys. (1941) 9,341-351
[17] Banci L., Bertini I., Luchinat C. Nuclear and electron relaxation (1991), VCH, Weinheim
[18] Noack F., Progr. NMR Spectrosc. (1986) 18, 171-276

Molecular Dynamics from High-Resolution Magnetic Relaxation Dispersion Experiments

T. R. J. Dinesen, and R. G. Bryant
Department of Chemistry, University of Virginia, Charlottesville, VA 22901
trd3f@virginia.edu, rgb4g@virginia.edu

The frequency-dependent power spectral densities that directly scale relaxation are significant in that they are the Fourier transforms of the correlation functions governed by molecular motions. The Magnetic Relaxation Dispersion (MRD) experiment directly determines the form of these spectral densities by measuring the relaxation rates as a function of the applied magnetic field strength. With a suitable dynamical model, these results can be interpreted in terms of geometries, time-scales of motion, and other physically relevant parameters.

High-Field Sensitivity and Resolution

We have developed an instrument that overcomes the sensitivity limitations of related field-cycling techniques, permitting the study of low-concentration, or otherwise insensitive nuclei, with the resolution and sensitivity inherent to a super-conducting solenoid. Our home-built probes enable the physical movement of a spin-polarized sample between a 7.05 Tesla solenoid, and an independent shielded electromagnet, where relaxation of interest occurs. Detection in the high field by some pulse sequence completes the field-cycle. Instruments that utilize a rapid current switch field cycle may suffer from poor resolution and relatively small polarization fields.

Ionic Solutes in Aqueous Phase

Application of this technique to the study of ionic solutes has produced the first direct evidence supporting the formation of cation-cation aggregates with lifetimes longer than the rotational correlation times in aqueous solution. From the calculated inter-nuclear distances, any electrostatic repulsion in this high dielectric medium could be overcome by the formation of hydrogen bonds between bridging water molecules and those of the inner co-ordination spheres. The presence of counter-ions further stabilizes these complexes, which have been observed for +1/+2 and +2/+2 systems. Furthermore, it is shown that the relaxation of alkali metals in the presence of substituted nitroxides is dominated by the Fermi contact interaction, owing to a very small concentration of co-ordinated ion-nitroxide complexes.

Anisotropic and Internal Motion

Results from model chemical systems in reduced dimension environments, and those which display motional anisotropy along a molecular axis are also shown, as are preliminary results from spin-labeled polypeptides and nematic liquid-crystal systems.

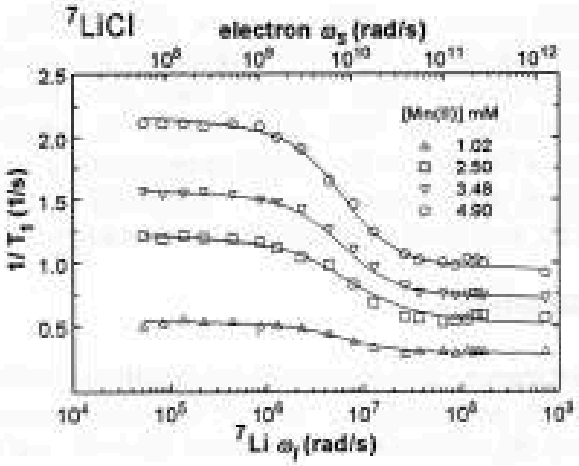

MRD of ^{7}Li / Mn(II) system. Parameters from best fit to data of paramagnetic relaxation model suggest formation of cation-cation pairs. [1]

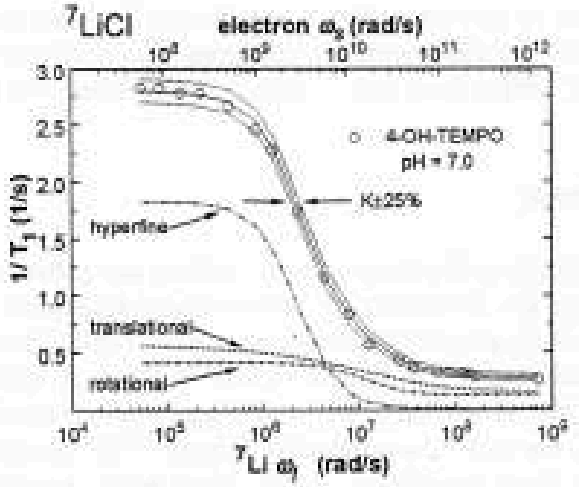

MRD of ^{7}Li in dilute nitroxide solution. The relaxation is dominated by the Fermi contact interaction owing to a small concentration of RNO-Li complexes. [2]

[1] T. R. J. Dinesen, S. Wagner, and R. G. Bryant, submitted, 1998.
[2] T. R. J. Dinesen, and R. G. Bryant, J. Magn. Reson. in press, 1998.
[3] C. C. Lester, and R. G. Bryant, in "Biological Magnetic Resonance, vol. 12: NMR of Paramagnetic Molecules" (L. J. Berliner and J. Reuben, Eds.), Plenum, New York (1993).

THE CALCULATION OF THE SPIN-LATTICE RELAXATION TIME IN ENTANGLED POLYMER MELTS

K.Fenchenko
Kazan State University, Kremlevskaya str.18, 420008, Russia

INTRODUCTION

Recently, Schweizer [1] developed a microscopic model describing the critical slowing down of dynamics of the polymer melts with the molecular weight (M_w) above the critical value (M_e) for the entanglement formation. This model based on the polymeric analogue of the mode-mode coupling approximation has been studied in the work [2]. Namely, the authors of paper [2] have given a estimation of the spin-lattice relaxation time in the form: $T_1 \propto \omega^{0.4} N^{3/2}$, where ω is the resonanse frequincy and N is the number of segments in a polymer chain. However they have not taken into account a contribution on the spin-lattice relaxation time connected with stress arrest in the time limit $\tau_0 << t << \tau_0 N^{3/2}$ where τ_0 is the minimal relaxation time of the polymer chain in the Rouse model. Taking into account this contribution can leads to a quite different power lows of molecular - weights and frequency dependencies.

In the work [3] formulated twice renormalized Rouse model, describing of dynamics in melts of entangled macromolecules ($M_w >> M_e$) using pairs interactions. In the same place has been shown that the power lows of frequency dependence of the spin-lattice relaxation time obtained in the frame of this model are in a good agreement with experimental data.

In the present work it is derived the expressions for the spin-lattice relaxation time on the basis of the mode-mode coupling approximation. Besides, it are given the numerical estimations of the spin-lattice relaxation time in melts of entangled power owing to the twice renormalized Rouse model. A comparison with experimental data is carried out.

RESULTS

For calculations, in a good accuracy it can suggest, that the dominating contribution on the T_1 time gives «intrasegmental» dipole-dipole interactions. On this basis the following expressions for the spin-lattice relaxation time in melts of entangled macromolecules ($M_w >> M_e$) are obtained : (a) mode-mode coupling approximation, $T_1^{-1} = 0.7 M_2 æ \psi^{4/5} \tau_e / [N(\omega\tau_e)^{6/5}]$; (b) twice renormalized Rouse model, $T_1^{-1} \approx 64 M_2 \psi^{4/3} \tau_e / (\omega\tau_e)^{1/3}$,where $N^{-1/2} << \omega\tau_e << 1$, Here æ and ψ is a dimensionless parameters describing the interactions between polymer chain segments in the melt. Namely, $æ = S_0 \rho b^3$, where S_0 is a static collective structure factor, ρ is the number of segments per unit volume, b is the segment length of the polymer chain. In addition to this fact $\psi = \rho d^3 (d/b)^3 S_0 g^2(d)$, where d is the «diameter» of the segment, g(r) is the intermolecular pair correlation function. Besides, $M_2 = \gamma^4 \eta^2 (I+1)I / r_i^6$, where γ it the gyromagnetic ratio; η is the Plank constant, r_i is the distance between spins. Further the values of the parameters ψ, M_2, æ, and τ_e are shown. Ones are obtained by numerical calculations $\psi = 0.13$, $æ = 0.64$ [1]. So does owing to experimental data for the melts without entanglements ($M_w < M_e$):

(i) polyisobutelene (PIB) ($M_w = 111 \times 10^4$, $M_e = 15 \times 10^3$), $\tau_e(T=357K) = 1.8 \times 10^{-9}$s, $M_2 = 0.4 \times 10^{10} c^{-2}$;

(ii)polydimethilsiloxane (PDMS) ($M_w = 25 \times 10^4$, $M_e = 19 \times 10^3$), $\tau_e(T=293K) = 1.2 \times 10^{-10}$s, $M_2 = 0.4 \times 10^{10} c^{-2}$.

Below the rations of the spin-lattice relaxation time (T_1^{th}) calculated using formulas (a)-(b) measured T_1^{exp} in PIB and PDMS melts are shown:

1. mode-mode coupling approximation $T_1^{exp}/T_1^{th}(\omega=3x10^4Hz)\approx9$(PIB), $T_1^{exp}/T_1^{th}(\omega=1.2x10^6Hz)$ ≈18(PDMS).

2.twice renormalized Rouse model: $T_1^{exp}/T_1^{th}(\omega=3x10^4Hz)\approx0.98$(PIB), $T_1^{exp}/T_1^{th}(\omega=1.2x10^6Hz)$ ≈0.3(PDMS).

CONCLUSION

Thus, the twice renormalized Rouse model not only gives scaling frequency dependencies of the spin-lattice relaxation rates that correspond with the experiment, but also yields the absolute values of the relaxation rates having the same order of magnitude as the experimental ones. In contrast to this fact the expressions obtained using by mode-mode coupling approximation gives the absolute values of T_1 time not having the same order of magnitude of the experimental ones. Moreover, it contains molecular weight and frequency dependence, which are not observed in experiment.

[1] K.S. Schweizer, J.Chem.Phys.91, 5802-5821 (1989).
[2] R. Kimmich, N. Fatkullin, H. W. Weber , J. Non Cryst. Solids, №3, 303- 349(1994)
[3] N. Fatkullin, R. Kimmich, J. Chem. Phys. (submitted).

Pure Quadrupole Resonance of Metal Ions and Other Species in Proteins and Other Biopolymers

Dimitri Ivanov and Alfred G. Redfield
Biophysics Program and Department of Biochemistry
Brandeis University
Waltham, MA 02254, USA
FAX (USA) 781-736-2349

If appropriate I will talk briefly about the early days of field cycling NMR in metals (1), and field cycling NMR in general (2). Then I will review our attempt to make field-cycling pure quadrupole resonance (FCPQR) simple and generally applicable to proteins. PQR has been observed without field cycling in at least one protein (of Cu(I) in Cu-Zn Superoxide dismutase, by G. Harbison's group (unpublished)), and quadrupole interactions can be estimated by high-field central transition NMR and other methods. However, we hope that FCPQR will be useful and not too difficult for accurate high-sensitivity observations of low frequency transitions. Our emphasis is on the "rotating frame" methods introduced by one of us and by Slusher and Hahn, and developed by many others including the groups of Minier and Seeger. We are also evaluating a multiple-level crossing method described only, as far as we know, in the thesis of J. C.-K. Koo (with E. L. Hahn, Berkeley, 1969). These are rigid-lattice methods, and to freeze out thermal methyl rotations which would shorten T_1 we operate below 50°K, in a flow dewar (3). The field is cycled by sucking the sample from the center of a 500 MHz magnet to its upper edge, about 1 M above, where the .03 T field and its gradient can be bucked out with a Helmholz coil. The temperature at the top (low field) is 2-4°K higher than at the bottom. We expect to use protein samples dissolved in H_2O-PEG or H_2O-Glycerol, fast-frozen to inhibit water crystallization and, in the case of PEG, as a precipitate, spinning the protein down into the NMR tube just before freezing, to get high concentration. We have obtained promising FCPQR signals from ^{11}B and ^{17}O in small

molecules frozen in glycerol-water glass (3). Generally, we are hampered by short T_1's at zero field, some of which may be due to O_2 that we did not remove, or other impurities. We are now trying to understand the low field T_1's as well as other problems that may make it hard to observe FCQPR of interesting species like Mg and Zn.

1. Y. Masuda in the Encyclopedia of NMR (Wiley 1996, D. Grant, ed.), A. Genack, Phys. Rev. B13, 68 (1976).
2. A. Redfield in "NMR as a Structural Tool" (Plenum, 1996; Rao & Kemple, eds.), D. B. Zax in the Encyclopedia (above); Oja and Lounasmaa, Rev. Mod. Phys. 69, 1 (1997); J. H. Walton et al., Chem. Phys. Lett. 203, 237 (1993).
3. Ivanov and Redfield, Zeit.fur Naturforschung, in press (1998).

Synthesis and Structural Analysis of Modified TiO_2/SiO_2 Mixed Oxides Prepared by Sol-Gel Process

Miewon Jung, Eunja Yoo

Department of Chemistry, Sungshin Women's University, Seoul 136-742, Korea
mwjung@cc.sungshin.ac.kr

The systematic modifications of silica matrix as a function of modified Ti-alkoxide content have been investigated by the sol-gel process. Depending on the modified Ti/Si molar ratio and the properties of the ligand used, flexible to brittle gels have been obtained. A structural analysis of the various steps of the hydrolysis-condensation process as well as of the final solid powder determined by IR, UV-Visible, liquid and solid state ^{1}H, ^{13}C, ^{29}Si NMR spectroscopy. It has been identified an optimal homogeneous distribution of the heterometal bond(direct and/or indirect Si-O-Ti bonds) at molecular level exists in this process. ^{29}Si CP/MAS spectra are characterized by broad lines for the three type of sites. Different contributions observed for Q2, Q3, Q4 sites in these TiO_2/SiO_2 samples are relate to the amounts and types of ligand used on modified titanium alkoxides. The modification of titanium alkoxide have been determined by the synthetic condition before hydrolysis-condensation. Proper control of the process condition improves the homogeneity of Ti ion-Si matrices and also controls the distribution of metal oxides.

Reference

[1]Dagobert Hoebbel, Tomas Reinert and Helmut Schmidt, J. Sol-Gel Science and Technology, 6, 139-149 (1996)

[2]G. De, A. Licciuli, C. Massaro, L. Tapfer, M. Catalano, G. Battaglin, C. Meneghini, P. Mazzoldi, J. Non-Cryst. Solids, 194, 225-234 (1996)

[3]K. L. Walther and A. Wokaun, J. Non-Cryst. Solids, 134, 47-57 (1991)

[4]C. J. Brinker, Sol-Gel Sci., New York (1990)

Conformational Equilibrium Isotope Effects on Selectively Deuterated Cyclooctanone

Miewon Jung

Department of Chemistry, Sungshin Women's University, Seoul 136-742, Korea.
mwjung@cc.sungshin.ac.kr

Conformational equilibrium isotope effects are found in selectively deuterated cyclooctanone isotopomers(cyclooctanone-2-D, cyclooctanone-2,2,7,7-D_4, and cycloocta-none-2,2,8-D_3) by observing equilibrium NMR isotope shifts in ^{13}C spectra. The temperature dependence of the isotope shifts are included for the complete analysis of cyclooctanone conformation. Equilibrium constants and the changes in the free energies, enthalpies, and entropies are also reported for these cyclooctanone isotopomers. Molecular mechanics (MM2) calculations of steric interactions and molecular geometry strongly support the steric and hyperconjugative origin of the observed isotope shift results.

References

[1](a) P. E. Hansen, Ann. Rept. NMR Spectr., 15, 105 (1983) (b) D. A. Forsyth, Isot. Org. Chem., 6, 1 (1984) (c) Y. Nakashima, T. Sone, T. Teranishi, K. Suzuki, and K. Takahash, Magn. Reson. in Chem., 32, 578 (1994)

[2]M. Saunders, M. Jaffe, and P. Vogel, J. Am. Chem. Soc., 93, 2558 (1971)

[3]Y. N akashima, H. Kanada, M. Fukunaga, K. Suzuki, and K. Takahashi, Bull Chem. Soc. Jpn., 65, 2894 (1992)

The signal of stimulated echo in three spin system

Kulagina T.P., Kamaukh G.E.

Institute of Chemical Physiks in Chernogolovka
Chernogolovka, Moscow region, 142432, Russia

The well known method of stimulated echo [1-4] is widely applied for studing molecular order and dynamics in polymers, liquid crystals, phorous medias,etc. The method is established on the basis of changing the amplitudes of primary and stimulated echoes in a sequence of three RF pulses:

$(\pi/2)_x \ldots \tau_1 \ldots (\pi/2)_x \ldots \tau_2 \ldots$ (primary echo)$\ldots(\tau_2 - \tau_1)\ldots (\pi/2)_y \ldots \tau_1$(stim. echo).

The appearance of a distinct echo in ingomogeneous external magnetic field was explained in [2] with additional phenomena affecting the amplitude of stimulated echo if the secular part of dipole interaction is not completely averaged out in the evolution intervals of the pulse sequence. In that work there were considered dipolar interations for two spin system and were found only amplitude of the primary and the stimulated echoes. All other Hahn echoes were not considered. In common case five Hahn echoes were shown experimentally [1,4] to appear at the moment $2\tau_1$, $\tau_2 + 2\tau_1$, $2\tau_2$, $2\tau_2 + \tau_1$, $2\tau_2 + 2\tau_1$. The echo at the moment $2\tau_2 + \tau_1$ has not been explained yet by dipolar interactions in two spin system. The purpose of this work is to study all Hahn echoes in three spin system in the presence of the dipolar interaction and a gradient of the external magnetic field.

We have considered the dynamics of three equivalent spins 1/2 , $\mathbf{I}_k$, $\mathbf{I}_l$ and $\mathbf{I}_n$. The local rotating - framer Hamiltonian is composed of a RF term, H_{rf}, a second term representing the local field gradient offset, H_g, and the secular part of dipolar coupling $H_d^{(0)}$:

$$H = H_{rf} + H_g + H_d^{(0)},$$

where $H_g = -\hbar\Omega_g(\mathbf{r})\,(I_{kz} + I_{lz} + I_{nz})$, $\hbar\Omega_g(\mathbf{r}) = \Delta$,

$H_d^{(0)} = \hbar\Omega_d\,(I_{kz} I_{lz} - 1/3\,\mathbf{I}_k \mathbf{I}_l + I_{lz} I_{nz} - 1/3\,\mathbf{I}_l \mathbf{I}_n + I_{nz} I_{kz} - 1/3\,\mathbf{I}_n \mathbf{I}_k)$, $\hbar\Omega_d = 3b$,

$b=b_{kl}-(3\cos^2\theta_{kl}-1)/r_{kl}^3$ – the dipolar coupling constant, which is the same for all pairs of spin.

The system of three spins was considered as the sum of two effective spin systems, one of them was affected by the Zeeman field only, another was represented as the effective spin 3/2 under influence of Zeeman and quadrupole interactions with Hamiltonian $H_q = 3b/2\,(I_z^2 - 5/4)$, I_z –is the operator of z-projection for spin 3/2. Such method allowed to determine the amplitude of all echoes exactly.

We obtained the following expressions for the amplitude of primary echo

$$A(2\tau_1) = -(1/16)\cos(\Delta(t-2\tau_1))[2 + 3\cos(3b(t-2\tau_1)) + 2\cos(3b(t-\tau_1)) + 2\cos 3b\tau_1 - \cos 3bt],$$

and for amplitude of stimulated echo

$$A(2\tau_1+\tau_2) = -(1/32)\cos(\Delta(t-\tau_2-2\tau_1))[6 + 3\cos(3b(t-\tau_2-2\tau_1)) + 2\cos(3b(t-\tau_2-\tau_1)) + 2\cos 3b\tau_1 + 3\cos 3b((t-\tau_2))].$$

Our calculations allowed to determine the amplitude of all five Hahn echoes and to explain the appearance of the echo at the moment $2\tau_2 + \tau_1$ due to dipolar interactions of multispin system.

1. E.L. Hahn, Phys.Rev.,80,580(1950).

2. R. Kimmich, E. Fisher, P. Callaghan, N. Fatkullin, J.Magn.Res.A,117,53(1995).

3. F. Grinberg, R. Kimmich, J.Chem.Phys.,103,365(1995).

4. R. Kimmich, NMR– Tomography, Diffusometry, Relaxometry,Springer(1997).

Design and construction of a fast field-cycling spectrometer with high B_0 homogeneity for the investigation of superionic conductors.

O. Lips, M. Nolte, A. F. Privalov and F. Fujara
Fachbereich Physik, Universität Dortmund, 44221 Dortmund, Germany

The design and partly the construction of a fast field-cycling spectrometer with B_0 up to 2.4T, an inhomogeneity less than 10ppm within $1cm^3$ and switching times below 1ms is described.

Motivation

Our aim is the investigation of motional heterogeneity in superionic conductors (SICs), which are solids with an unusually high ionic conductivity comparable to that of liquid electrolytes. In recent years there has been growing interest in superionic conductors, because they can be used for a variety of applications e.g. sensors, batteries and fuel cells. To study dynamic processes in SICs on the microscopic scale the frequency dependence of the T_1 relaxation time can be analysed, since it is sensitive to the spectral density of molecular motions [1,2]. Furthermore it is particularly suited to the investigation of a possible motional heterogeneity in the superionic state. First test measurements were performed on the fluorine conductor LaF_3 with a tysonite structure in the frequency range of $9 \cdot 10^6 - 4 \cdot 10^8$ Hz and have shown a deviation from a BPP-behavior which was successfully explained by a distribution of correlation times [3]. The study of ^{19}F has the advantage of a high sensitivity and of a pronounced chemical shift which makes it possible to resolve different structural positions. The necessary spectral resolution accounts for the need of a good B_0 homogeneity. Furthermore short switching times are required, since the T_1 relaxation time is expected to become smaller than 1ms in low magnetic fields.

Concept

According to the need of a short switching time (<1ms) a low inductance, air-cored, resistive solenoid with an electronic switching circuit was chosen. The bore diameter of the magnet is desired to be 30mm, so that a commercial cryostat and a homebuilt high temperature probe head can be used to cover a temperature range of 4-1500 K.

A special coil optimization and design is applied to achieve the required field homogeneity and a low inductance. The width of the conducting wire is varied, causing a variable current density, while the gap between the windings is kept constant (Fig. 1). To find the most favorable wire shape an algorithm is used to optimize functions which describe the boundaries of a coiled conductor as functions of the winding angle [4]. In our case Chebyshev polynomials of 6^{th} order are chosen as boundary functions. The thickness of the conductor is taken into account for the correct calculation of the coil geometry. By this technique the magnetic field in a volume of 1 cm^3 can be homogenized theoretically to a

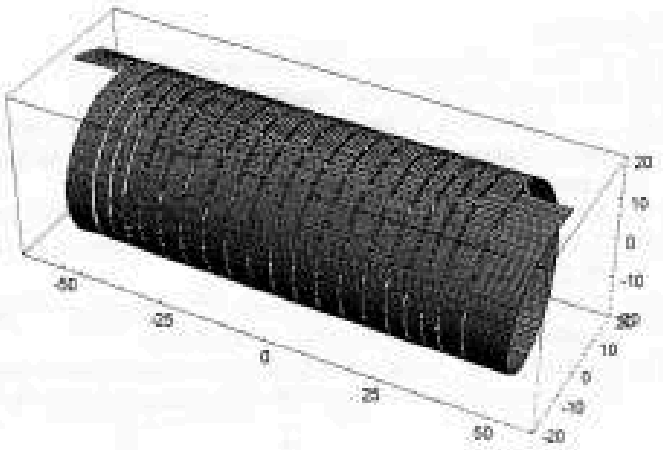

Fig. 1: Coil with variable wire width, optimized for 100 mm length, 19.5 mm diameter and 20 windings. Axis scale in mm.

few ppm. As an example the calculated field profile along the z-axis is shown in Fig. 2 for a coil with a length of 100 mm, an inner diameter of 19.5 mm, a wire thickness of 1.8 mm, a gap width of 0.7 mm and 20 windings.

Furthermore the optimization algorithm can also be used to reduce the effective volume of the magnetic field, and hence the inductance, by adjusting the field at appropriate target points to predefined values.

The current through the coil must be altered by electronic switching to achieve fast field transients. An energy storage principle utilizing a capacitor will be applied [1,5].

It is planned to control the spectrometer by a computer which sets the switches and adjusts the magnetic field to the desired values. The latter will be carried out by a MOSFET bank that regulates the current with a stability of better than 10ppm.

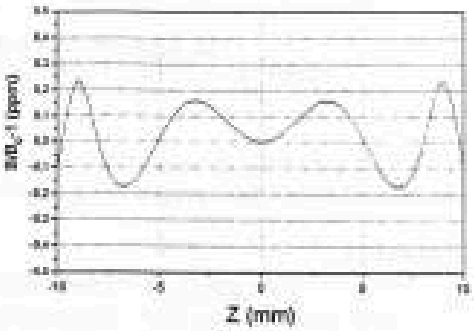

Fig. 2: Relative deviation of the field along the axis from the center of the coil. See text for parameters.

Realization

It was found that a 6 layer design with 20 windings per layer is optimal for our current source (40V, about 1000A). It offers the additional advantage that the gap between the windings can be 1mm wide without a significant rise in resistance. This wide gap simplifies the manufacturing without destroying the homogeneity in radial direction. Therefore all layers can be manufactured from a copper tube by a computer controlled milling tool in the workshop of our physics department and expensive techniques like spark erosion, laser or waterjet cutting can be avoided.

The field cycling circuit will be realized using insulated gate bipolar transistors (IGBTs) as switches, since they are faster than GTO thyristors, which are implemented in several field cycling spectrometers [5]. Principally it is also possible to use IGBTs working in the active zone for the current regulation [6], but nowadays it is still easier and cheaper to employ a MOSFET bank. We decided to apply low voltage MOSFETs, since they offer a better regulation characteristic and a lower drain-source on-resistance $R_{ds(on)}$ than high voltage MOSFETs.

For data acquisition and the control of the spectrometer a computer running LabVIEW will be utilized [7]. The computer will be equipped with a pulse programmer card, a transient recorder, a GPIB-card and a standard I/O-card. The reference signal for different magnetic fields will be generated using an external 20-bit DAC.

References

[1] F. Noack (1986), *Progr. NMR Spectrosc.* **18**, 171-276

[2] R. Kimmich (1980), *Bull. Magn. Res.* **1**, 195-217

[3] A. F. Privalov, S.V. Dvinskikh, F. Fujara and H.-M. Vieth, Frequency Dependent Spin-Lattice Relaxation Study of the Transport Processes in Superionic Conductors, to be represented at Congress AMPERE , Berlin 98

[4] A.F. Privalov, S.V. Dvinskikh and H.-M. Vieth (1996), *J. Magn. Reson.* A **123**, 157-160

[5] E. Rommel, K. Mischker, G. Osswald, K.H. Schweikert and F. Noack (1986), *J. Magn. Res.* **70**, 219-34

[6] D.M. Sousa et al. (1997), *Proc. 7th European Congress on Power Electronics and Applications, Trondheim* 1997, 2.285-2.290

[7] M. Nolte et al., Setting up a field-cycling spectrometer control, to be represented at Symposium Field-Cycling NMR Relaxometry, Berlin 98

Field Cycling NMR Study of Structure and Dynamics in Liquid Crystals

D. Loganathan, K. Venu and V. S. S. Sastry
School of Physics, University of Hyderabad, Hyderabad - 500 046. INDIA

Of the various dynamic processes like order director fluctuations (ODF), self diffusion (SD) and reorientations (R), ODF is the one unique to liquid crystals which can be best studied by FCNMR technique[1]. Butyloxy benzylidene alkylanilenes (4O.m) are well investigated due to the rich polymorphism exhibited by these systems. Effect of molecular structural variations on the physical properties like phase stability, polymorphism and other properties are rather well known. Especially the end chain properties like Odd-Even effects, length of the end chains and etc.,are considered as common properties affecting static and dynamic properties of mesophases. The systematic studies of liquid crystals considering all these factors together so far are very few[1]. So we have taken a family of samples (4O.m) in which there is a systematic variation in structure alone and there are no other major factors which could affect NMR relaxation times in these systems.

FCNMR Spectrometer :

Field Cycling NMR spectrometer operating at 3 MHz is fabricated and standardized [2] which mainly consists of a pulsed rf spectrometer and an electromagnet which allows fast switching of the fields in lesser than 3 ms. These magnet coils are energized through a bank of power MOSFETs and a stability of the field of about 1 in 10^3 is achieved with the help of a PID type controller and a compensating circuit. Switching circuits are made using power MOSFETs instead of GTOs [1] in our simple FCNMR spectrometer.

Experiments:

Observation of proton spin-lattice relaxation time (T_1) as a function of Larmor frequency over a wide frequency range (~10^4 to ~10^8 Hz), and of temperature (T), in the Nematic, phases of 4O.2, 4O.3, 4O. 4 , 4O. 5, 4O. 7 and 4O. 9 were carried out. Analysis of the data were done based on a composite model[1,3], incorporating the three relevant molecular mechanisms [order director fluctuations (ODF), molecular self-diffusion (SD) and individual reorientations (R)], reflecting the differing influences of the microscopic dynamics on the magnetic dipolar interactions among the spins. The higher frequency data were collected [4,5] as a function of temperature in different phases, while the FCNMR data were measured at fixed temperatures in each of the phases of this sample.

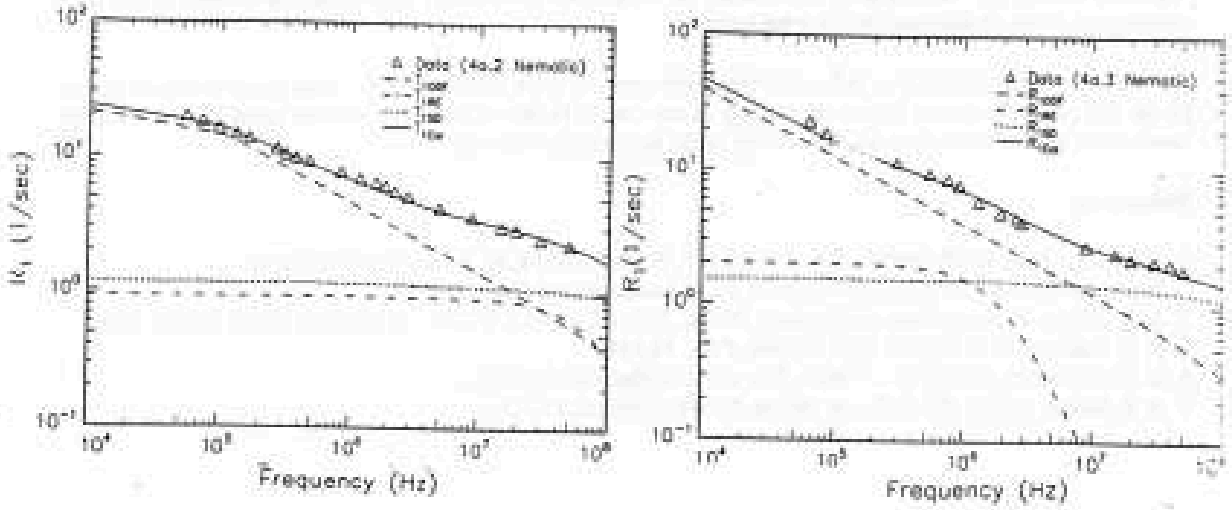

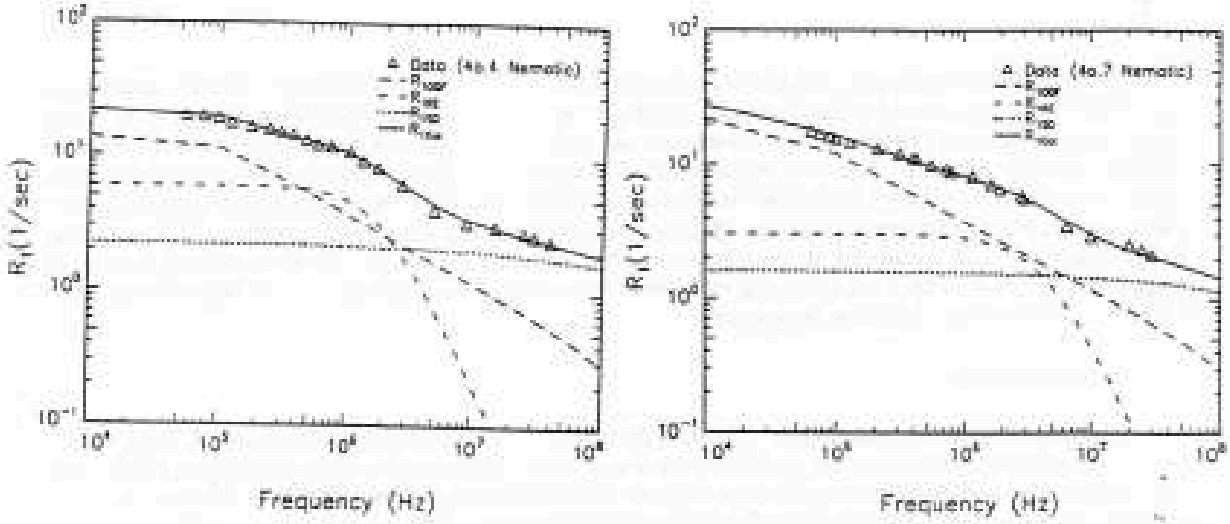

Results and Discussion:

The plots shows the experimental data and theoretical calculations from all the three contributions interms of spectral densities ($1/T_1 = R_1$), where the solid line connecting the data points represents the best ecombination of the three mechanisms. Along with the effect of end chain lengths there is another property which influences the ODF behaviour namely the 'balancing of end chains'. In comparison with earlier high frequency studies on the same samples it is worth considering the following points.

Odd chain samples behaves differently from even chain samples which generally shows more prominent effects on the Molecular Dynamics due to unbalancing of end chains. In case of odd chain samples increase of chain length seems to be more effective than the unbalancing of the end chains of the core.

References:

1. F. Noack , Prog. NMR Spectro. 18, 171 (1986) ; F. Noack and K.H. Schweikert (1994),233 Molecular Dynamics of Liquid Crystals Ed. G. R. Luckhurst and C. A. Veracini.
2. A. S. Sailaja, D. Loganathan and K. Venu, PROC. IND.ACAD.SCI.INDIA, 66 (A) SPL. ISSUE (1996) p-161
3. R. R. Vold and R. L. Vold (1988) J. Chem. Phys. 88,4655
4. G. Ravindranath (1991) Ph. D Thesis, University of Hyderabad, INDIA.
5. A. S. Sailaja (1994) Ph. D Thesis, University of Hyderabad, INDIA.

NMR Proton Dipolar Order Relaxation in Nematics Studied by Field Cycling Technique

O. Mensio, R. C. Zamar and D. J. Pusiol
Facultad de Matemática, Astronomía y Física, Universidad nacional de Córdoba
Ciudad Universitaria, 5000 Córdoba, Argentina

S. Becker and F. Noack
Physikalisches Institut, Universität Stuttgart
Pfaffenwaldring 57, 70550 Stuttgart, Germany

NMR studies of molecular motions in liquid crystals are usually performed by two different kinds of spin-relaxation experiments which provide experimental data useful to disentangle the underlying spectral densities of superimposed molecular reorientations, namely: one being a combination of high-field Zeeman relaxation T_1 with high-field dipolar or quadrupolar order relaxation T_{1D} and T_{1Q} temperature dependent measurements at constant Larmor frequency (υ_L),[1,2] the other kind are frequency dependent T_1 studies over a broad υ_L range, often applying fast-field cycling techniques.[3,4] Nowadays, with the Fast Field-Cycling technique, such frequency dependent measurements are also applicable to T_{1D}. However, it has only been seldom tried and not systematically, mainly because of experimental limitations.

Recently we reported experimental results of T_{1D} and T_1 nematic thermotropic liquid crystals measured over a broad Larmor frequency range (10^3 - 7. 10^7 Hz) by combining the Jeener-Broekaert pulse sequence and Fast Field-Cycling NMR technique. [5] We found that the experimental results clearly disagree with the predictions of the standard two-spins approach for dipolar spin-lattice relaxation rate in nematics.[6] This model considers as the spin system the nearest protons of the benzene rings of the molecule, neglecting the remaining interactions among the protons of the tails and the benzene ring. The predicted dipolar order relaxation is significantly slower than the observed one. As a remarkably feature the difference between the theoretical and experimental T_{1D} in the intermediate and high field range shows the typical frequency dependence of the OFD, $\upsilon_L^{1/2}$. The observed discrepancy indicates the existence of important mechanisms of dipolar relaxation driven by the OFD that are not included into the oversimplified two-spins model. However, at present the nature of such processes remains unknown.

In this work we investigate both theoretically and experimentally the influence of multi-spin interactions and correlations involving more than two spins on the dipolar relaxation rate. With the aim of distinguishing the contributions from the protons of the core and the tails to the dipolar relaxation rate, we measured T_1 and T_{1D} in PAA (para-azoxyanisole) and in the partially deuterated PAA_{ds} in the frequency range 10^3 -10^7 Hz. The former material reflects the dynamics of the complete spin system and the latter the dynamics of the core of the molecules. We found that the OFD are the main mechanism of dipolar order relaxation, similarly to our previous results in nematics 8CB and HpAB.[5] Here, there are also noticeable gaps between the prediction of the isolated spin-pair model and experimental data for both compounds (see Figure). This fact suggests that the failure of the standard model to account for the experimental results is not related directly to the neglecting of the protons of the tails, and that the source of the discrepancy should be ascribed to the omission of relaxation processes associated to the benzene-ring protons. However, after calculating T_{1D} for PAA_{ds} in a general way, within the semiclassical theory and involving all the core spins, we found a negligible correction. This result indicates, in consistence with the observed proton spectra ,[7] that the relevant dipolar interaction is that of the first neighbors and that the failure should be sought in the basic assumptions of the semiclassical weak-order relaxation theory.

Summarizing, the present study shows that a thorough theoretical revision of the effect of the slow fluctuations of the director on the dipolar relaxation rate becomes necessary. In particular, the role of the spin interactions during the lifetime of the fluctuations should be investigated.

Figure

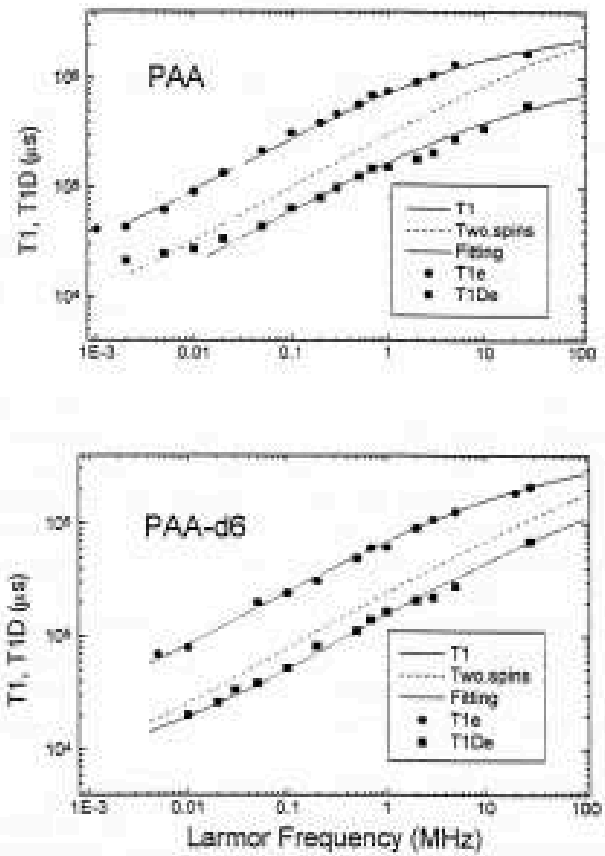

Zeeman and dipolar relaxation rate , measured with the Field Cycling Technique. The dots and squares are experimental T_1 and T_{1D} data respectively. The upper full lines represent the semiclassical model for Zeeman spin-lattice relaxation in nematic liquid crystals. The dashed lines are the predictions of the semiclassical two-spin model for dipolar order relaxation. The disagreement between theory and experiment is similar for both compounds. Finally, the lower full lines are fittings including an additional term related to the OFD.

References

[1] R.Y. Dong, *Nuclear Magnetic Resonance of Liquid Crystals* (Heidelberg, Springer), (1994).
[2] R.L. Vold, W.H. Dackerson, and R.R. Vold, J. Mag. Reson., 43, 213 (1981).
[3] F. Noack, M. Notter, and W. Weiss, Liq. Cryst. 3, 907 (1988).
[4] R.Kimmich, *NMR. Tomography. Diffusometry. Relaxometry* (Berlin , Springer), (1997).
[5] R.C. Zamar, E. Anoardo, O. Menzio, D.J. Pusiol, S. Becker and F. Noack, J. Chem. Phys. , in press.
[6] R.G.C. Mc. Elroy, R.T. Thompson, and M.M. Pintar, Phys.Rev. A **10** (1), 403 (1974).
[7] J.J. Visintainer, E. Bock, R.Y. Dong, and E. Tomchuk. Can. J. Phys., **53**, 1483 (1975).

Setting up a field-cycling spectrometer control

M. Nolte, O. Lips, A. F. Privalov, T. Feiweier and F. Fujara
Fachbereich Physik, Universität Dortmund, 44221 Dortmund, Germany

To control a new built field-cycling spectrometer [1] and to standardize the NMR software used on different spectrometers in our laboratories we need a development environment which allows programs to be quickly designed, modified and adapted to various hardware. LabVIEW [2], a product developed by National Instruments, ideally suits our needs. LabVIEW uses the graphical programming language "G": Programs consist of graphical symbols rather than of textual language. For example the NMR signal is represented as a "data source"-object, which is connected to a "waveform graph"-object. The waveform graph object is predefined in LabVIEW for output of data to the screen and the data source object is either supplied by the data acquisition hardware manufacturer or can be build in conjunction with standard drivers. To present acquired data in the graph two objects are simply wired to each other. A Fourier transformation of the data can be included by inserting a "Fourier transformation"-object between the two existing ones (Additional information is necessary to successfully pass it to the waveform graph, see figure 1). In this way it is simple for the developer and the user to apply modifications to an existing program.

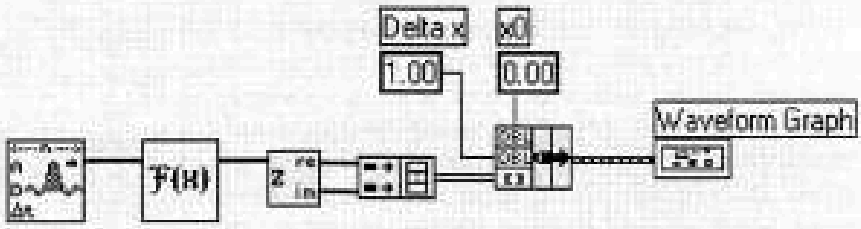

Fig. 1: Example of NMR programming in LabVIEW

The whole system centers on LabVIEW. In a dedicated computer running 32-bit Windows we can easily access the installed hardware with the help of LabVIEW objects. In this way it is possible to control the whole spectrometer from a simple window on the screen, showing only the information and controls we want to see.
The hardware periphery consists of a pulse programmer card, a transient recorder and a gpib-card as shown in figure 2. Furthermore we plan to use a standard I/O-Card and an external device with a 20 Bit-DAC form Analog Devices [3] to control the B_0-field with high stability. We have chosen an external device to minimize noise at the DAC. To be able to switch the values of the B_0-field in a minimum of time, these values have to be stored in the external device containing the DAC. For this reason, the device needs its own memory. The pulse programmer card will have a "reset"- and a "next"-line connected to this device. All values of the B_0-field get transmitted to the device with a standard I/O-Card before the pulse program is run. A pulse programmer card from s.m.i.s. Ltd., which offers 16 TTL output- and 8 TTL input-channels with a time resolution of 100 ns, is used.
Data acquisition is carried out by a transient recorder from IMTEC. The start of the data acquisition is triggered by the pulse programmer card. When the acquisition is finished the data will be transferred to the computer, processed if required and shown on the screen by LabVIEW.

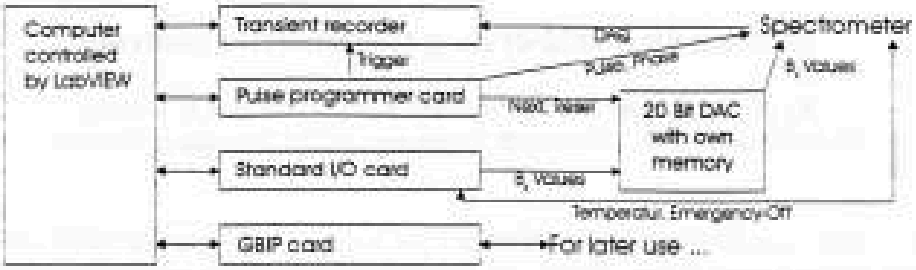

Fig. 2: Block diagram of the controlling hardware

Beside transferring B_0-field values to the external device the I/O-Card will be used for additional purposes e.g. the temperature corrections. The B_0-field value is controlled by taking the voltage at a reference resistor. Since the resistance changes with temperature, these changes have to be taken into account. The temperature of the coil conductor has to be measured as well [4]. If it gets too high, an emergency shutdown will be executed. Other security mechanisms will be implemented without computer control to gain response time.

Forth is the programming language used by the s.m.i.s. pulse programmer card, but less suited for programming purposes. So we defined our own pulse programming language that takes care of the timing specifications of the card and makes it much easier to write pulse programs. The example shown in figure 3 is a pulse command, which applies a pulse of 500 nanoseconds to output no. 11.

Our pulse programming language:
pulse channel11 5e-7

Translated to forth:
6 g@ dup [56832 , 1024 ,]
xor 24 g!
1 times noop
24 g!

Fig. 3: Pulse programming example

Using LabVIEW we hope to build a universal field-cycling spectrometer with fast switching time, which offers an intuitive user-interface and easy data acquisition.

References

[1] O. Lips et al., Design and construction of a fast field-cycling spectrometer with high B_0 homogeneity for the investigation of superionic conductors, to be represented at Symposium Field-Cycling NMR Relaxometry, Berlin 98
[2] http://www.natinst.com/labview/
[3] C. Job, J. Zajicek, M. F. Brown, Rev. Sci. Instrum. 67 2113-2122 (1996) Fast field-cycling nuclear magnetic resonance spectrometer
[4] Thesis of K.-H. Schweikert, University of Stuttgart (1990)

Cross polarisation techniques in fast field cycling NMR spectroscopy

N.F. Peirson and J.A.S. Smith,

Department of Chemistry, King's College London, Strand, London, WC2R 2LS, United Kingdom.

Field cycling NMR is a technique which can provide a wealth of information [1] concerning molecular structure and molecular motion . The Fast Field Cycling (FFC) spectrometer used in this work [2] has a number of advantages over mechanical field cycling [1]. In particular we use the ability of our instrument to maintain intermediate field strengths for variable periods, which would not be practical for a mechanical system.

This paper reports the ^{14}N study of the NH_4^+ ion in $(NH_4)_2S_2O_8$, in which we have previously studied the ^{17}O quadrupole dip spectra [3]. The experiments were performed by monitoring changes in the ^1H NMR signal at about 40 MHz as the field is successively cycled to lower fields (5 kHz to 5 MHz) for variable periods. Three lines are observed in the low frequency spectrum at 20, 48 and 73 kHz, due to cross relaxation of ^1H with the ^{14}N in the NH_4^+ ion. Using multiple switches between high and low fields it is possible to store magnetisation in the ^{14}N bath, saturate the ^1H signal, and then observe the remaining ^{14}N magnetisation. This provides a spectrum for the ^{14}N transitions which is not obscured by the effects of ^1H relaxation. This method can now be used to measure cross polarisation, cross relaxation and ^{14}N relaxation times.

We are also able to populate specific ^{14}N transitions by polarisation from the ^1H bath. This allows the study of the connectivity between transitions. We observe an interesting pattern which might suggest that it is possible to determine the sign of the quadrupole coupling constant.

1. F. Noack, Prog. NMR Spec., **18** (1986) 171 - 276.
2. M. Blanz, T.J. Rayner and J.A.S. Smith, Meas. Sci. Technol., **4** (1993) 48 - 59.
3. N.F. Peirson, J.A.S. Smith and D. Stephenson, Z. Naturforsch. **49a**, (1994) 351 - 353.

E - mail: neil.peirson@kcl.ac.uk
john.smith@kcl.ac.uk

Field-Cycling Dynamic Nuclear Polarization and Relaxometry in Low Magnetic Fields: Techniques and Applications

V. Sapunov, A. Sabanin, A. Denisov, O. Dekusar, D. Savel'ev
Quantum Magnetometry Laboratory
Department of Theoretical and Applied Physics
Urals State Technical University
Mira St., 19, Ekaterinburg, 620002, Russia
E-mail: sva@ktf.rcupi.e-burg.su

The laboratory QM develops the methods of a weak magnetic field NMR with the purpose of research of geological objects and creation of the geophysical equipment. The best results are reached by method of field-cycling, that is caused by increase of relation signal/noise and opportunity of research of spectral density of nuclear movements in a wide range. In the report are submitted the FC NMR equipment and number of examples of its application [1-6].

1. FC DNP spectrometer of a range 0,05-200 Oe [1]

The sequence of action consists of three periods: polarization at a field induction 10-200 Oe; relaxation or Overhauser's polarization at 0,05-20 Oe with frequency electronic pumping in a range 30-200 MHz; registration by a spin echo methods at the fixed field 11,74 Oe. To create magnetic fields in any of periods are using solenoid and Helmholtz coils. The given realization of experiment is chosen for measurement T_1 in a range of magnetic fields 0,05-200 Oe and, mainly, for research DNP at various kinds of electron pumping ($h_1 \perp H_0$ at usual saturation; $h_1 \parallel H_0$ when parallel pumping and DNP under circular $h_1\pm$ polarization). Field-cycling method allows to raise signal/noise ratio at the 3-40 cm^3 samples volume and it to set norms DNP signals.

Table shows the results of experiment and account on FC parallel DNP [2-3] in solutions TANO (A^{∞}/f - normalized DNP amplification, α/β - parity of spin rotation and anisotropy hyperfine interaction, T_1 - total and T_2^{sr} - spin rotation times electron relaxation, τ_R - time of radical rotary diffusion and a_h - settlement hydrodynamic radius). Ho=3 Oe. Transition 2-6 forbidden in strong magnetic field is saturated.

Solution	A^{∞}/f	α/β	T_1, 10^{7},s	T_2^{sr}, 10^{7},s	τ_R, 10^{11},s	a_h, A°
Water	200 ± 10	0,14 ± 0,04	2,53	6,88	1,9 ± 0,6	2,6 ± 0,3
Ethanol	146 ± 9	1,04 ± 0,16	0,87	1,07	1,6 ± 0,3	2,6 ± 0,2
Dimetil-formamide	98 ± 9	1,00 ± 0,20	2,27	2,80	1,3 ± 0,3	2,5 ± 0,2
Dekane	95 ± 20	1,06 ± 0,41	1,52	1,85	0,9 ± 0,4	2,2 ± 0,3
Heptane	< 20	> 5,7	0,87	0,9	< 0,34	< 2,0
Toluene	123 ±16	1,7 ± 0,5	1,44	2,9	0,4 ± 0,1	1,9 ± 0,2

At present analogous experiments in porous media (powder) are preparing.

2. Proton relaxometer of Earth's magnetic field

The principle of action of the equipment is similar to item 1. The polarization and registration is carried out by the double solenoid (noiseproof) with an internal diameter 120 mm. The solenoid is perpendicular to a magnetic field of the Earth. The signal proton precession is formed by switching off polarization current for 30 μS. The broadband connection on noise is used, that allows to register times relaxation up to 10 mS. The computer processing and accumulation of a signal provide sensitivity up to 0,1% of a liquid in volume of a sample D115x60 mm.

Relaxometer is intended for non-destructive evaluation of porosity and permeability of the rock (cores) near to drillhole. An index of free fluid and curves of proton magnetic relaxation are determined. For example "T2 cutoff" around 30 mS represent the ability of fluid to be produced or remain in drillhole [4].

3. Nuclear magnetic logging tools

The NMR methods is known to be used for provide direct information of the pore structure and pore fluid in the drillholes. In order to improve FC NMR of Earth's magnetic field we use the simultaneous signal recording of the Overhauser proton sensors and proton precession signal of oil. This ensures the signal/noise increasing and the possibility to use the spin echo method. Simple spin echo method also allow to realize radial tomography that is impotent to excluding of the harmful indrillhole proton signal. To similar we investigate using of the gradient magnetic impulse [5].

4. FC Overhauser's magnetometer [6]

The given device is practical application of a method of a field-cycling NMR and accompanies with all mentioned above equipment. The effective polarization field at registration of a proton precession is 2000-5000 Oe. Special algorithms and processor processing for definition of frequency of a signal are used. The mode of broadband connection on noise and digital processing used in the given equipment, allow to expand reception band of a signal without decrease of sensitivity and to increase speed of operation. In our industrial magnetometer POS-1 the accuracy and sensitivity in the range above 0.2 Oe up to 0.00001% is achieved.

Acknowledgments

The authors thank RFFI for Grant No. 98-03-332a and ZapSibNIIGeofizika, Bison, Newmont Exploration Ltd. for supporting our studies, of which this work is part.

References

[1] V. Sapunov, A. Doroshek A, A. Filatov... PTE, N 4, p. 114-116 (1988)
[2] V. Sapunov, A.Gavrilin, A. Denisov... Ampere, p.32 (1996)
[3] V. Sapunov, A.Chirkov Radiospectroscopy, Perm Univ.press, p.59-63 (1989)
[4] J. White. Applications of Downhole MRI..., SPE, Aberdeen (1997)
[5] A. Denisov... Radiospectroscopy, Perm Univ.press, p.187-192 (1993)
[6] O. Dekusar., A. Denisov... 29th Ampere (1998) [to be represented]

FIELD CYCLING CIRCUIT FOR A NUCLEAR MAGNETIC RESONANCE SPECTROMETER

D. M. Sousa *, P. Verdelho *, G. D. Marques *, A. C. Ribeiro *,#, P. J. Sebastião *,#

* Universidade Técnica de Lisboa, IST, Av. Rovisco Pais 1, 1096 Lisboa Codex, Portugal

Centro de Física da Matéria Condensada, Universidade de Lisboa, Av. Prof. Gama Pinto, 2, 1699 Lisboa Codex, Portugal; pedros@lince.cii.fc.ul.pt

In this paper a new field cycling circuit for a NMR spectrometer is proposed. The topology, the operating principle of the circuit and some simulation results are presented and discussed. Our circuit is based on a well-known topology and uses a specific hysteretic control circuit with state-of-the-art power semiconductors. Our simulations show that fast current transient responses and good dynamics can be obtained. Fast Field Cycling power supplies based on this circuit can present better performances and easier maintenance.

INTRODUCTION

Experimental Fast Field Cycling (FFC) Nuclear Magnetic Resonance (NMR) is a powerful spectroscopic technique which is strongly dependent on the performance of the used magnet and suitable power supply [1, 2, 3]. The continuous development of new power semiconductors can be useful on the design of new fast switchable current supplies to increase the performance of FFC NMR spectrometers. In particular the new circuits should be more efficient and easy to maintain, both important aspects of home built equipment.

The induction magnetic field is a function of the cycling current. This current depends on the power capacity and the electrical parameters of the magnet. The current should be as high as possible and with the minimum possible ripple. The current source must supply the magnet with sharp current pulses of variable length having adjustable and smooth high and low current levels. Different concepts and operating principles have been used to implement these requirements [4, 5, 6].

In this work, we propose a new field cycling circuit based on a different circuit topology. It uses semiconductors with high current and voltage handling capacities and a different concept for the control circuit.

MAIN CIRCUIT AND OPERATION

The main circuit is shown in fig. 1. It represents a well-known power circuit with switching semiconductors.

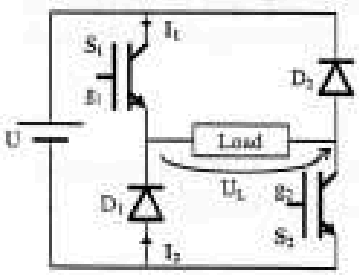

Figure 1 - Main circuit topology

This circuit has the following simple transfer function, $U_L = \left(g_1 - \overline{g_2}\right) \cdot U$, where $g_j = 0$ when the semiconductor j is OFF and $g_j = 1$ when the semiconductor j is ON.

The load current increases when $U_L > 0$ and it decreases when $U_L < 0$.

In order to be used in a fast field cycling NMR spectrometer, this circuit needs a specific control circuit with the characteristic shown in fig. 2. This circuit is an hysteretic controller with three levels (1, 0, -1). The control circuit output signal is a function of control error signal (ΔI), defined as the difference of the reference current (i_{ref}) and the magnet current (i_{Load}).

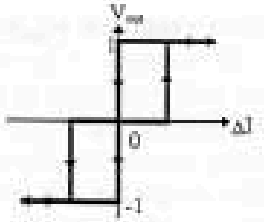

Figure 2 - Control circuit characteristic

The semiconductor's state is controlled in such a way that different paths for the current can be established. For the level 1 both semiconductors are ON ($g_j = 1$); for the level -1 both semiconductors are OFF ($g_j = 0$); for the level 0: if $\Delta I > 0$, S_1 is switched ON and S_2 is switched OFF and vice-versa if $\Delta I < 0$ (see fig. 2). Figs. 3 and 4 present all the above situations.

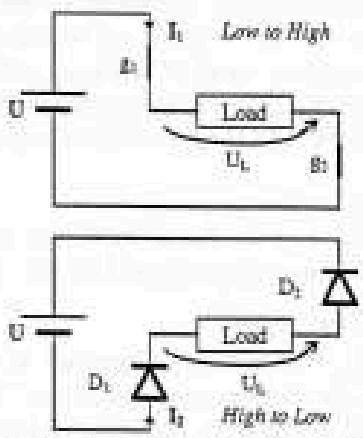

Figure 3 - Current paths for the different transients

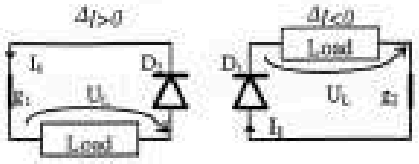

Figure 4 - Current paths for the steady state

SIMULATION RESULTS

The simulation results of the proposed current cycling circuit are shown in the figs. 5 and 6. These results were obtained considering the electrical parameters of a real magnet [6].

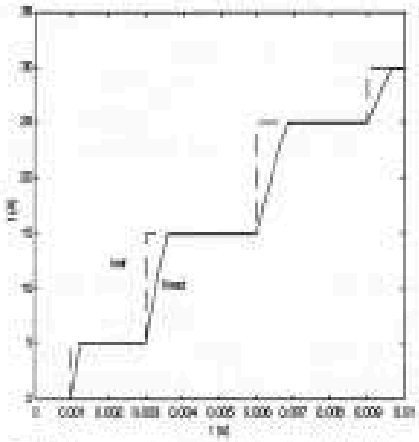

Figure 5 - Current transients from low to high levels of the reference and load signals (— i_{ref}; — $i_{L\,(mod)}$)

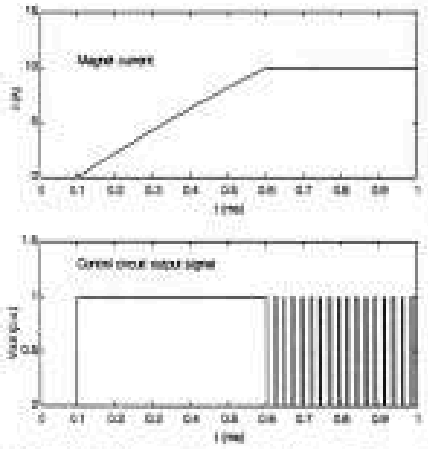

Figure 6 - Magnet current and control circuit output signal for i_{ref} = 10 A

The results shown in fig. 5 are similar to other referred in the literature and are adequate for a PFC NMR spectrometer [4, 5, 6]. Current transients from a high level to a low level have the same behavior.

The time evolution of the output control circuit signal and respective magnet current are presented in fig. 6. The control circuit output signal has the expected behavior.

Another important parameter for the field stability is the current ripple. In fig. 7 we show the typical triangular wave form of the current's ripple (for the sake of clarity the amplitude of the ripple was increased). The current ripple can be reduced, in principle, down to the operational amplifiers noise level, with a well dimensioned and implemented control circuit.

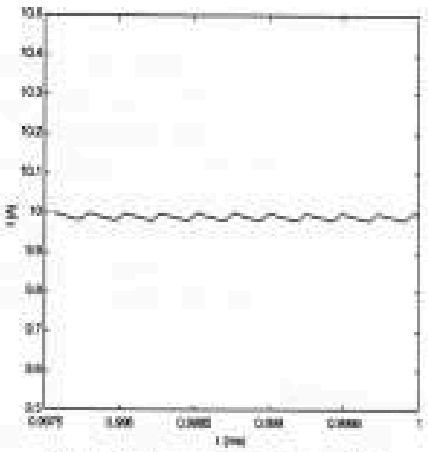

Figure 7 - Current ripple for i_{ref} = 10 A

Another important signal to analyze is the static error which has the same form of the ripple signal. The amplitude of this signal can also be adjusted acting on the control circuit.

As final remarks we would like to point out that with a simple circuit topology, state-of-the-art power semiconductors and a different control concept, a simple fast switchable, low ripple and easy to maintain PFC NMR spectrometer's power supply can be implemented.

REFERENCES

[1] Noack, F.; Progress in NMR Spectroscopy, Vol. 18, pp. 171-276, 1986

[2] Schweikert, Karl-Heinz: Thesis, Physikalisches Institut der Universität Stuttgart, Stuttgart, FGR, 1990

[3] Rommel, E. ; Thesis, Physikalisches Institut der Universität Stuttgart, Stuttgart, FGR, 1988

[4] Rommel, E.; Mischker, K.; Osswald, G.; Schweikert, K.H. and Noack, F., Journal of Magnetic Resonance, 70, pp. 219-234, 1986

[5] Job, Constantin; Zajicek, Jaroslav; Brown, Michel F., Review of Scientific Instruments, 67 (6): 2113-2122, June 1996

[6] Sousa, D.M.; Rommel, E.; Santana, J.; Fernando Silva, J.; Sebastião, P.J.; Ribeiro, A.C., 7th European Conference on Power Electronics and Applications, pp. 2.285-2.290, Norway, 1997

Pulsed Field-Cycled ENDOR Spectroscopy

G. Sturm, D. Kilian, A. Lötz, J. Voitländer
Institut für Physikalische Chemie der Universität München, Sophienstr. 11, D-80333 München
aloetz@olymp.phys.chemie.uni-muenchen.de

An experiment is described that detects hyperfine transitions in zero field with pulsed EPR and field cycling.

Introduction

One way of improving the resolution of powder spectra in EPR spectroscopy is high-field EPR [1] with its "single crystal like" spectra on account of the enhanced spectral resolution. Yet, complete removal of the inhomogeneous line broadenings of disordered samples is possible in zero field with its spatial isotropy (zero field resonance, ZFR [2]). The main disadvantage of ZFR is its low sensitivity. However, it is possible to combine the sensitivity of X-band EPR and the resolution of zero-field EPR by *field-cycling spectroscopy*, with excitation of transitions between splittings in zero field and detection in high field. Recently, a *CW* field-cycled ENDOR experiment has been described [3]. In this paper we present the first report on a *pulsed* version of this experiment.

Experimental

The experiment was carried out with our field-cycling spectrometer described elsewhere [4]. The field-cycling EPR probehead [5] was modified (Fig. 1) and now includes a 14-turn ENDOR coil for the excitation of zero-field transitions. The coil is twisted around a cylindrical Rexolite support and fixed by a teflon ribbon. Inside the ENDOR-coil there is a rexolite holder for a bridged loop-gap resonator [6] made by chemical deposition of silver at room temperature.

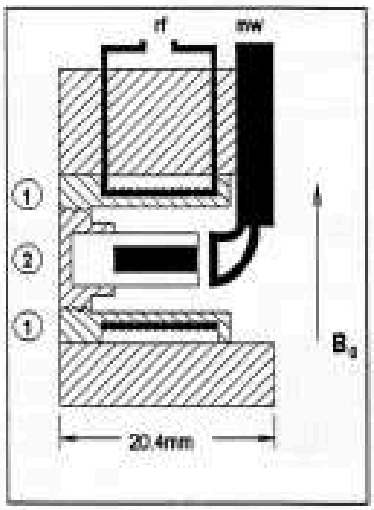

Fig. 1: Probehead for pulsed field-cycled ENDOR. ❶ Rexolite ENDOR coil support. ❷ Rexolite holder for the bridged loop-gap resonator.

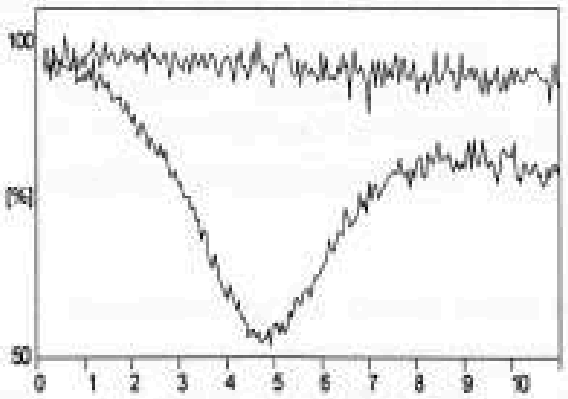

Fig. 2: Pulsed field-cycled ENDOR spectrum of a coal sample. Echo intensity in % versus rf irradiation frequency in MHz. Lower trace: Recovered EPR amplitude, after irradiation in zero field. No accumulation. Upper trace: Equal experimental conditions, yet without rf irradiation. This baseline of the spectrum represents only 30 % of the EPR signal without field cycling on account of spin-lattice relaxation in zero field.

Results and Discussion

Fig. 2 (lower trace) shows the first pulsed field-cycled ENDOR spectrum, the sample being coal at 4.2 K (impregnation pitch HL, VfT AG Castrop-Rauxel). The magnetic field dropped within 0.5 ms from high field to zero field. In zero field the sample was irradiated for 800 µs with a frequency stepped by an equal increment of 50 kHz after each cycle. The echo intensity was monitored 2.5 ms after switching back to high field. Only one broad ENDOR line can be seen, similar to the broad powder patterns found in room temperature HYSCORE-experiments of the same sample, and assigned to ^{13}C hyperfine couplings [7]. A comparison with the upper trace of Fig. 2, obtained without rf irradiation in zero field, shows the remarkably strong ENDOR effect of 50 %. Studies with an improved magnetic field-cycling apparatus and samples for which we expect narrower ENDOR lines are still in progress.

Conclusion

The first pulsed field-cycled ENDOR spectrum is presented. We expect that future studies with other samples will show the high-resolution capability of this method.

[1] Y. S. Lebedev, In: Modern Pulsed and Continous-Wave Electron Spin Resonance, L. Kevan and M. K. Bowman (eds.), J. Wiley, New York, pp. 365-404 (1990)
[2] R. Bramley and S. J. Strach, Chem. Rev. 98, 49-82 (1983)
[3] J. Krzystek, M. Notter, and A. L. Kwiram, J. Phys. Chem. 98, 3559-3561 (1994)
[4] J. Olliges, A. Lötz, D. Kilian, and J. Voitländer, J. Chem. Phys. 103, 9568-9573 (1995)
[5] G. Sturm, A. Lötz, and J. Voitländer, J. Magn. Res. 127, 105-108 (1997)
[6] S. Pfenninger, J. Forrer, and A. Schweiger, Rev. Sci. Instrum. 59, 752-760 (1988)
[7] P. Höfer, J. Magn. Res. 111, 77-86 (1994)

Field-cycling NMR study of slow molecular dynamics in nematic liquid crystals in porous glass

M.V.Terekhov, S.V.Dvinskikh
Institute of Physics, St.Petersburg State University, 198904, St.Petersburg, Russia
e-mail: terehov@snoopy.niif.spb.su

Microconfined liquid crystals are of considerable interest from the both of theoretical and technological point of view. In recent years the NMR method has been successfully applied to these systems to obtain an information on director field configuration, order parameter distribution, features of phase transition and molecular anchoring on liquid crystal-pore wall interface. Confinement of the liquid crystals in submicron pore matrix results in considerable change of molecular dynamics. The main change in spin-lattice relaxation due to restriction geometry effect, as compared with bulk sample, is expected in a low Larmour frequency range.

In current work we present an investigation of slow molecular dynamics in nematic 5CB liquid crystals confined in submicron size porous glass by field cycling proton NMR relaxometry in a wide frequency range $1\cdot10^2$-$2\cdot10^7$Hz. Also the results of the application of zero-field NMR spectroscopy to this system are reported and compared with relaxation data. In liquid crystals in glassy porous matrix the cross-relaxation contribution [1] is absent, thus giving the opportunity to observe more clearly, as compared with the previous studies, the other relaxation mechanisms appeared under confinement. Different continuos-pore glass matrices with average pore size from 7 nm to 200 nm were used. Home-built field-cycling relaxometer and its modification for zero field NMR measurements is described in [2].

In the entire frequency range spin-lattice relaxation rate is smallest for bulk sample and enlarges with the pore size decrease. The relaxation rate difference between bulk and confined samples is strongest in kHz frequency range. The numerical analysis of the experimental data have been performed to distinguish the most effective relaxation mechanisms in the samples with different pore size. It was found that in samples with large mean pore size the translational-induced reorientation (TR) relaxation mechanism dominates in range 10^2-$3\cdot10^4$ Hz, while in $3\cdot10^4$-10^6 Hz frequency range the order director fluctuations (ODF) is more effective process. In sample with 7 nm mean pore size the main contribution to the relaxation was accounted for by the self-diffusion processes (SD) slowed down in near-surface area, while the effect of TR and ODF processes is negligible in the studied frequency range. The numerical analysis of relaxation process in large pore

samples have been updated with account of molecular motion slowing down in the near-surface layers. This approach allows improvement the relaxation data fit within 30-700KHz frequency region [3].

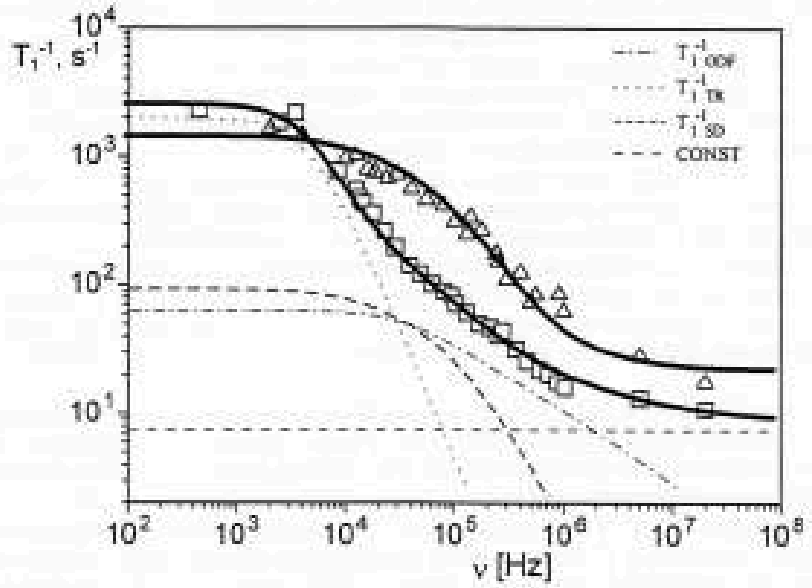

Fig 1. T_1^{-1} dispersion of nematic 5CB confined in 200nm (□) and 7nm (Δ) average size glassy pores. Solid lines represent the numerical fit with account of order directory fluctuation, translational-induced molecular reorientation and self-diffusion relaxation contributions. Broken lines are the separate contributions for 200nm sample.

Zero-field ^{1}H NMR spectrum of the 5CB in 200 nm and 80 nm pore shows a characteristic doublet structure. By contrast, zero-field spectrum of the 7nm sample has no resolved structure. A narrowing of spectrum, as compared with bulk sample and sample with large pore size, is accounted for by the combined effect of the motional averaging caused by translational diffusion induced reorientation and order parameter distribution [3].

References

[1]D.Schwarze-Haller, F.Noack, M.Vilfan, G.P.Crawford, J.Chem.Phys **105**, 4823 (1996).

[2] (a) S.V.Dvinskikh, Yu.V.Molchanov, S.R.Filippov. Instr.Exp.Tech., **31**, 1287 (1988), (b) M.V.Terekhov, S.V.Dvinskikh, Instr.Exp.Tech., **39**, 452 (1996).

[3] M.V.Terekhov, S.V.Dvinskikh, A.F.Privalov. Submitted to Appl.Magn.Res.

Properties Effecting The Relaxivity of Dendrimer MRI Contrast Agents: FCR and EPR Studies
E.C. Wiener*, M.W. Brechbiel+, J. Chen, L. Belford*, and R. Clarkson*, *University of Illinois @ Urbana-Champaign, +National Institutes of Health, NCI, USA.

Introduction:

We have prepared macromolecular MRI contrast agents based on dendritic polymers.[1] The geometric increase in the number of surface groups coupled with only a linear increase in the diameter of these polymers give them a unique potential application in systems that require amplification. The preparation of contrast agents for medical diagnostic imaging is one such application. The exquisite synthetic control over the critical molecular design parameters of dendrimers also allows us to examine many features that might effect the efficiency of these agents. These polymers are prepared by a series of reiterative reactions starting with an initiator core. Each iteration defines a generation. We have coupled various ion-chelate complexes to the surface groups of either ammonia or ethylenediamine core polyamidoamine and 1,4-diaminobutane core polyethyleneimine core dendrimers.

Field cycling relaxometry and EPR were used to characterize the various contributions of the rotational correlation time, electronic relaxation time, and water residence time. We report that both dendrimer family and generation effect the relaxivity of dendrimer-based agents. The dendrimer family also effects the size of the polymer at which the water residence time limits the relaxivity.

Methods:

Ammonia and ethylenediamine core polyamidoamine (PAMAM), pharmaceutical grade, were provided by the Michigan Molecular Institute, and 1,4-diaminobutane core polypropyleneimine (PPI) dendrimers were provided by Dutch State Mines. The chelating agents 2-(4-isothiocyanatobenzyl)-6-methyl-diethylenetriaminepentaacetic acid and 2-(4'-isothiocyanatobenzyl)-1,4,7,10-tetraazacyclododecane-N,N',N'',N'''-tetraacetic acid were prepared following the methods of Brechbiel[2] and McMurry[3], respectively. Conjugation of the isothiocyanates to the terminal amines on the dendrimers were carried out as described by Wiener.[1] This procedure results in a thiourea bond linking the chelate to the dendrimer to form PAMAM-TU-DTPA and PAMAM-TU-Bz-DOTA derivatives.

Longitudinal relaxation rates, $1/T_1$, were obtained on an IBM field cycling relaxometer built by Koenig and Brown. Nuclear magnetic relaxation dispersion, NMRD, profiles were obtained as described by Wiener et. al..[1] The magnetic field ranged from 0.47 mT to 1.17 T. Relaxivities were obtained from the slope of the graph of $1/T_1$ vs [Gd] and/or by subtraction of the relaxation rate in the absence of the paramagnetic ion from that containing Gd(III) and dividing this difference by the [Gd(III)].

The [Gd(III)] in each sample was determined by inductively-coupled argon plasma-mass spectroscopy using a Perkin-Elmer Sciex ELAN 5000 ICP-MS instrument.

EPR measurements and vanadyl complexation were carried out as described by Wiener et al..[4] Best values for the A- and g- matrices were determined from the rigid limit spectra with SIMPOW. Both isotropic and anisotropic rotational correlation times are determined using the program FIT. For the anisotropic fits two diffusion times were used. All computations were performed on an IBM RS/6000 320 MHZ. The powder patterns of the dendrimers converge by ~130 °C.

Results and Discussion:

Unlike contrast agents made from linear polymers those prepared from some families of dendrimers show an increase in relaxivity as the molecular weight or generation increases. We observed this with two different ammonia core PAMAM derivatives one with an N,N-dipropionate surface and the PAMAM-TU-DTPA derivative. For gadolinium complexes of the N,N-dipropionate PAMAMs, the relaxivity increased from 65 to 120 $(mM * s)^{-1}$ as the generation increased from 1.5 to 8.5. For gadolinium complexes of the PAMAM-TU-DTPA derivative the relaxivity increase from 21.3 ± 0.03 to 34 ± 4 $(mM * s)^{-1}$ at 20 °C and 25 MHz as the generation went from 2 to 6.

We next tested the hypothesis that this increase in relaxivity was associated with an increase in the rotational correlation time. Early studies by Metzler et al indicate that ammonia core PAMAMs have

two types of motions which he calls internal and terminal. The rotational correlation times of the terminal motions increase by only a factor of about two as the generation increases from 1 to 7. Those of the internal motions increase by more than twenty times. Calculations of the rotational correlation times from EPR data of vanadyl complexes of the generation 2 and 6 PAMAM-TU-DTPA derivatives give average rotational correlation times that match the range of internal motions obtained by Metzler for the corresponding generation. Analysis of the data with an anisotropic model consisting of two rotational correlation times resulted in little change in the time corresponding to rotation about the axis that linked the chelate to the ammonia core for the generation 2 and 6 PAMAM-TU-DTPA derivative. However the rotational correlation time that corresponds to the overall molecular tumbling of the two molecules increased from 10 to 31 ns at 25 °C as the generation went from 2 to 6.

The dependence of the relaxivity on either the rotational correlation time or the water residence time can be determined by examining the NMRD profiles at different temperatures. Increasing the temperature decreases both the rotational correlation time and the water residence time. Decreasing the rotational correlation time also decreases the relaxivity of a rotationally dependent ion-chelate complex. Decreasing the water residence time will increase the relaxivity for ion-chelate complexes with long limiting water residence times. Therefor an increase in the relaxivity associate with an increase in temperature implies that the relaxivity is limited by the water residence time. Our data for gadolinium complexes of the PAMAM-TU-DTPA and PAMAM-TU-Bz-DOTA derivative indicate that as the system becomes rotationally constrained the water residence time can limit the relaxivity. The relaxivity of the generation 6, for both the PAMAM-TU-DTPA and PAMAM-TU-Bz-DOTA derivatives, increased with increasing temperature. Indicating that the water residence time dominates the relaxivity of these agents. Only the relaxivity of the generation 2 PAMAM-TU-DTPA derivative decreased.

The temperature studies indicate that the rotational correlation time dominates the relaxivity of the generation 2 PAMAM-TU-DTPA derivative. This implies that a dendrimer of a different family and shape might have a higher relaxivity. In particular an ellipsoid derivative should have a higher rotational correlation time and therefor a higher relaxivity. The polypropyleneimine and EDA core PAMAMs should have elongated structures and higher relaxivities. We tested this hypothesis. The relaxivity of the generation 2 PPI-TU-DTPA derivative is 30 ± 2 relative to 21.3 ± 0.03 $(mM * s)^{-1}$ for the same generation ammonia core PAMAM-TU-DTPA derivative. EPR studies indicate that the rotational correlation time of the motion about the axis connecting the chelate to the core is the same for both derivatives. However the rotational correlation time for the overall molecular tumbling of the molecules are quite different and are 10 and 33 ns at 25 °C for the ammonia core PAMAM-TU-DTPA and PPI-TU-DTPA derivatives respectively. This is consistent with an elongated structure.

These findings characterize the dependence of dendrimer-based contrast agents. They show that the relaxivity of these agents increases with the rotational correlation time, and that the water residence time of Gd(III)- DTPA and Gd(III)-DOTA can limit the relaxivity of the larger derivatives. The data show that the dendrimer family, and generation can effect the relaxivity. Further more as different chelates have different water residence times, the chelate can also determine the generation that the water residence time becomes important.

Acknowledgments:

We thank Dr. Paul Lauterbur for his helpful comments. This work was supported by PHS 5 P41 RR05964-06, and 1 R29 CA61918, the University of Illinois, the Beckman Institute, and the Servants Foundation.

References:

1. Wiener, E.C., Brechbiel, M.W., Brothers, H., Magin, R.L., Gansow, O.A., Tomalia, D.A., and Lauterbur, P.C. 1994. Magn. Reson. Med. 31(1): 1.
2. Brechbiel, M.W. and Gansow, O.A. 1991. Bioconjugate Chem. 2, 187.
3. McMurry, T.J., Brechbiel, M., Kumar, K., and Gansow, O.A. 1992. Bioconjugate Chem. 3, 108.
4. Wiener, E.C., Auteri, F.P., Chen, J.W., Brechbiel, M.W., Gansow, O.A., Schneider, D.S., Belford, R.L., Clarkson, R.B., and Lauterbur, P.C. 1996. J. Am. Chem. Soc. 118, 7774.

Field Cycling Method for Dipolar Order Relaxation Study in Liquid Crystals.

R. Zamar, E. Anoardo, O. Mensio and D. Pusiol.
Facultad de Matemática, Astronomía y Física. Universidad Nacional de Córdoba. Medina Allende y Haya de La Torre. Ciudad Universitaria. 5010 - Córdoba - Argentina.

S. Becker and F. Noack
Physikalisches Institut der Universität Stuttgart. Pfaffenwaldring 57. 7000 Stuttgart 80. Germany.

Dipolar energy relaxation measurements using conventional Jeener-Broekaert sequence becomes a dificult experiment for Larmor frequencies under 2 MHz. In the low frequency regime, the signal to noise ratio of the dipolar echo becomes strongly reduced because of the poor spin polarization. The field cycling method consist in polarizing the spin system and performing the Zeeman to dipolar order transfer in a high field, while allowing the system to relax in a lower field [1]. The polarizing magnetic field is switched off after the solid echo and the detection Zeeman field is switched on to aquire the dipolar echo (figure 1).

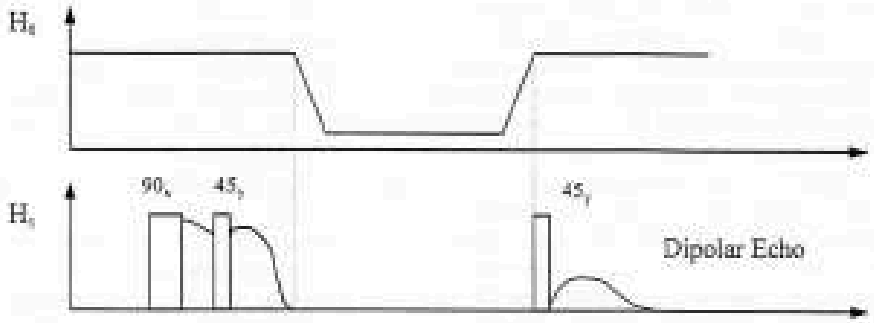

Figure 1

As an application, in this work we present an experimental study of T_{1D} in nematic thermotropic liquid crystals measured over a broad Larmor frequency range (10^3 - $6x10^7$ Hz).

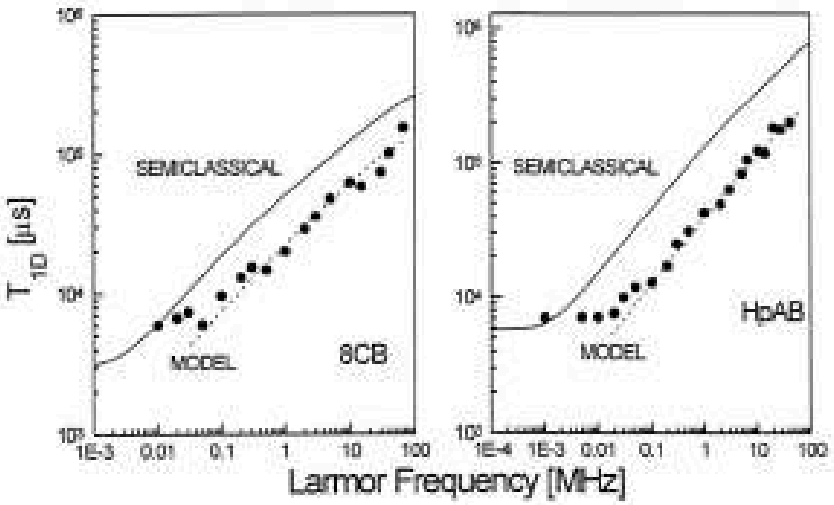

Figure 2 shows experimental T_{1D} values for two thermotropic nematogens: 8CB (309 ^{0}K) and HpAB (383 ^{0}K). The solid line shows the expected T_{1D} frequency dependence obtained from the semiclassical two spin model relaxation theory. To obtain this curve we fited T_1 dispersion data of these compounds (in the same experimental conditions) in order to evaluate the envolved spectral densities. Experimental results are in clear disagreement with the predictions of the standard two-spin approach for dipolar spin-lattice relaxation rate in nematics (the difference between theory and experiments has a noticeably dependence on the Larmor frequency). To fit the experimental data (dashed line in figure 2) in the high and intermediate field range, a $\omega^{1/2}$ correction term must be added to the traditional model [2]. This aditional contribution shows a typical frequency dependence corresponding to order fluctuations of the nematic director (OFD). These results reveal the existence of important mechanisms of dipolar relaxation which are driven by the OFD and that are not included into the usual two-spins model. We found a strictly zero correction for T_1 after including multispin correlations, within the assumption of spin temperature. This result does not depend neither on the location of the involved spins, nor on the kind of the molecular motions.

References.

[1] F. Noack, S. Becker and J. Struppe; Annual Repports on NMR Spectroscopy (1996).

[2] R. Zamar, E. Anoardo, O. Mensio, D. Pusiol, S. Becker and F. Noack, J. Chem. Phys., in press (1998).

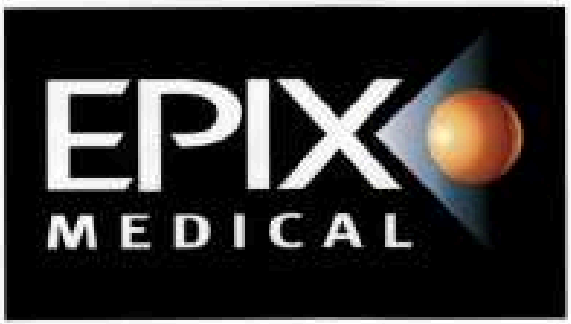

EPIX Medical, based in Cambridge, MA, is developing targeted contrast agents to improve the capability of MRI as a tool to diagnose a variety of diseases. The Company's principal product under development, MS-325, is an investigational new drug currently in Phase II clinical trials for peripheral vascular disease, coronary artery disease, and breast cancer. MS-325 is a gadolinium chelate which binds to the blood protein albumin, remains at high concentrations in the bloodstream throughout the MRI exam, and is designed to be excreted safely through the kidneys over time. Because of its affinity for albumin, MS-325 provides the image time and signal strength needed to obtain a high-contrast, high-resolution image of the cardiovascular system.

EPIX also performs research in the areas of water proton relaxation of metal chelates, coordination chemistry, biophysics, and biochemistry.

EPIX Medical, Inc.
71 Rogers St.
Cambridge, MA 02142
Phone: 617-499-1400
Fax: 617-499-1414
Internet: www.epixmed.com

SPINMASTER-FFC

The versatile Fast Field Cycling NMR Relaxometer

STELAR s.n.c.

Via E. Fermi, 4 27035 Mede (PV) ITALY
Tel. +39 384 820096 Fax. +39 384 805056
e-mail: stelinf@tin.it

List of Participants

Name	email		Pages
Anoardo, Esteban	anoardo@famaf.fis.uncor.edu	Córdoba, Argentina	9,29, 57,92
Assfalg, Michael	michael.assfalg@physik.uni-ulm.de	Ulm, Germany	59
Bryant, Robert G.	rgb4g@virginia.edu	Charlottesville, VA, USA	22,44, 63
Caravan, Peter	pcaravan@epixmed.com	Cambridge, MA USA	
Digilio, G.		Torino, Italy	55
Denisov, Vladimir	vladimir.denisov@fkem2.lth.se	Lund, Sweden	16
Dinesen, Timothy R. J.	trd3f@virginia.edu	Charlottesville, VA, USA	63
Fantazzini, Paola	sciennin4@ingbo1.ing.unibo.it	Bologna, Italy	
Fasano, Mauro	fasano@ch.unito.it	Torino, Italy	53
Fatkullin, Nail	nfatkull@phys.ksu.ras.ru	Kazan, Russia	33,59
Fenchenko, Konstantin	oleg.opanasyuk@ksu.ru	Kazan, Russia	65
Ferrante, Gianni	stelinf@tin.it	Mede (PV), Italy	55,61
Fischer, Elmar	elmar.fischer@physik.uni-ulm.de	Ulm, Germany	
Gille, Klaus	klaus.gille@physik.uni-ulm.de	Ulm, Germany	
Gillis, Pierre	pierre.gillis@umh.ac.be	Mons, Belgium	15
Gottschalk, Michael	michael.gottschalk@fkem2.lth.se	Lund, Sweden	
Grimmer, A. R.	ar.grimmer@rz.hu-berlin.de	Berlin, Germany	
Grinberg, Farida	farida.grinberg@physik.uni-ulm.de	Ulm, Germany	37,59

Halle, Bertil	bertil.halle@fkem2.lth.se	Lund, Sweden	16,35
Horsewill, A. J.	A.Horsewill@nottingham.ac.uk	Nottingham, UK	25
Jung, Miewon	mwjung@cc.sungshin.ac.kr	Seoul, Korea	69,70
Karnaukh, Grigorii E.,	tan@icp.ac.ru	Chernogolovka, Russia	71
Kimmich, Rainer	rainer.kimmich@physik.uni-ulm.de	Ulm, Germany	37,46, 57,59
King, J. Derwin	dking@swri.edu	San Antonio, Texas, USA	7
Korb, Jean-Pierre	jpk@pmcsun1.polytechnique.fr	Palaiseau, France	44
Krushelnitsky, Alexey G.	Krushelnitsky@sci.kcn.ru	Kazan, Russia	20
Kulagina, T. P.	tan@icp.ac.ru	Chernogolovka, Russia	71
Lips, Oliver	oliver@e3.physik.uni-dortmund.de	Dortmund, Germany	73,79
Loetz, Albert	aloetz@olymp.phys.chemie.uni-muenchen.de	München, Germany	86
Loganathan, Doraisamy	phy041s@uohyd.ernet.in	Hyderabad, India	75
Luchinat, Claudio	luchinat@risc1.lrm.fi.cnr.it	Florence, Italy	27
Lurie, David J.	lurie@aberdeen.ac.uk	Aberdeen, UK	5
Michl, Günter	guenter.Michl@schering.de	Berlin, Germany	
Muller, Robert N.	Robert.Muller@umh.ac.be	Mons, Belgium	13,15
Müller, Klaus	klaus@b01.chemie.uni-stuttgart.de	Stuttgart, Germany	
Nolte, Markus	markus@e3.physik.uni-dortmund.de	Dortmund, Germany	73,79
Peirson, Neil	neil.peirson@kcl.ac.uk	London, UK	81
Petit, Dominique	dpe@pmc.polytechnique.fr	Palaiseau, France	
Philippot, Samuel	samuel@pmmh.espci.fr	Paris, France	

Pierart, Corinne	corinne.pierart@umh.ac.be	Mons, Belgium	
Platzek, Johannes	johannes.platzek@schering.de	Berlin, Germany	
Pusiol, Daniel	pusiol@fis.uncor.edu	Córdoba, Argentina	9,29, 77,92
Redfield, Alfred		Waltham, MA, USA	3,67
Rinck, Peter A.	parinck@aol.com	Mons, Belgium	13
Roduner, Emil	roduner@psi.ch	Stuttgart, Germany	23
Rommel, Eberhard	eberhard@lucy.physik.uni-wuerzburg.de	Würzburg, Germany	
Sabanin, Anton A.	ants@dpt.ustu.ru	Ekaterinburg, Russia	82
Sapunov, Vladimir A.	sva@ktf.rcupi.e-burg.su	Ekaterinburg, Russia	82
Seitter, Ralf-Oliver	ralf.seitter@physik.uni-ulm.de	Ulm, Germany	11,59
Sousa, Duarte M.	pedsousa@alfa.ist.utl.pt	Lisboa Codex, Portugal	84
Spohn, Karl-Heinz	karl-heinz.spohn@physik.uni-ulm.de	Ulm, Germany	
Stapf, Siegfried	pczssx@unix.cc.c.nottingham.ac.uk	Nottingham, UK	37,48
Strange, John H.	j.h.strange@ukc.ac.uk	Canterbury, UK	
Struppe, Jochem Otto F.	jstruppe@chem.ucsd.edu	San Diego, Ca, USA	32
Terekhov, Maxim V.	terehov@snoopy.phys.spbu.ru	St. Petersburg, Russia	88
Valiullin, Rustem	RUSTEM@phys.ksu.ras.ru	Kazan, Russia	50
Vander Elst, Luce	Luce.Vanderelst@UMH.AC.BE	Mons, Belgium	13
Venu, Kandadai	kvsp@uohyd.ernet.in	Hyderabad, India	16,35, 39,75

Vilfan, Mika	mika.vilfan@ijs.si	Ljubljana, Slovenia	42
Wiener, Erik	e-wiener@uiuc.edu	Urbana, Il, USA	18,90
Zanni, Helene	zanni@pmmh.espci.fr	Paris, France	
Zavada, Tatjana	tatjana.zavada@physik.uni-ulm.de	Ulm, Germany	46
Zick, Klaus	klz@bruker.de	Rheinstetten, Germany	